PETROGENESIS OF A BIMODAL ASSEMBLAGE OF
ALKALI-BASALT AND RHYOLITIC IGNIMBRITE, GRAVELLY RANGE,
SOUTHWEST MONTANA

by

MALIA KAY SPAID-REITZ

B.A., Wright State University, 1978

A MASTER'S THESIS

submitted in partial fulfillment of the

requirements of the degree

MASTER OF SCIENCE

Department of Geology

KANSAS STATE UNIVERSITY
Manhattan, Kansas

1980

Approved by:

Sambhudas Chaudhuri

Major Professor

Spec. Coll.
LD
2668
.T4
1980
S676
c.2

CONTENTS

TABLES

FIGURES

A C K N O W L E D G E M E N T S

Those who have contributed their time, effort, and support to aid the completion of this thesis are gratefully acknowledged. My major professor, Dr Sambhudas Chaudhuri; provided guidance throughout this research and aided in the Sr isotope analyses and in interpretation. Dr. Robert Cullers, Dr. Herbert Moser, and Dr. Charles Walters served on my supervisory committee and provided constructive editorial remarks. Dr. James Underwood also reviewed the manuscript and provided constructive editorial remarks. Dr. Robert Cullers also aided in trace-element analyses and in petrogenetic interpretation. Dr. Paul Pushkar inspired me to do this study and provided guidance throughout.

The Department of Geology, Kansas State University, provided a Graduate Teaching Assistantship and the use of facilities. The Department of Geology, Wright State University, provided field equipment and photomicrograph equipment. Dr. Gerard W. James, Kansas Geological Survey, provided X-ray fluorescence facilities and assisted with analyses. The Geological Society of America and Sigma Xi, the Scientific Research Society, financially supported this study with Grants-in-Aid for research.

Dr. James Gutmann, Wesleyan University, provided assistance while the author was in Montana, and made helpful suggestions for spectrophotometric analyses. Bruce Reitz, my husband, assisted and encouraged me throughout this project. Joseph Smalley, fellow graduate student from KSU, artistically illustrated petrographic thin sections for this study. Roger Wadleigh and Dave Eichen, students from WSU, provided friendship and aid while in the field in Montana.

INTRODUCTION

STATEMENT OF THE PROBLEM

Volcanic rocks typical of Tertiary extrusive activity in southwestern Montana and adjacent areas are located in the Gravelly Range (fig. 1). Previous studies of these rocks are few and consist only of the determination of broad field relationships and of very generalized petrographic data (Mann, 1954; 1960). Stratigraphic correlations and evolutionary modes of the volcanic rocks have yet to be determined.

This investigation focused on the petrogenesis of the Tertiary volcanic rocks in the Gravelly Range. Field relations, petrographic, major-element, trace-element, and strontium isotope data from four of the major outcrop areas, Black Butte, Wolverine Basin, Lion Mountain-Windy Hill, and Divide Mountain, were determined (fig. 2). These data were used to develop possible melting and crystallization models for the magmas and to examine the relationships with nearby igneous bodies of similar age for which isotopic and chemical data are available.

REGIONAL VOLCANO-TECTONIC SETTING

Widespread volcanism occured in the western United States during the Cenozoic. Types of magma and their tectonic associations changed markedly during that time in a 1,500-km zone from the Pacific margin eastward. Although a direct relationship between volcanism and tectonic

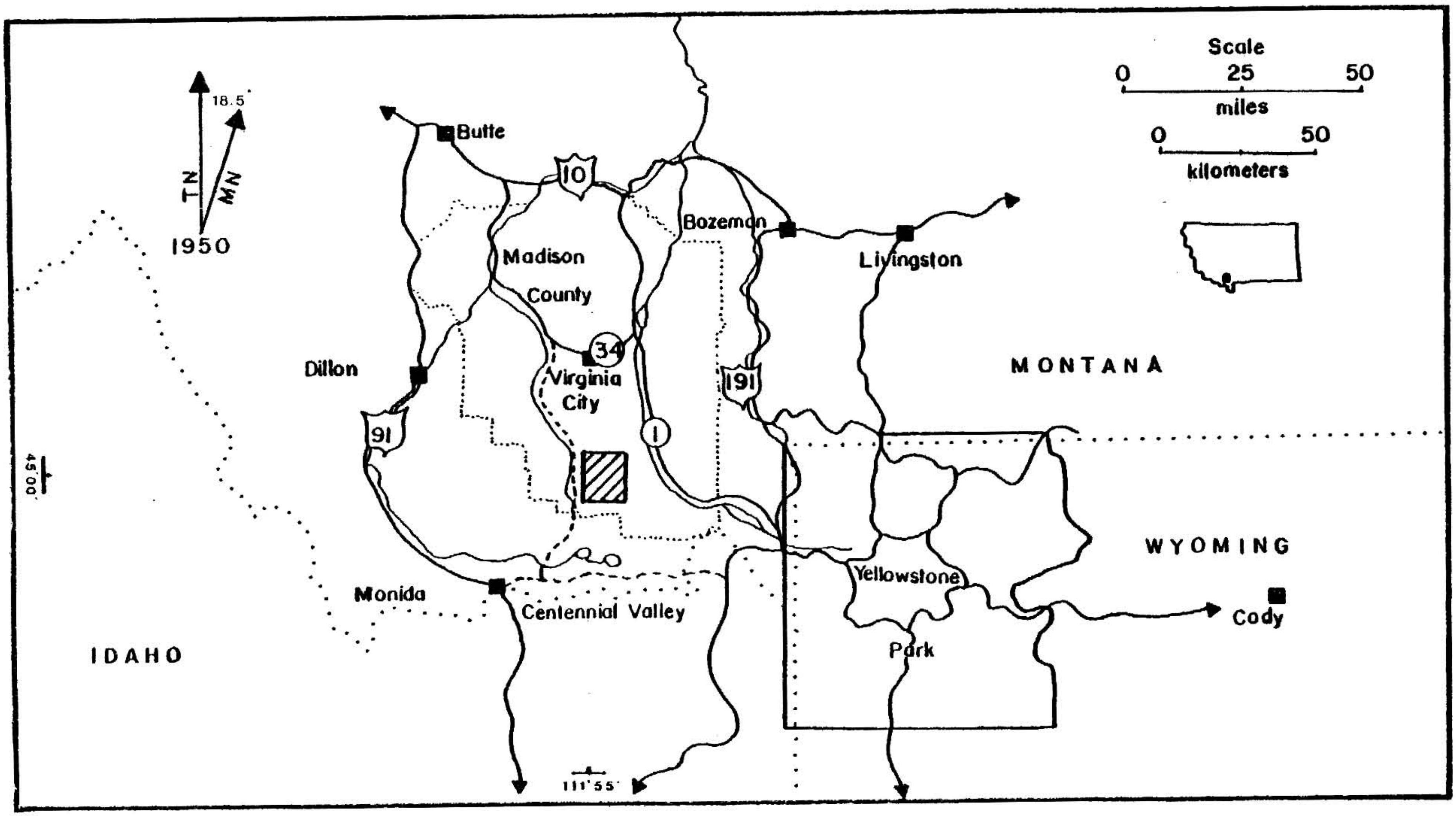

Figure 1. Index map of the Gravelly Range, Madison County, Montana. Diagonal lines denote the study area of this investigation (after Mann, 1954).

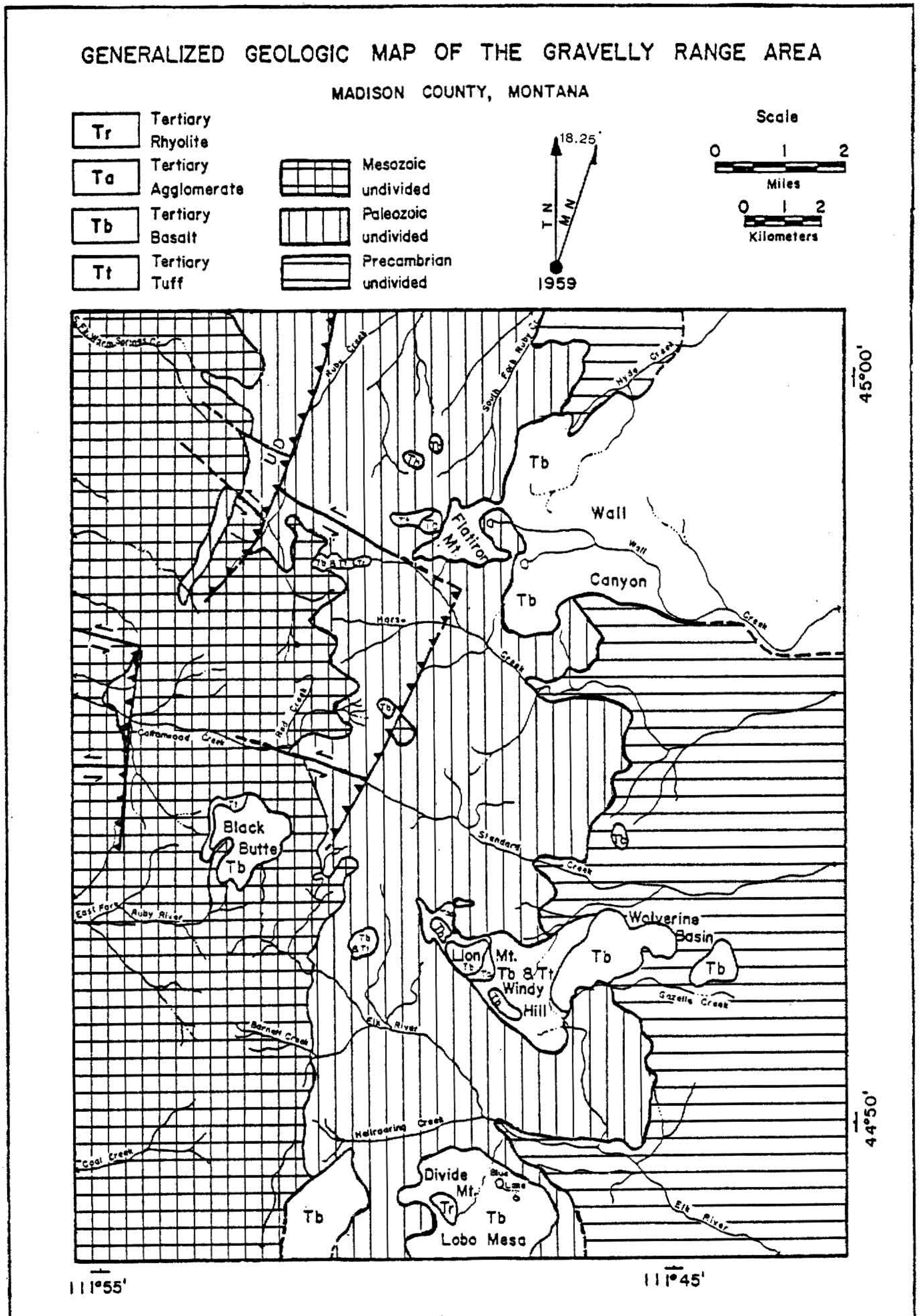

Figure 2. Generalized geologic map showing major volcanic outcrop areas on the southeastern flank of the Gravelly Range. Modified from Mann (1954).

regime has been challenged (Gilluly, 1971; 1973), many authors conclude that such a relationship exists in the western United States (Dickenson, 1972; Lipman et al., 1972; Christiansen and Lipman, 1972). From Late Cretaceous through the middle Tertiary, largely calc-alkaline andesite of intermediate composition and associated silicic differentiates that were related to a regime of continental-margin plate convergence, characterized the orogenic phase of volcanism. Associated structural features include folds and thrust faults. Regional metamorphism also occured. The post-orogenic phase of volcanism represented by Eocene and younger sequences, may be related to a regime of extension that resulted in extrusion of mainly bimodal basalt and high-silica rhyolite. Associated structural features include regional normal and strike-slip faults.

A similar change of volcanism associated with tectonic regime is exemplified in southwestern Montana, although the shift from calc-alkaline andesite to alkali basalt occured much earlier there than in much of the western United States (Chadwick, 1978). Extensional tectonism may have been active 40 m.y. B.P. (Kuenzi and Fields, 1971), inasmuch as post-Eocene andesite is uncommon in southwestern Montana.

G R A V E L L Y R A N G E

LOCATION AND ACCESS

The Gravelly Range is a north-trending feature in the southern part of the Northern Rocky Mountain physiographic province. It extends more than 80 km from Virginia City in the north to Centennial Valley in the south, and it covers approximately 800 sq km (fig. 1). The study area is located in southern Madison County, Montana, in the Cliff Lake and Monument Ridge U.S. Geological Survey 15-minute quadrangles, on the southeastern flank of the Gravelly Range. A dirt and gravel road provides access to the area from Highway 287 at the West Fork Campground. Access within the area is provided by additional dirt and gravel roads and pack trails.

RELIEF, TOPOGRAPHY, AND VEGETATION

Elevations vary from approximately 2,300 m in the lower valleys to 3,200 m on the top of the highest butte; maximum relief is 900 m. The average elevation of the crest of the range is 3,000 m; the crest is smooth and rounded. The west flank is a gentle slope controlled by westward dipping sediments, whereas the east flank is steep and disected by active streams that are transverse to the structure and drain into the Madison Valley. Black Butte is the most prominent feature in the range, rising 450 m above its base. Spruce and Douglas fir dominate the upper elevations, and birch and aspen dominate the river valleys and lower elevations. Lodgepole pine now also thrives in the lower elevations since much of the natural timber was disturbed by logging. The timberline, with meadows above, occurs at approximately 2,700 m (Mann, 1954).

G E N E R A L   G E O L O G Y

INTRODUCTION

Early geologic investigations included a reconnaissance of the Gravelly Range. Peale (1896) conducted the earliest study during which he mapped the surface geology and named the metamorphosed basement rocks the "Cherry Creek beds". Douglas (1909) described the general physiography during a trip through the west. Condit et al. (1927) reported on the phosphate rock in the Yellowstone-Three Forks area.

Scott (1938) and Atwood and Atwood (1945) investigated the area around Black Butte for evidence of glaciation and found the gravels for which the range was named to be of glacial origin. Atwood and Atwood also studied the regional structure of the area and found the core of the range to consist of metamorphosed Precambrian sedimentary rocks. Paleozoic and early Mesozoic sedimentary rocks overlie an erosional surface. Their present 10° westward dip was the result of uplift during the late Mesozoic. Fissure volcanism then poured lava over much of the surface in the mid-Tertiary; erosion which followed reduced the range to its present configuration.

STRATIGRAPHY

Mann (1954; 1960) provided a detailed description of Paleozoic through early Cenozoic sedimentary rocks with only brief mention of Precambrian metamorphic rocks and Tertiary igneous rocks (fig. 3).

Era	Period	Epoch	Unit	Thickness	Description
CENOZOIC	Quat.		Pleistocene glacial material and Recent alluvium		
CENOZOIC	Tertiary	Oligo-cene	Volcanics	0-150 m	Flow basalt and volcanoclastic rocks
CENOZOIC	Tertiary	Eo-cene	Black Butte gravel	0-30+ m	Gray-brown, ashy gravel
CENOZOIC	Tertiary	Paleo-cene	Limestone cobble conglomerate	0-40 m	Reddish cobble conglomerate
MESOZOIC	Creta-ceous		Colorado Formation	610+ m	Gray, orange sandstone, porcellanite, gray and black shale
MESOZOIC	Creta-ceous		Kootenai Formation	120-150 m	Gray conglomerate and sandstone, varie-gated claystone, "gastropod limestone", and reddish-brown sandstone
MESOZOIC	Jurassic		Morrison Formation	40 m	Varigated claystones and gray-brown sandstone
MESOZOIC	Jurassic		Ellis Formation	5-24 m	Greenish-gray glauconitic sandstone, sandy limestone and gypsum
MESOZOIC	Triassic		Thaynes (?) Formation	0-30 m	Gray and yellowish-orange sandstone and siltstone
MESOZOIC	Triassic		Woodside Formation	0-120 m	Red beds
MESOZOIC	Triassic		Dinwoody Formation	120-180 m	Yellowish-orange siltstone and dolomite
PALEOZOIC	Permian		Phosphoria Formation	60+ m	Yellowish-gray and gray sandstone, shale oolitic phosphorite, chert, and orthoquartzite
PALEOZOIC	Carboniferous	Pennsyl-vanian	Quadrant Formation	160+ m	Grayish-orange dolomite and quartzitic sandstone
PALEOZOIC	Carboniferous	Pennsyl-vanian / Missis-sippian	Amsden Formation	40+ m	Red beds, silty limestone and dolomite
PALEOZOIC	Carboniferous	Missis-sippian	Mission Canyon	260+ m	Brown and gray cherty limestone
PALEOZOIC	Carboniferous	Missis-sippian	Lodge-pole	200+ m	Yellow-brown and gray limestone
PALEOZOIC	Devonian		Three Forks Formation	60+ m	Yellowish siltstone, limestone and gray-green shale
PALEOZOIC	Devonian		Jefferson	90+ m	Yellow-brown to dark brown limestone
PALEOZOIC	Devonian		Basal Unit	30+ m	Tan limestone and silty limestone
PALEOZOIC			Ordovician and Silurian missing		
PALEOZOIC	Cambrian		Meagher- (?) Pilgram Formation	300+ m	Yellowish-brown and gray-mottled limestone
PALEOZOIC	Cambrian		Wolsey Formation	60+ m	Gray, green sandstone and shale
PALEOZOIC	Cambrian		Flathead Sandstone	15-37 m	Brown, tan, yellow quartzitic sandstone
PRECAMBRIAN			Cherry Creek Series		Phyllite, quartzite, amphibolite, quartz-feldspar gneiss

Figure 3. Summary of the stratigraphic units exposed in the Gravelly Range (after Mann, 1960).

The Cherry Creek Series consist of a sequence of metamorphosed sediments, and they make up the basement rocks of the Gravelly Range. Phyllite, quartz-feldspar gneiss, amphibolite, and quartz-biotite-garnet gneiss are the major rock types. Radiometric ages indicate that similar metasedimentary rock sequences in nearby ranges are Archean (2,762 $\pm$ 113 m.y. B.P.)(James and Hedge, 1980); this age corresponds to the "Beartooth orogeny."

An angular unconformity separates the Paleozoic sequence from the Precambrian sequence. With the exception of the Ordovician and Silurian periods, all of the periods in the Paleozoic Era are represented in the Gravelly Range by approximately 1,300 m of sedimentary rocks. Major exposed lithologies include limestone, dolomite, shale, and sandstone with minor chert, silty limestone, and oolitic phosphorite.

The Mesozoic sequence lies conformably on the Paleozoic sequence. All of the periods in the Mesozoic Era are represented in the Gravelly Range by approximately 1,200 m of sedimentary rocks. Major exposed lithologies include siltstone, dolomite, red beds, sandstone, claystone, conglomerate, and shale with minor limestone and gypsum.

An angular unconformity seperates the Cenozoic from the underlying Mesozoic sequence. The Cenozoic Era is represented by 0-200 m of sediment, sedimentary rocks, and assorted volcanic rocks. The sedimentary lithologies include cobble conglomerate, gravel, volcanic tephra, glacial material, and alluvium.

TECTONIC SETTING

During the Late Cretaceous Epoch, the Gravelly Range area was a basin into which was deposited more than 600 m of miogeosynclinal sediments

(Eardly, 1960). The Laramide uplift developed northwest-trending thrust faults south of the Gravelly Range area and created folds of similar trend within the Gravelly, Madison, Ruby, and Centennial Mountain ranges (Hamilton, 1960; Honkala, 1960).

By the early Cenozoic, two systems of thrust faults were dominant (Eardly, 1960). One is located northeast of the Gravelly and Madison ranges, where the overriding block of sedimentary rocks moved southwest. The second, along which the overriding block moved sedimentary rocks to the northeast, is located west of the Gravelly Range. An intricate wedge of material was caught between the two fault systems, and this wedge forms the core of the Gravelly Range and the adjacent Madison, Ruby, and Centennial ranges (Hamilton, 1960).

During the middle through late Cenozoic, the strata were offset along normal faults which followed Laramide fault trends. Recent normal faults were then superimposed on all previous faults in the Gravelly Range and the surrounding vicinity. The area now resembles the Basin and Range area of Nevada (Honkala, 1960).

VOLCANIC GEOLOGY

INTRODUCTION

Gravelly Range volcanic rocks include a bimodal assemblage of alkali basalt of mid-Tertiary age and minor rhyolitic ignimbrite of unknown age. Based on relative stratigraphic positions, the rocks may be divided into four units: (1) basal crystal tuff, (2) alkali basalt suite and associated volcanoclastic rocks, (3) olivine diabase dikes, and (4) uppermost rhyolitic ignimbrite.

Recent studies indicate that several volcanic centers, which include fissures and central vents, are present in the Gravelly Range (Marvin et al., 1979; Burke-Griffin, 1978; Burke-Griffin and Pushkar, 1979; Eichen, 1979; Eichen and Pushkar, 1979; this investigation). Based on the major rock types represented, these volcanic rocks are assumed to be associated with recent extensional tectonism (Lipman et al, 1972; Christiansen and Lipman, 1972; Burke-Griffin, 1978; Eichen, 1979). Previous studies have shown that the field relations of the major rock units as well as the petrography of the major units are similar from one outcrop area to another (Burke-Griffin, 1978; Eichen, 1979).

FIELD RELATIONS OF THE MAJOR ROCK TYPES

BASAL CRYSTAL TUFF

Approximately 10 percent of the volume of Gravelly Range volcanic rocks consists of crystal tuff. Where exposed, this unit crops out beneath flow basalt, and is commonly intruded and overlain by basaltic units. Locally, where the tuff is in contact with later units, metamorphic aureoles are present. Exposed thicknesses vary from 2 to 200 m, and weathered portions have steep smooth slopes (30°-40°). Poorly defined subhorizontal beds of varied thickness are observed on the slope of Lion Mountain and in Wolverine Basin.

ALKALI-BASALT SUITE

Approximately 75 percent of the volume of Gravelly Range volcanic rocks belongs to the alkali-basalt unit. Rock types, which range from alkali-olivine basalt to basaltic andesite; silicic-alkalic basalt is the most voluminous. Minor amounts of associated tephra are interbedded with basalt from the Lion Mountain-Windy Hill. Flow basalt may retain sinuous stream patterns, or they may cap sedimentary sequences. A prominant set of closely-spaced subhorizontal joints is ubiquitous and defines a fissility which allows the rock to break into slabs. Individual flows may be as thick as 60 m, and crude columnar joints are observed in massive flows. Steep scarps with broad talus aprons indicate the original basaltic cover was once more extensive. Tops and bases of individual flows are observed only in a few areas, e.g. Wolverine Basin, Lion Mountain, and Windy Hill.

OLIVINE DIABASE

Medium-grained olivine diabase makes up 10 percent of the Gravelly Range volcanic rocks. The attitude of these rocks ranges from sub-horizontal sills concordant with basaltic fissility to near-vertical dikes which tend to follow columnar joints. Complex interfingering and cross-cutting relationships are formed by this rock type in the vicinity of volcanic vents and feeder dikes. Thicknesses vary, but are usually less than 20 m in the largest dimension. Outcrops of this rock type are less resistant to weathering than outcrops of the basalt, although there are steep scarps in Wolverine Basin. Exposures on Black Butte and Lion Mountain tend to be more rounded, although there are some scarps.

RHYOLITIC IGNIMBRITE

Approximately 5 percent of the volume of Gravelly Range volcanic rocks consists of rhyolitic ignimbrite. Outcrop of this rock type has been observed only in Wolverine Basin, although the loose boulders that are abundant on top of Divide Mountain may represent a disintegrated outcrop. In both areas, the ignimbrite overlies alkali-basalt. In Wolverine Basin, the rhyolitic ignimbrite appears to be conformable with the underlying alkali-basalt. As yet, no apparent source areas for this rock type have been found. Thickness of the observed exposures is only a few meters.

PETROLOGY OF THE MAJOR ROCK TYPES

BASAL CRYSTAL TUFF

The basal crystal tuff is a friable, deeply weathered pale orange volcanic ash. Locally where it is intruded by or is overlain by younger dikes and flows, it is baked into a well consolidated deep-orange rock which fractures into semiconchoidal fragments that resemble pottery shards. Chalcedony and opaline deposits are found in some baked zones. Petrographic studies reveal this rock is a hypocrystalline porphyritic ash-fall tuff which conatins anhedral to subhedral phenocrysts of sanidine, quartz, plagioclase (An_{35}-An_{55}), and traces of hornblende, biotite, and opaque minerals (fig. 4). Mesostatic fragments include glass shards and clay minerals (Eichen, 1979).

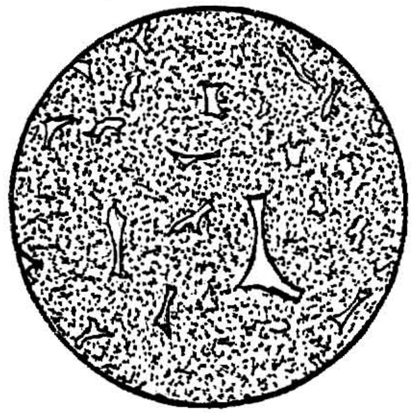

Figure 4. Petrographic illustration of glass shards in the basal crystal tuff. Uncrossed nicols.
0.02 mm

ALKALI-BASALT SUITE

Rock types within the alkali-basalt suite vary from fine-grained porphyritic basalt with millimeter sized phenocrysts of olivine and clinopyroxene or both, to fine-grained porphyritic basaltic andesite with phenocrysts of clinopyroxene and occasional resorbed plagioclase. The porphyritic basalt is black whereas the porphyritic basaltic andesite is dark gray. Several flows are vesicular and characteristically contain amygdaloidal carbonate. Minor crystal tuffs similar to the basal unit are interbedded together with lapilli and lithic tuff and interflow breccia. These units consist mostly of scoriaceous blocks, bombs, and lapille in an ashy matrix, and in most places are cemented by carbonate. Petrographic studies reveal these rocks vary from hypocrystalline to holocrystalline, and they are porphyritic (figs. 5 and 6). Intersertal alkali-olivine basalt with plagioclase (An_{55}-An_{75}) microlites, phenocrsyts of olivine and augite, and alkali-rich glass is the most mafic rock type (fig. 5). Intersertal basaltic andesite with phenocrysts of augite, resorbed plagioclase (calcic), and plagioclase (An_{30}-An_{50}) microlites in a groundmass of clinopyroxene and glass in the most silicic rock type (fig. 6). Intergranular texture is also commonly displayed in the alkali-olivine basalt. Ferromagnesian minerals commonly are altered to iddingsite, and amygdaloidal carbonate is common in vesicular to scoriaceous samples.

Figure 5. Petrographic illustration of an olivine phenocryst surrounded by plagioclase microlites and augite grains in the alkali-olivine basalt. Crossed nicols. 1.0 mm

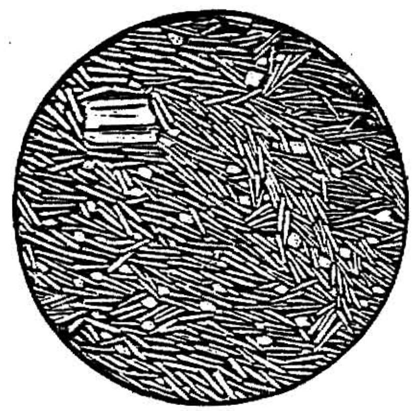

Figure 6. Petrographic illustration of a resorbed plagioclase phenocryst surrounded by plagioclase microlites and augite grains in the basaltic andesite. Crossed nicols. 1.0 mm

OLIVINE DIABASE

The olivine diabase is medium to dark gray, and its grain size varies from fine to coarse with medium the most common. Subhedral to euhedral white plagioclase and black hornblende with rounded brown iddingsite-rimmed clinopyroxene and olivine are present in the coarser zones (Burke-Griffin, 1978; Eichen, 1979). This rock weathers readily, and secondary carbonate mineralization is common particularly in the coarser zones. Petrographic studies reveal this rock is holocrystalline and displays intergranular to ophitic textures(fig. 7). Minerals present in the rock include euhedral to subhedral plagioclase (An_{40}-An_{55}), olivine, augite, hornblende, opaque minerals, and traces of apatite. Ferromagnesian minerals are highly altered to iddingsite; there is some chloritization and secondary carbonate mineralization (Burke-Griffin, 1978; Eichen, 1979).

Figure 7. Petrographic illustration of ophitic intergrowths of plagioclase and augite in the medium-grained olivine diabase. Crossed nicols.

0.01 mm

RHYOLITIC IGNIMBRITE

Fresh surfaces of the rhyolitic ignimbrite are densely welded and vary from pink to purple-gray; millimeter sized phenocrysts of sanidine are common. Deeply weathered samples are light pink to orange and are loosely consolidated. There are occasional pumice fragments up to a few millimeters in length; scattered mafic minerals are altered to iron oxides. Petrographic studies reveal this rock is a hypocrystalline porphyritic ash-flow tuff which contains anhedral phenocrysts of quartz, sanidine, and opaque minerals. Mesostatic fragments include glass shards and clay minerals.

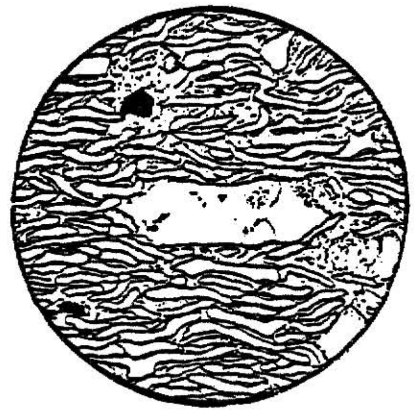

Figure 8. Petrographic illustration of welded glass shards that surround a sanidine phenocryst in the rhyolitic ignimbrite. Uncrossed nicols. 1.0 mm

MAJOR OUTCROP AREAS

BLACK BUTTE

Field relations, petrography, and major-element chemistry of volcanic rocks from Black Butte were examined by Burke-Griffin (1978) and Burke-Griffin and Pushkar (1979). Black Butte is a volcanic neck located near the crest of the Gravelly Range (fig.2) and is composed mainly of basalt (fig. 9). Radiometric ages indicate Black Butte basalt is approximately 23 m.y. old and may represent the latest activity in the area (Marvin et al., 1974). Major volcanic rock types, in ascending stratigraphic order include: (1) alkali-basalt, (2) crystal tuff, (3) agglomerate, and (4) olivine diabase.

Black Butte basalt is interpreted as the erosional remnant of a large volcanic neck that may have been the source for much of the activity in the Gravelly Range (Marvin et al., 1974; Burke-Griffin, 1978; Burke-Griffin and Pushkar, 1979). No evidence of tops and bases of flows is exposed on the butte. Nearly vertical columnar-jointed exposures of basalt reach heights of more than 60 m, thus the initial eruption was probably quiescent. Sub-horizontal, concordant tuff lenses occur interspersed with basalt near the top of the butte and may indicate minor intermittent pyroclastic eruptions. Fragments of medium- to coarse-grained olivine diabase are plentiful in the talus although outcrop occurs only near the top of the butte where an olivine diabase dike intrudes the basalt flows. A large pipe of agglomerate, called vent facies by Burke-Griffin, is exposed over most of the top of the butte, and it cross-cuts all other rocks. There is a similar smaller agglomerate pipe on the southeast flank of the butte. These pipes are indicative of a change to more explosive activity during the latter stages of the volcanic activity.

WOLVERINE BASIN

Field relations and petrography of volcanic rocks from Wolverine Basin were examined by Eichen (1979) and Eichen and Pushkar (1979). Flow basalt is the most voluminous rock type exposed in the area (fig. 10). Based on their similar field relations and petrography, basalt of the Wolverine Basin is assumed to be the same age as Black Butte basalt (Eichen, 1979). Major volcanic rock types, in ascending stratigraphic order, include: (1) crystal tuff, (2) alkali-basalt, (3) olivine diabase, and (4) rhyolitic ignimbrite.

Wolverine Basin basalt was emplaced as a relatively quiescent flow from an easterly-trending fissure, although only the faulted segments of a basaltic feeder dike system remain as illustrated by Eichen (fig. 11). Pyroclastic material is characteristically absent in this area with two exceptions. Orange-red ash-fall tuff (basal crystal tuff) underlies the basalts adjacent to the feeder dike, and a purple-gray welded tuff (rhyolitic ignimbrite) overlies the basalt flows in Roger's Meadow (fig. 10). No evidence of the source of either of these units was found in Wolverine Basin.

Figure 9. Geologic map and generalized cross section of Black Butte, a volcanic neck in the Gravelly Range (modified from Burke-Griffin, 1978). Solid black aquares indicate sample locations of rocks analyzed in this study.

26 = BB-26B-77

9 = BB-9-77

EXPLANATION

(Symbols after Burke-Griffin, 1977).

Tertiary Volcanic Rocks

- alkali-basalt talus
- agglomerate
- olivine diabase
- crystal tuff
- alkali basalt

Country Rocks

- Mesozoic sedimentary rocks, undivided

Symbols

- Contact, dashed where approximate
- Contour line, interval: 200 ft
- Sample location

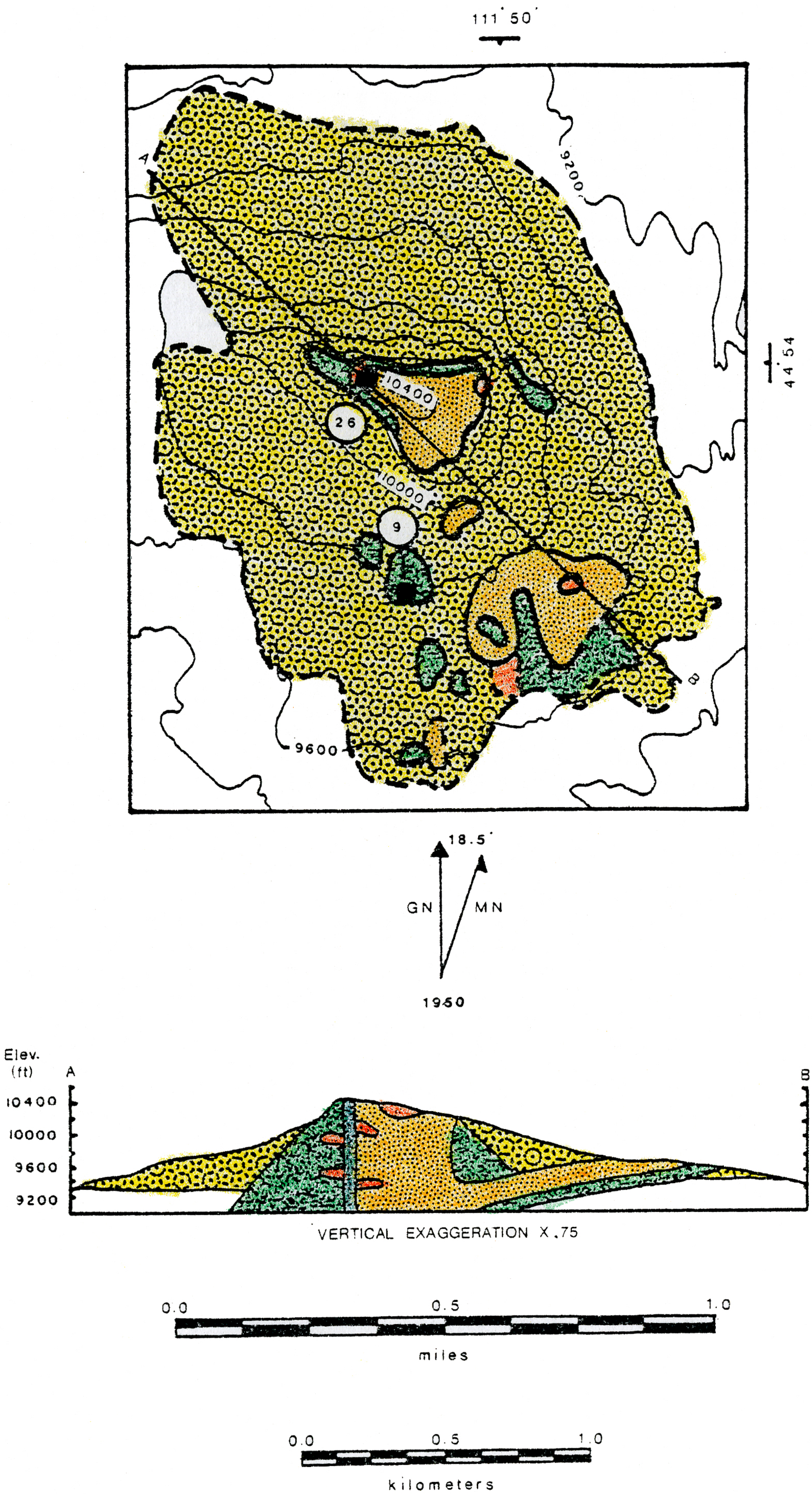
111° 50'
44° 54'
9200
10400
10000
9600
26
9
A
B
18.5°
GN
MN
1950
Elev. (ft)
10400
10000
9600
9200
VERTICAL EXAGGERATION X.75
0.0
0.5
1.0
miles
0.0
0.5
1.0
kilometers

Figure 10. Geologic map and generalized cross section of Wolverine Basin volcanic rocks in the Gravelly Range (modified from Eichen, 1979). Solid black squares indicate sample locations of rocks analyzed in this study.

62 = P-62B-78

30 = P-30B-77

13 = P-13F-77

5 = P-5-77

EXPLANATION

(Symbols after Eichen, 1979).

Tertiary Volcanic Rocks

rhyolitic ignimbrite

olivine diabase

alkali basalt

crystal tuff

Country Rocks

Paleozoic sedimentary rocks and Precambrian metamorphic rocks, undivided

Symbols

Contact, dashed where approximate

Contour line, interval: 200 ft

Sample location

Fault, dashed where approximate

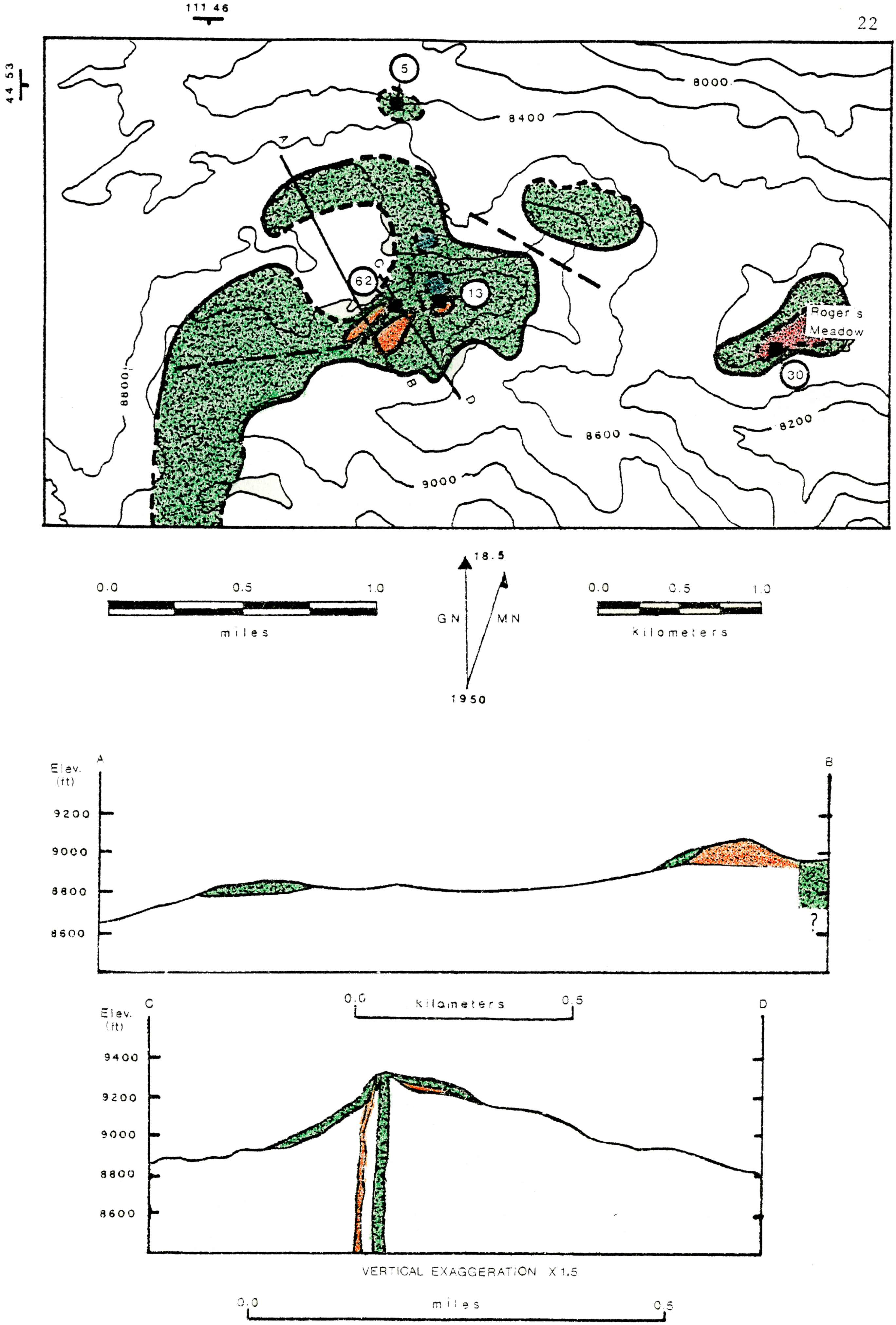
111 46
44 53
5
8000
8400
A
C
62
13
Roger's
Meadow
30
8800
B
D
8600
8200
9000
0.0
0.5
1.0
miles
18.5
GN
MN
1950
0.0
0.5
1.0
kilometers
Elev.
(ft)
A
B
9200
9000
8800
8600
?
C
D
0.0
kilometers
0.5
Elev.
(ft)
9400
9200
9000
8800
8600
VERTICAL EXAGGERATION X 1.5
0.0
miles
0.5

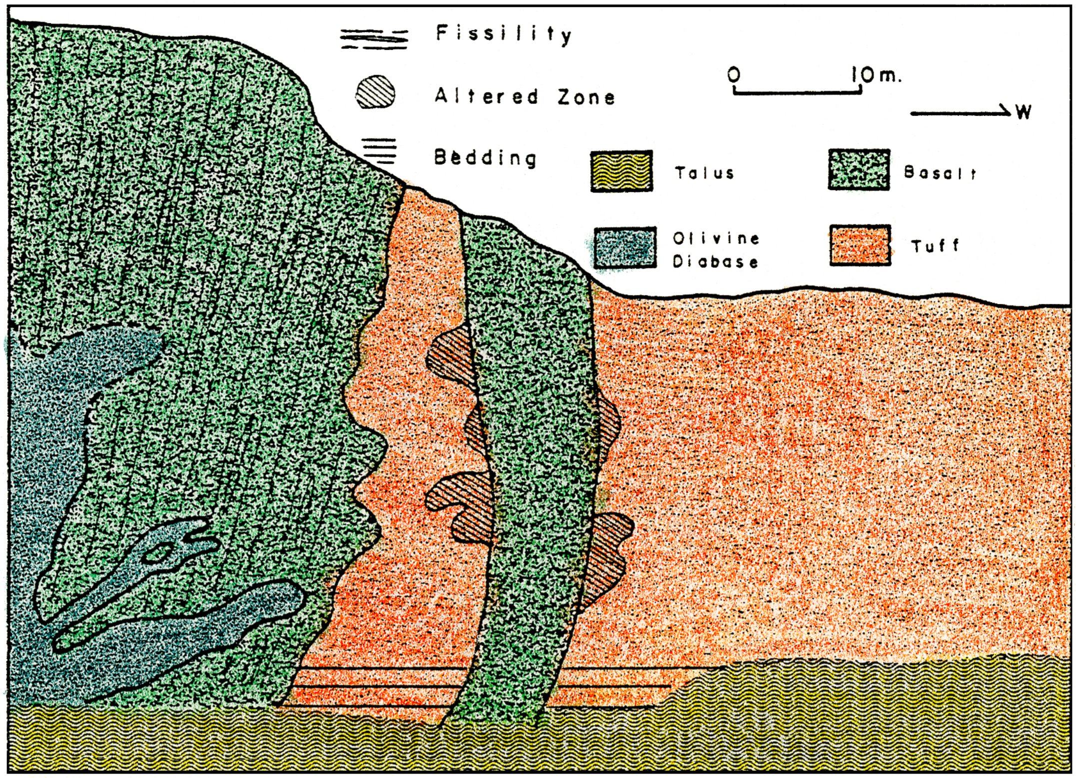

Figure 11. Idealized cross section of the field relationships in the vicinity of the Wolverine Basin feeder dike system (Eichen, 1979).

In addition, several dikes of medium-grained olivine diabase are found with the feeder dike system. Individual flows of basalt may be as thick as 60 m, and definite tops and bases of flows are distinguished only in Roger's Meadow. Crudely columnar-jointed scarps and large talus piles indicate that the original basalt cover was more extensive. Fissility is commonly sub-horizontal except in vent areas where it steepens to near vertical.

LION MOUNTAIN-WINDY HILL

Lion Mountain and Windy Hill form a northwest-trending ridge east of the crest of the Gravelly Range (fig. 2). Flow basalt is the most voluminous rock type (fig. 12). Mann (1954) determined the basal crystal tuff from Lion Mountain was mid-Oligocene in age. Major volcanic rock types, in ascending stratigraphic order, include: (1) crystal tuff, (2) alkali basalt

Figure 12. Geologic map and idealized crossectional view of the northeast flank of Lion Mountain-Windy Hill, a center of volcanic activity in the Gravelly Range. Solid squares indicate sample locations of rocks analyzed in this study.

22 = SR-22B-79

19 = SR-19-79

15 = SR-15B-79

14 = SR-14B-79

1 = SR-1C-79

E X P L A N A T I O N

Tertiary Volcanic Rocks

- agglomerate
- olivine diabase
- alkali basalt
- crystal tuff

Country Rocks

- Paleozoic sedimentary rocks, undivided

Symbols

- Contact, dashed where approximate
- Contour line, interval: 200 ft
- Sample location

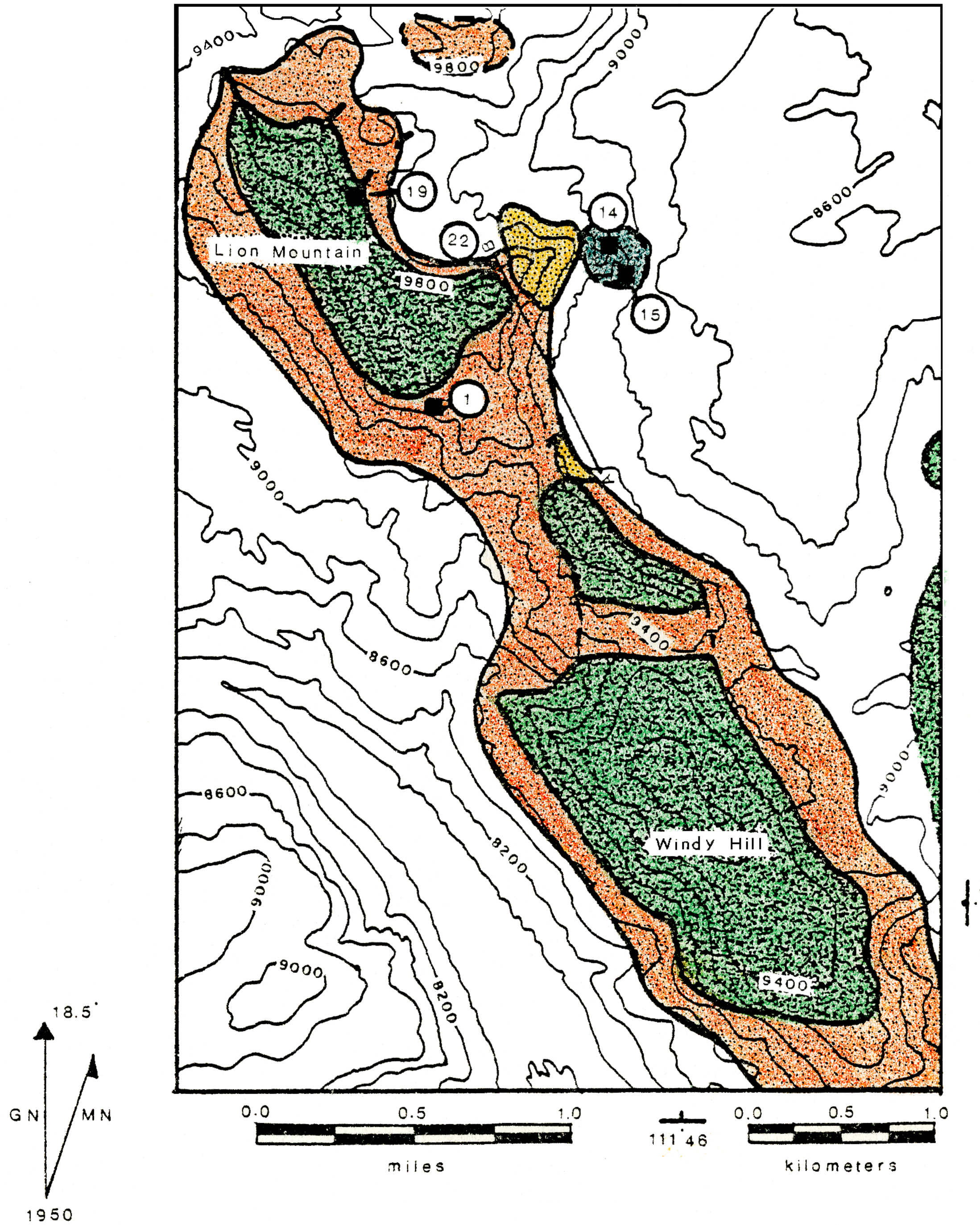
9400
9800
9000
8600
19
22
14
15
B
Lion Mountain
9800
1
9000
9400
8600
8600
9000
8200
9000
Windy Hill
9000
8200
9400
44 51
18.5
GN
MN
1950
0.0
0.5
1.0
miles
111 46
0.0
0.5
1.0
kilometers

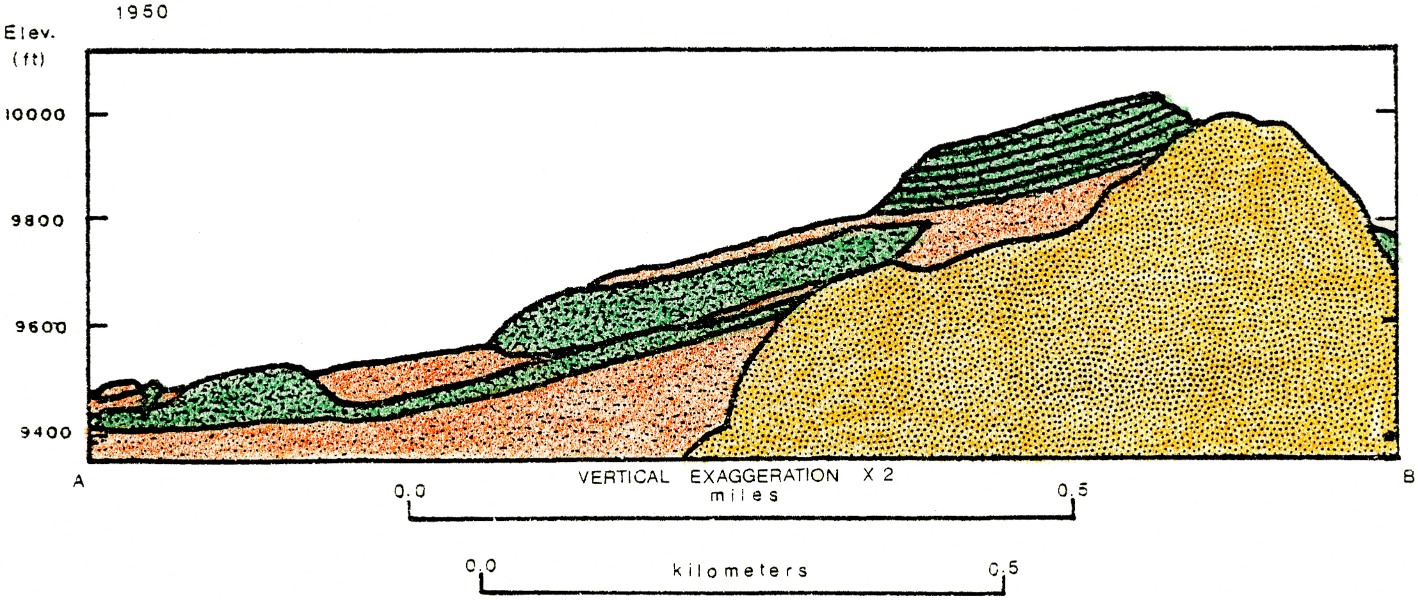
Elev. (ft)
10000
9800
9600
9400
A
B
VERTICAL EXAGGERATION X 2
0.0
0.5
miles
0.0
kilometers
0.5

(3) agglomerate, and (4) olivine diabase.

Lion Mountain is a basalt-capped erosional remnant of a volcanic center which was a major source of much of the activity in the Gravelly Range. Windy Hill is a basalt capped northwest-trending ridge connected to Lion Mountain by a saddle. Near the central portion of the dissected volcanic pile, the remnants of a cone of agglomerate approximately 250 m high and a columnar pipe of lava with vertical foliation exist adjacent to each other and probably represent the center of much of the activity. The presence of abundant pyroclastic material indicates very explosive activity with intersperced eruptions of basalt. Massive flows which cap much of the area indicate a transition to more quiescent activity in the latter stages of the eruptive episode.

Crystal tuff with interlayered sub-horizontal flow basalt underlies the area. Thickness varies from approximately 10 to 200 m. Locally, where the tuff is intruded by basalt dikes, the tuff is baked. Flow basalt which is approximately 60 to 90 m thick overlies the tuff. At least six individual flows cap Lion Mountain; at least 13 individual flows cap Windy Hill. A small breccia pipe several meters thick and minor basalt flows occur near the diabase, and although the details are obscure, all three appear to cross-cut the cone of agglomerate. Olivine diabase crops out near the major tephra cone although the extent of the olivine diabase is uncertain inasmuchas vegetation and talus obscure its outcrop.

DIVIDE MOUNTAIN

Divide Mountain is located a few kilometers east of the Gravelly Range and several kilometers south of Lion Mountain-Windy Hill (fig. 2). Only a brief reconnaissance of the field relations of the volcanic rocks of this area was made due to its inaccessible location (fig. 13).

Divide Mountain is underlain by basalt which crops out on the slopes of

Figure 13. Geologic map of Divide Mountain volcanic rocks (after Mann, 1954). Solid squares indicate sample locations of rocks analyzed in this study.

24 = SR-24-79

25 = SR-25A-79

= SR-25B-79

E X P L A N A T I O N

Tertiary Volcanic Rocks

rhyolitic ignimbrite

alkali basalt

Country Rocks

Paleozoic sedimentary rocks, undivided

Symbols

Contact

Contour line, interval: 200 ft

Sample location

Fault, dashed where approximate

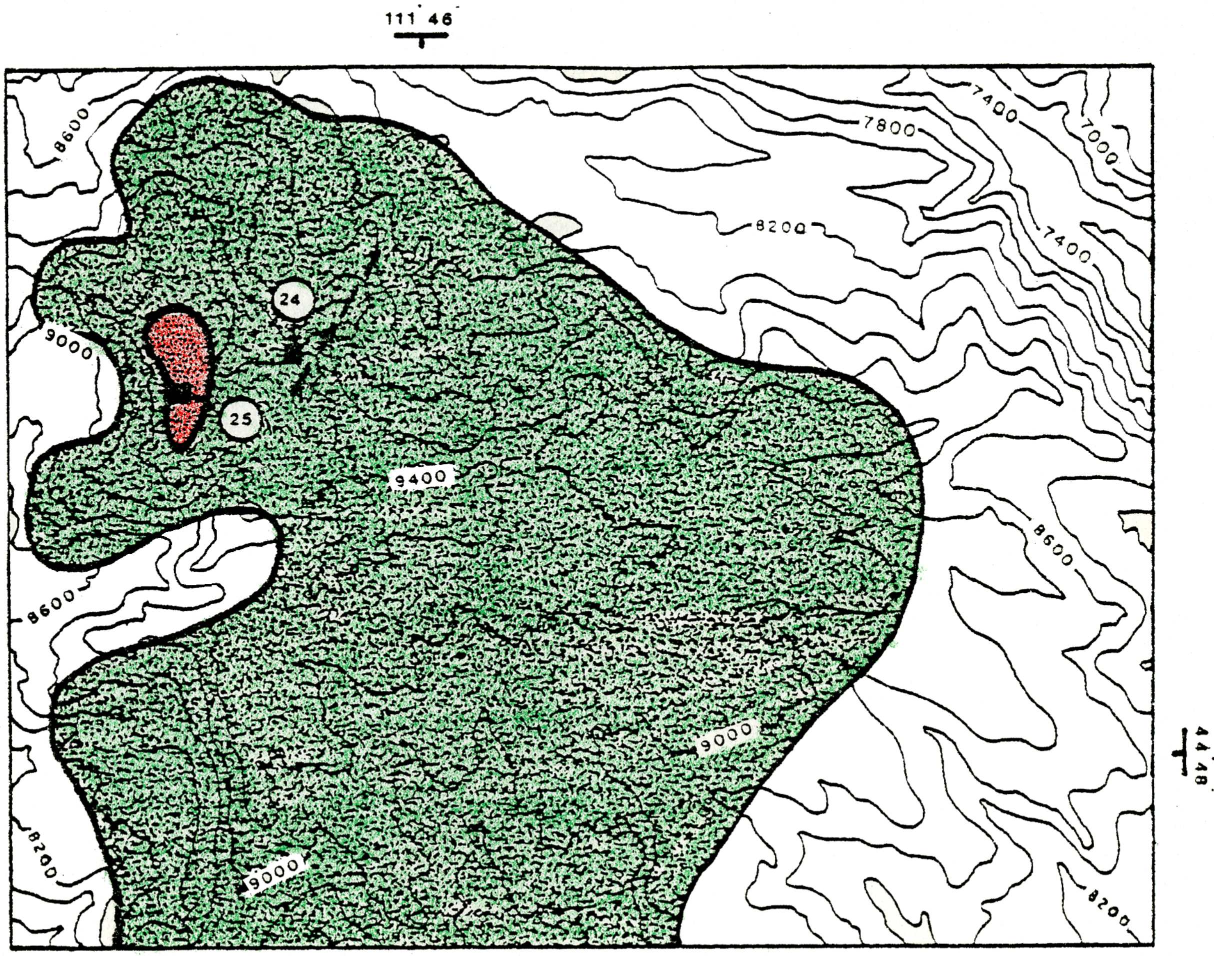
111°46'
44°48'
8600
7800
7400
7000
8200
7400
9000
24
25
9400
8600
8600
9000
8200
9000
8200

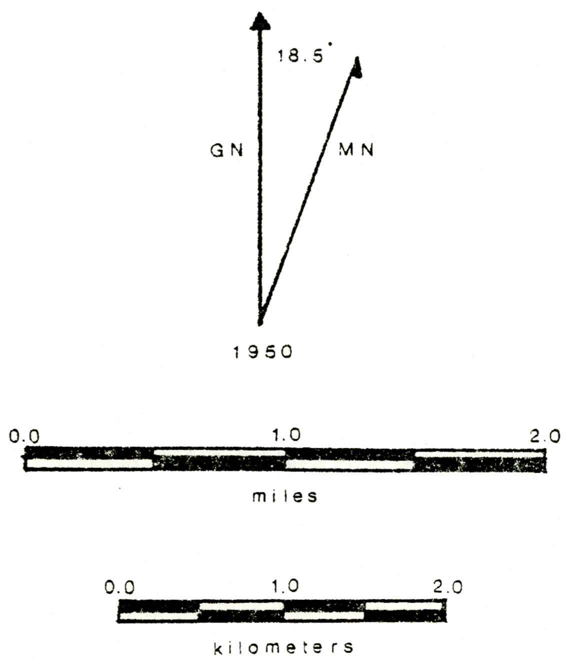
18.5°
GN
MN
1950
0.0
1.0
2.0
miles
0.0
1.0
2.0
kilometers

the mountain. The broad treeless summit crown does not have an outcrop but is dotted with accumulations of boulders of rhyolitic ignimbrite. No source for the volcanic rocks in this area has been observed. Mann (1954) assigned a Tertiary age for these rocks. Major volcanic rock types, in ascending stratigraphic order, include: (1) alkali basalt and (2) rhyolitic ignimbrite.

GEOCHRONOLOGY

Mann (1954) reported a mid-Oligocene age for the basal tuff unit of Lion Mountain. Thus, volcanic rocks of the Gravelly Range are assigned a maximum age of mid-Tertiary (35 m.y. B.P.) based on their stratigraphic position.

Nine K-Ar ages are reported by Marvin et al. (1974) on igneous rocks from eight localities in southwestern Montana. Basalt from Black Butte yields an age of 23 m.y. B.P. Radiometric ages on the igneous rocks north of Black Butte indicate volcanic activity continued over a 10 m.y. period from mid-Oligocene (34 m.y. B.P.) through early-Miocene (23 m.y. B.P.). Black Butte basalt has been considered by many to be the youngest evidence of volcanic acitivity in this area. More recent published K-Ar ages suggest the volcanic activity of the Gravelly Range may have started as early as 51 m.y. B.P. (Marvin and Dobson, 1979).

P R O C E D U R E

SAMPLE COLLECTION

Samples from Lion Mountain-Windy Hill and Divide Mountain were collected in the field for this investigation by the author during the summer of 1979. Locations are plotted on geologic maps of these areas (figs. 9-13) which were prepared from blow-ups of U.S. Geological Survey 15-minute quadrangle maps with a 40 ft contour interval. Other rock samples from Black Butte and Wolverine Basin which were analyzed in this project were provided by Dr. Paul Pushkar of Wright State University. Locations for these samples were plotted on geologic maps prepared by Burke-Griffin (1978) and Eichen (1979).

SAMPLE PREPARATION

Thin sections of samples from Lion Mountain-Windy Hill and Divide Mountain were prepared and examined for this investigation. Thin sections from Black Butte were described by Burke-Griffin (1978). Thin sections from Wolverine Basin, with the exception of one slide (P-30B-77) which was described by the author, were described by Eichen (1979). Only the freshest samples as determined petrographically were chosen for chemical analyses.

Approximately 100 g of fresh sample was placed in a Spex mixer/mill and milled for 30 minutes. The milled sample was next passed through a 200-mesh sieve and stored in a clean glass vial.

SPECTROPHOTOMETRY

Analyses for the elements Si, Al, Fe, Ca, Na, K, Ti, and Mn were made on 15 samples and five U.S. Geological Survey standard rocks with a Perkin-Elmer model 305-B atomic absorption and flame emmission spectrophotometer with a chart recorder. Lithium metaborate fusion as described by Gutman (personnal communication), Medlin et al. (1969), and Suhr and Ingamells (1966) was used to digest powdered rock samples. Aliquot portions of each sample solution were then diluted to the necessary linear concentration range for each element. Details of this procedure and the instrumental settings used are described by Reitz (1980).

Synthetic standards were prepared from stock solutions to bracket the approximate concentrations of the rock samples. Duplicate analyses of the U.S. Geological Survey standard rocks G-2, AGV-1, STM-1, BCR-1, and W-1 were conducted to monitor analytical accuracy. Table 1 summarizes the recommended values reported by Flanagan (1973; 1976). Estimated maximum deviations of spectrophotometric analyses are: SiO_2, Al_2O_3, and K_2O = $\pm$ 1 percent; Fe_2O_3 and Na_2O = $\pm$ 3 percent; MgO = $\pm$ 4 percent; TiO_2 = $\pm$ 8 percent.

GRAVIMETRIC ANALYSES

Total water and volatile contents of 15 samples and five U.S. Geological Survey standard rocks were determined using methods similar to those ofRiley (1958), Maxwell (1968), and described in Hutchison (1974). H_2O^- was determined by baking approximately one gram of powdered sample at 110°C for one hour in a clean previously dried platinum crucible. After cooling the crucible and sample to room temperature in a dessicator, the residue was

TABLE 1. Major-element content (weight percent) of U.S. Geological Survey standard rocks.

STANDARD	STM-1	STM-1	W-1	W-1	AGV-1	AGV-1	G-2	G-2	BCR-1	BCR-1
	Nepheline Syenite		Diabase		Andesite		Granite		Basalt	
REFERENCE	(1)	(2)	(1)	(3)	(1)	(3)	(1)	(3)	(1)	(3)
NO. Analyses	3		3		3		2		2	
OXIDE										
SiO_2	59.68	59.54	52.41	52.64	59.23	59.00	68.90	68.96	53.59	54.50
Al_2O_3	18.47	18.60	15.07	15.00	17.11	17.25	15.26	15.18	13.55	13.61
Fe_2O_3(T)	5.21	5.14	11.52	11.52	11.09	6.77	2.46	2.44	13.42	13.40
MgO	0.08	0.01	6.69	6.62	1.51	1.53	0.76	0.75	3.49	3.46
CaO	1.07	1.16	11.04	10.96	4.92	4.90	1.92	1.88	6.73	6.92
Na_2O	8.76	8.96	2.16	2.15	4.27	4.26	4.08	4.19	3.22	3.27
K_2O	4.24	4.24	0.64	0.64	2.85	2.89	4.52	4.55	1.64	1.70
TiO_2	0.11	0.14	1.13	1.07	1.01	1.04	0.43	0.47	2.14	2.20
MnO	0.21	0.22	0.17	0.17	0.09	0.10	0.03	0.03	0.17	0.18
H_2O-	0.03	0.18	0.14	0.16	0.87	0.16	0.07	0.11	0.57	0.80
ignition	1.54	---	0.09	---	0.80	---	0.60	---	0.44	---
H_2O+ and CO_2	---	1.57	---	0.59	---	0.87	---	0.63	---	0.80
TOTAL	99.40	99.85	101.06	101.09	99.43	98.76	99.03	99.19	98.96	100.84

(1) This study (2) Flanagan (1976) (3) Flanagan (1973)
(T) Total iron calculated as Fe_2O_3

weighed and the percentage weight lost was reported as adsorbed water (H_2O^-). Ignition was then performed on the residual sample by placing the crucible and sample in a muffle furnace at 1,000°C for 15 minutes. Ignited samples were cooled in a desiccator and the weight lost was recorded as loss on ignition.

Fair agreement was obtained with this method for all standard samples except for sample W-1 (Table 1). Discrepancies are most likely a result of the oxidation of iron which would tend to reduce the amount of weight lost during ignition. Estimated maximum deviation for ignition values is ± 25 percent, except for sample W-1 is approximately 75 percent in error.

MASS SPECTROMETRY

$^{87}Sr/^{86}Sr$ isotopic ratios for seven samples were determined with a 15 cm, 60° Nier-type mass spectrometer using a Ta filament. Sample preparation procedures used were described by Chaudhuri (1966), Methot (1973), and Kilbane (1978). Prior to analysis, the approximate concentrations of Rb and Sr were determined spectrophotometrically and sample sizes selected so that 25 to 40 ppm pf Sr were separated from each sample for analysis. To remove instrumental-induced fractionation, all the $^{87}Sr/^{86}Sr$ data were normalized to an $^{86}Sr/^{88}Sr$ value of 0.1194. Replicate analyses of the Eimer and Amend $SrCO_3$ standard yields a value of 0.7082 ± 0.0003. The decay constant of ^{87}Rb used for this study is $1.42 \times 10^{-11} yr^{-1}$.

Rb and Sr concentrations, measured in ppm, were determined for nine samples on a Phillips 1410 X-ray spectrometer located at Ks. Geol. Survey, with an Mo target and LiF analyzing crystal. Instrumental settings were: 50 kv, 50 ma, baseline = 2.1, and window = 2.1. Rb was measured at 2θ = 38.00°, and Sr was measured at 2θ = 30.00°. Sample concentrations were determined by camparison to a calibration curve of counts per second versus concentration determined from five U. S. Geological Survey standard rocks (G-2, W-1, GSP-1, AGV-1, and BCR-1). Values obtained from the standard rock samples are compared to the recommended values of Flanagan (1973) in Table 2. Estimated maximum deviations of X-ray fluorescent data are: Rb and Sr = $\pm$ 5 percent.

INSTRUMENTAL NEUTRON ACTIVATION ANALYSIS

Concentrations of the elements Ba, Ce, Co, Cr, Cs, Eu, Fe, Hf, La, Lu, Na, Sb, Sc, Se, Sm, Ta, Tb, Th, U, Yb, and Zn were determined for ten samples and three U.S. Geological Survey standard rocks by instrumental neutron activation analysis (INAA), using a method developed by Gordon et al. (1968) and Jacobs et al. (1977), and modified by Koch (1978) and Kilbane (1978). Samples were irradiated in the Kansas State University Triga Mark II reactor and radioassayed on a 25 cm^3 Ge (Li) detector coupled with a magnetic tape interface (model 8531 A). A computer program adapted from Jacobs et al. (1977) was then used to determine standard-to-sample peak-height ratios for the desired elements. Several U.S. Geological Survey standard rocks and a Canadian reference soil (SO-4) were analyzed during the study. Close agreement with the published results of Flanagan(1973) was obtained. Table 2 presents a comparison of the results. Estimated maximum deviations for INAA data are: Co, Hf, Ce, La, and Sm = $\pm$ 5 percent; Ba, Fe, Na, Sb, Sc, Th, Eu, Lu, Nd, and Yb = $\pm$ 10 percent; Cr, Ta, and Tb = $\pm$ 15 percent; Cs and Rb = $\pm$ 20 percent; and U, Zn, and Se > $\pm$ 25 percent.

TABLE 2. Trace-element content (ppm, unless noted otherwise) of U.S. Geological Survey standard rocks.

STANDARD	AGV-1	AGV-1		BCR-1	BCR-1		W-1	W-1	
	Andesite			Basalt			Diabase		
REFERENCE	(1)	(2)		(1)	(2)		(1)	(2)	
ELEMENT (3)									
Ba	1100	1210	R	599	675	R	88	160	R
Ce	59	63	A	47.6	53.3	R	23	23	M
Co	13.8	14.1	A	35	38	M	52	47	A
Cr	11.2	12.2	A	14.1	17.6	A	164	114	A
Cs	1.0	1.4	M	0.6	0.9	A	0.7	0.9	R
Eu	1.4	1.7	A	1.6	1.9	R	1.2	1.1	R
Fe (4)	6.16	6.76	R	12.68	13.40	R	13.02	11.09	R
Hf	5.1	5.2	A	4.7	4.7	A	3.2	2.7	A
La	34	35	M	24	26	A	13	9.8	A
Lu	0.25	0.28	A	0.51	0.55	R	0.41	0.35	A
Na (4)	4.02	4.26	R	3.05	3.27	R	2.58	2.15	R
Nd	38	39	A	30	29	R	18	15	R
Rb	81	67	R	120	47	R	25	21	R
Sb	4.5	4.5	A	0.6	0.7	A	---	1.0	R
Sc	10.7	13.4	A	31	33	M	41	35	A
Se	0.8	0.1	A	0.3	0.1	M	0.2	0.1	M
Sm	5.4	5.9	A	6.2	6.6	A	3.7	3.6	A
Ta	1.1	0.9	R	0.8	0.9	R	0.5	0.5	R
Tb	0.48	0.70	R	0.79	1.0	R	0.65	0.71	R
Th	6.90	6.41	R	6.6	6.0	R	3.18	2.42	R
U	1.8	1.9	A	1.0	1.7	A	0.2	0.6	A
Yb	1.5	1.7	A	3.16	3.36	A	2.4	2.1	R
Zn	60	84	R	74	120	R	120	86	R

(1) Combined results of this study and Reitz (1980) (2) Flanagan (1973)
(3) Elemental content determined by instrumental neutron activation.
(4) Oxides expressed as weight percent Fe_2O_3 and Na_2O.
U.S. Geological Survey values; R = recommended, A = average, M = magnitude.

R E S U L T S

PETROGRAPHY

Petrographic details of thin sections of samples analyzed for this investigation are shown in Table 3. Normative rock types represented include alkali-olivine basalt, silicic-alkalic basalt, basaltic andesite, crystal tuff, and rhyolitic ignimbrite.

Basalt samples vary from holocrystalline to hypocrystalline, and they are porphyritic-aphanitic to medium-grained phaneritic. Textures displayed include intergranular, intersertal, subophitic, and ophitic. Most samples show ferromagnesian mineral grains rimmed by iddingsite with a few completely altered. Amygdaloidal carbonate is present in one vesicular sample. Common phenocryst minerals are olivine and augite with less common plagioclase and hornblende. Opaque minerals are restricted to the groundmass with plagioclase microlites, augite, and in a few samples apatite or glass.

Crystal tuffs are hypocrystalline and porphyritic. Less silicic samples are not welded, though silicic samples are eutaxitic. Common phenocryst minerals include quartz, sanidine, opaque minerals and augite in less silicic samples. In silicic samples, phenocryst minerals are less common, and ferromagnesian minerals are completely altered to iron oxides. Mesostatic glass shards are slightly altered to clay minerals.

ILLEGIBLE

THE FOLLOWING DOCUMENT (S) IS ILLEGIBLE DUE TO THE PRINTING ON THE ORIGINAL BEING CUT OFF

ILLEGIBLE

TABLE 3. Petrographic details of samples for which analytical data have been obtained. Abbreviations for localities: 1) BB=Black Butte, 2) WB=Wolverine Basin, 3) WH-LM=Windy Hill-Lion Mountain, and 4) DM=Divide Mountain. Abbreviations for authors: 1) BG=Burke-Griffin (1978), 2) E=Eichen (1979), and 3) SR=Spaide-Reitz (this study).

SPECIMEN Locality Author	ROCK TYPE Rock Name Normative Classification	PHENOCRYSTS	ALTERATION	GROUNDMASS	TEXTURE/COMMENTS
BB-9-77 BB BG	Medium-grained Basalt Alkali-olivine Basalt		Fe-Mg min. rimmed by Idd	Pl(15-50 pct., <2.5 mm, An_{50-70}), Ol(10-35 pct., 1-3 mm), Cpx(5-30 pct., <2 mm), Op min.(15 pct, <1 mm), Ap(tr,<0.5 mm)	Holocrystalline, Equigranular, Intergranula Zoned Pl, Twinned Ol
P-5-77 WB E	Porphyritic Basalt Silicic-alkalic Basalt	Ol(15 pct., <1.5 mm)	Very fresh	Pl(60-70 pct., <1 mm, An_{50-70}), Cpx(15-20 pct., <0.5 mm), Op min.(<5 pct., <0.5 mm)	Holocrystalline, Inequigranular, Intergranular
SR-24-79 DM SR	Porphyritic Basalt Silicic-alkalic Basalt	Opx(<5 pct., <1 mm), Ves(<5 pct., <2 mm), Ol pseud(<10 pct., <1.5 mm)	Fe-Mg min. altered to Idd, myg. car.	Pl(<70 pct., <0.02 mm, An_{50-70}), Op min.(<10 pct., <0.02 mm), Gl(<5 pct., <1 mm)	Hypocrystalline, Inequigranular, Intersertal, Vesicular
BB-26B-77 BB BG	Medium-grained Olivine Diabase Silicic-alkalic Basalt	Pl(30-40 pct., <2 cm, An_{50-70}) Ol(5 pct., <5 mm) Lb(tr,-15 pct., <2 cm)	Ferromagnesians rimmed by Idd, see car	Cpx(30-40,<2 mm) Op min. (5-10 pct., <1 mm)	Holocrystalline, Equigranular, Intergranula to Ophitic
SR-14B-79 WH-LM SR	Porphyritic Basalt Silicic-alkalic Basalt	Cpx(20 pct., <1.5 mm)	Fe-Mg min. rimmed by Idd	Pl(55%,<0.4 mm, An_{50-70}), Cpx(15%, <0.4 mm), Op min. (5 pct., <0.04 mm)	Holocrystalline, Inequigranular, Intergranular
P-36A-77 WB E	Porphyritic Basalt Silicic-alkalic Basalt	Ol(15 pct., <1.5 mm)	Fe-Mg min. rimmed by Idd	Pl(60-70 pct.,<1 mm, An_{50-70}), Cpx(15-20 pct., <0.5 mm), Op min. (<5 pct., <0.5 mm)	Holocrystalline, Inequigranular, Intergranular

TABLE 3. Petrographic details of samples for which analytical data have been obtained. Abbreviations for localities: 1) BB=Black Butte, 2) WB=Wolverine Basin, 3) WH-LM=Windy Hill-Lion Mountain, and 4) DM=Divide Mountain. Abbreviations for authors: 1) BG=Burke-Griffin (1978), 2) E=Eichen (1979), and 3) SR=Spaide-Reitz (this study).

SPECIMEN Locality Author	ROCK TYPE Rock Name Normative Classification	PHENOCRYSTS	ALTERATION	GROUNDMASS	TEXTURE/COMMENTS
BB-9-77 BB BG	Medium-grained Basalt Alkali-olivine Basalt		Fe-Mg min. rimmed by Idd	Pl(15-50 pct., <2.5 mm, An_{50-70}), Ol(10-35 pct., 1-3 mm), Cpx(5-30 pct., <2 mm), Op min.(15 pct, <1 mm), Ap(tr,<0.5 mm)	Holocrystalline, Equigranular, Intergranular Zoned Pl, Twinned Ol
P-5-77 WB E	Porphyritic Basalt Silicic-alkalic Basalt	Ol(15 pct., <1.5 mm)	Very fresh	Pl(60-70 pct., <1 mm, An_{50-70}), Cpx(15-20 pct., <0.5 mm), Op min.(<5 pct., <0.5 mm)	Holocrystalline, Inequigranular, Intergranular
SR-24-79 DM SR	Porphyritic Basalt Silicic-alkalic Basalt	Opx(<5 pct., <1 mm), Ves(<5 pct., <2 mm), Ol pseud(<10 pct., <1.5 mm)	Fe-Mg min. altered to Idd, myg. car.	Pl(<70 pct., <0.02 mm, An_{50-70}), Op min.(<10 pct., <0.02 mm), Gl(<5 pct., <1 mm)	Hypocrystalline, Inequigranular, Intersertal, Vesicular
BB-26B-77 BB BG	Medium-grained Olivine Diabase Silicic-alkalic Basalt	Pl(30-40 pct., <2 cm, An_{50-70}) Ol(5 pct., <5 mm) Lb(tr,-15 pct., <2 cm)	Ferromagnesians rimmed by Idd, see car	Cpx(30-40,<2 mm) Op min. (5-10 pct., <1 mm)	Holocrystalline, Equigranular, Intergranular to Ophitic
SR-14B-79 WH-LM SR	Porphyritic Basalt Silicic-alkalic Basalt	Cpx(20 pct., <1.5 mm)	Fe-Mg min. rimmed by Idd	Pl(55%,<0.4 mm, An_{50-70}), Cpx(15%, <0.4 mm), Op min. (5 pct., <0.04 mm)	Holocrystalline, Inequigranular, Intergranular
P-36A-77 WB E	Porphyritic Basalt Silicic-alkalic Basalt	Ol(15 pct., <1.5 mm)	Fe-Mg min. rimmed by Idd	Pl(60-70 pct.,<1 mm, An_{50-70}), Cpx(15-20 pct., <0.5 mm), Op min. (<5 pct., <0.5 mm)	Holocrystalline, Inequigranular, Intergranular

TABLE 3 (Cont.) Petrographic details of samples for which analytical data have been obtained.

SPECIMEN Locality Author	ROCK TYPE Rock Name Normative Classification	PHENOCRYSTS	ALTERATION	GROUNDMASS	TEXTURE/COMMENTS
SR-15B-79 WH-LM SR	Fine-grained Olivine Diabase Silicic-alkalic Basalt		Fe-Mg min. altered to Idd, Sec. Cl min. and car.	Pl(60 pct., <3 mm, An_{40-60}), Cpx(25 pct., <2 mm), Ol(10 pct., <1 mm) Op min.(<5 pct., <0.5 mm) Ap(tr, <0.5 mm)	Holocrystalline, Equigranular, Intergranular to Subophitic
SR-19-79 WH-LM SR	Basanitoid Porphyry Silicic-alkalic Basalt	Ol(25 pct., <2 mm), Cpx(5 pct., 1-2 mm) Pl(tr, 1-2 mm An_{50-70})	Fe-Mg min. altered to Idd	Pl(50 pct., <0.1 mm, An_{40-60}), Gl(<20 pct.), Cpx(<5 pct., <0.5 mm) Op min.(<5 pct., <0.5 mm)	Hypocrystalline, Inequigranular, Intersertal
P-62B-78 WB E	Fine-grained Olivine Diabase Basaltic Andesite		Ol Corroded, Cpx altered to Idd	Pl(60 pct., <3 mm, An_{40-60}), Cpx(25 pct., <2 mm), Ol(10 pct., <1 mm) Op min. (<5 pct., <0.5 mm) Ap(tr, <0.5 mm)	Holocrystalline, Inequigranular, intergranular
SR-22B-79 WH-LM SR	Porphyritic Andesite Basaltic Andesite	Pl(<5%, <4 mm), An_{40-60}, Cpx (tr, <2 mm), Qtz(tr, <1 mm)	Fresh	Pl(60 pct, 0.1 mm, An_{30-50}), Gl(20 pct.) Cpx(10 pct., 0.2 mm), Op min.(5 pct., 0.1 mm)	Hypocrystalline, Inequigranular, Intersertal/Pl resorbed
SR-1C-79 WH-LM SR	Crystal Tuff Andesitic Crystal Tuff	San(<5 pct., <0.4 mm), Qtz(tr <0.4 mm), Fe-Mg min. (tr, <0.4 mm)	Gl altering to Cl min., oxidized Fe-Mg min.	Cl min.(80 pct), Gl shds (<10%, 0.005 mm)	Hypocrystalline, Inequigranular/ no welding
P-13F-77 WB E	Crystal Tuff Dacitic Crystal Tuff	Qtz(tr, <.4 mm) San(tr, <.4 mm), Fe-Mg min.(tr, <.4 mm)	Gl altering to Cl min., oxidized Fe-Mg min.	Cl min.(95 pct), Gl shds (<5 pct., <4 mm)	Hypocrystalline, Inequigranular/no welding

TABLE 3 (cont.) Petrographic details of samples for which analytical data have been obtained.

SPECIMEN Locality Author	ROCK TYPE Rock Name Normative Classification	PHENOCRYSTS	ALTERATION	GROUNDMASS	TEXTURE/COMMENTS
SR-25A-79 DM SR	Welding Crystal Tuff Silicic Ignimbrite	San(<15 pct, <2 mm) Pl(<15 pct., <2 mm), Qz(<10 pct., <2 mm)	Ferromagnesians oxidized, Gl altering to clay	Cl min.(95 pct), Gl(5 pct., 4 mm)	Hypocrystalline, In-equigranular, Eutaxitic/ Pink-Purple
SR-25B-79 DM SR	Welded Crystal Tuff Silicic Ignimbrite	San(<15 pct., <2 mm) Pl(<15 pct., <2 mm), Qz (<10 pct., <2 mm)	Ferromagnesians oxidized, Gl al-tering to clay	Cl min.(95 pct.), Gl(<5 pct., <4 mm)	Hypocrystalline, In-equigranular, Eutaxitic/Pink-Purple
P-30B-79 WB SR	Welded Crystal Tuff Silicic Ignimbrite	San(<15 pct., <2 mm) Pl(<15 pct., <2 mm), Qz (<10 pct., <2 mm)	Ferromagnesians oxidized, Gl altering to clay	Cl min.(95 pct.), Gl(<5 pct., <4 mm)	Hypocrystalline, In-equigranular, Eutaxitic/ Purple

MAJOR ELEMENTS

INTRODUCTION

Major-element contents of representative samples of the volcanic rocks from each of the major outcrop areas are reported in Table 4. Analyzed rock types include the following: alkali-olivine basalt, BB-9-77; silicic-alkalic basalt, P-5-77, SR-24-79, BB-26B-77, SR-14B-79, P-36A-77, SR-15B-79, and SR-19-79; basaltic andesite, P-62B-78 and SR-22B-79; crystal tuff, SR-1C-79 and P-13F-77; and rhyolitic ignimbrite, SR-25A-79, SR-25B-79, and P-30B-77.

CLASSIFICATION

Based on a plot developed by Kuno (1966) in which the total weight percent of alkali content ($\Sigma Na_2O + K_2O$) is plotted against the weight percent of SiO_2, Gravelly Range mafic rocks are classified as an alkalic suite (fig. 14). MacDonald and Katsura have subdivided the field of alkali-olivine basalts on the same plot with a more restricted SiO_2 range, and this classification has been used by Lipman and Mehnert (1975) to classify alkali basalts from New Mexico. The Gravelly Range basalt are contained in the silicic-alkalic basalt field with one sample in the alkali-olivine basalt field and two samples in the basaltic andesite field (fig. 15). Gravelly Range tuff is classified by normative color index and by normative plagioclase composition. Crystal tuffs vary from andesitic to dacitic compositions, and the ignimbrites are rhyolitic in composition (Irving and Barager, 1971)(fig. 16).

TABLE 4. Major-element content (weight percent) and CIPW normative mineral composition (percent) of Gravelly Range volcanic rocks.

OXIDE(1)	Alkali-olivine Basalt BB-9-77	P-5-77	SR-24-79	BB-26B-77	Silicic-alkalic Basalts SR-14B-79	P-36A-77	SR-15B-79	SR-19-79
SiO_2	47.50	48.81	49.54	48.20	51.40	50.05	48.91	49.43
Al_2O_3	17.18	12.78	14.90	16.33	13.91	15.50	14.54	15.30
Fe_2O_3(T)	9.70	10.46	9.31	10.2%	8.94	9.71	10.56	7.92
MgO	6.39	9.74	4.39	4.05	7.69	5.98	4.35	6.79
CaO	10.35	8.59	10.68	9.71	7.61	8.41	8.76	7.39
Na_2O	3.30	2.90	2.95	3.31	3.23	3.46	3.92	6.19
K_2O	1.46	1.76	1.64	2.52	1.80	2.19	2.58	1.69
ignition	1.30	2.06	3.83	2.23	1.42	2.42	2.49	1.82
H_2O^-	0.22	0.24	0.83	0.72	0.90	0.41	0.18	0.40
TiO_2	1.76	1.98	1.40	2.65	1.79	1.51	2.24	1.52
MnO	0.15	0.13	0.16	0.14	0.11	0.12	0.11	0.13
TOTAL	99.31	99.45	99.63	100.07	98.80	99.76	98.64	99.06
FeO(2)	8.26	8.96	7.85	9.14	7.58	8.18	8.90	7.08
Fe_2O_3(2)	1.24	1.34	1.18	1.37	1.14	1.23	1.34	1.06
Q	---	---	---	---	---	---	---	---
C	---	---	---	---	---	---	---	---
Or	8.62	10.39	9.68	13.16	12.93	12.93	15.23	9.98
Ab	18.22	23.55	24.94	20.50	27.48	26.44	21.55	23.58
An	27.28	16.69	22.55	22.78	16.89	20.28	14.45	8.96
Ne	5.79	0.48	---	4.38	---	1.52	6.28	15.58
Di	19.65	20.95	25.16	21.06	16.88	17.56	24.02	22.48
Hy	---	---	2.41	---	7.29	---	---	---
Ol	12.97	19.09	5.48	8.21	10.03	13.14	7.83	11.47
Mt	1.80	1.95	1.71	1.99	1.66	1.79	1.95	1.54
Il	3.35	3.77	2.66	5.04	3.40	2.87	4.26	2.89
DI(3)	32.54	34.42	34.62	38.04	40.40	40.89	43.06	49.14

(1) Elemental content determined by spectrophotometry and recalculated as weight percent oxide.
(2) Estimated FeO and Fe_2O_3 weight percent from FeO/Fe_2O_3 = 0.15. (Brooks, 1976), except silicic samples are calculated as outlined by Anderson, unpublished data (1978).
(3) DI = Differentiation Index
(T) Total Fe calculated as Fe_2O_3

TABLE 4 (cont.). Major-element content (weight percent) and CIPW normative mineral composition (percent) of Gravelly Range volcanic rocks.

	Basaltic Andesites		Andesitic-Dacitic Crystal Tuff		Silicic Ignimbrites		
	P-62B-78	SR-22B-79	SR-1C-79	P-13F-77	SR-25A-79	SR-25B-79	P-30B-77
SiO_2	52.55	54.68	57.20	69.13	71.18	73.80	72.47
Al_2O_3	16.22	17.16	12.74	11.84	12.87	12.83	12.41
Fe_2O_3(T)	9.68	8.02	4.17	4.02	1.76	1.88	1.98
MgO	4.81	2.07	3.29	0.89	0.20	0.25	0.02
CaO	8.41	6.03	2.40	2.08	1.10	1.17	0.41
Na_2O	4.05	4.40	1.28	2.15	3.42	3.48	3.75
K_2O	2.58	3.67	2.25	2.84	5.40	5.27	5.59
ignition	2.72	1.19	5.93	2.33	0.55	0.52	0.34
H_2O^-	0.59	0.47	8.20	2.39	0.14	0.18	0.69
TiO_2	0.11	0.12	0.54	0.52	0.12	0.13	0.17
MnO	0.11	0.12	0.12	0.03	0.03	0.02	0.03
TOTAL	102.61	99.39	98.12	98.22	96.77	99.53	97.86
FeO(2)	8.16	7.55	3.51	2.64	0.96	1011	1.08
Fe_2O_3(2)	1.22	1.13	0.53	1.04	0.66	0.76	0.70
Q	---	---	28.63	39.13	27.90	30.24	29.39
C	---	---	3.84	1.63	---	---	---
Or	15.23	22.02	13.28	16.64	31.87	31.10	31.10
Ab	28.43	35.49	10.82	17.33	18.58	29.42	31.20
An	18.44	15.33	11.90	10.31	3.99	3.82	1.73
Ne	3.15	1.66	---	---	---	---	---
Di	19.21	12.34	---	---	1.24	1.68	0.27
Hy	---	---	13.50	5.40	1.14	1.22	1.04
Ol	10.50	7.06	---	---	---	---	---
Mt	1.77	1.64	0.77	1.51	0.96	1.10	1.02
Il	2.70	3.01	1.03	0.99	---	---	0.32
DI	46.81	59.16	52.73	73.10	88.35	90.76	91.69

(1) Elemental content determined by spectrophotometry and recalculated as weight percent oxide,
(2) Estimated FeO and Fe_2O_3 weight percent from $FeO/Fe_2O_3 = 0.15$. (Brooks, 1976), except silicic samples are calculated as outlined by Anderson, unpublished data (1978).
(3) DI = Differentiation Index
(T) Total Fe calculated as Fe_2O_3

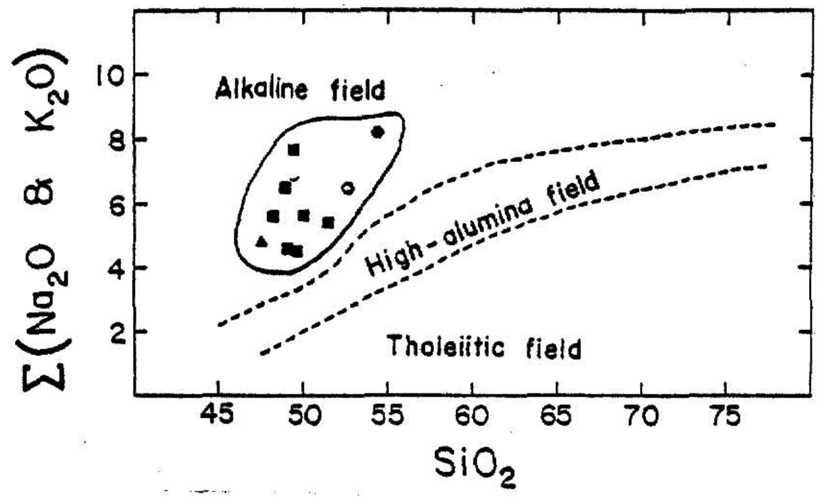

Figure 14. Chemical classification of Gravelly range basaltic rocks based on alkali-silica variations and field boundaries (Kuno, 1966). Alkali-olivine basalt (▲); Silicic-alkalic basalt (■); Basaltic andesite (●).

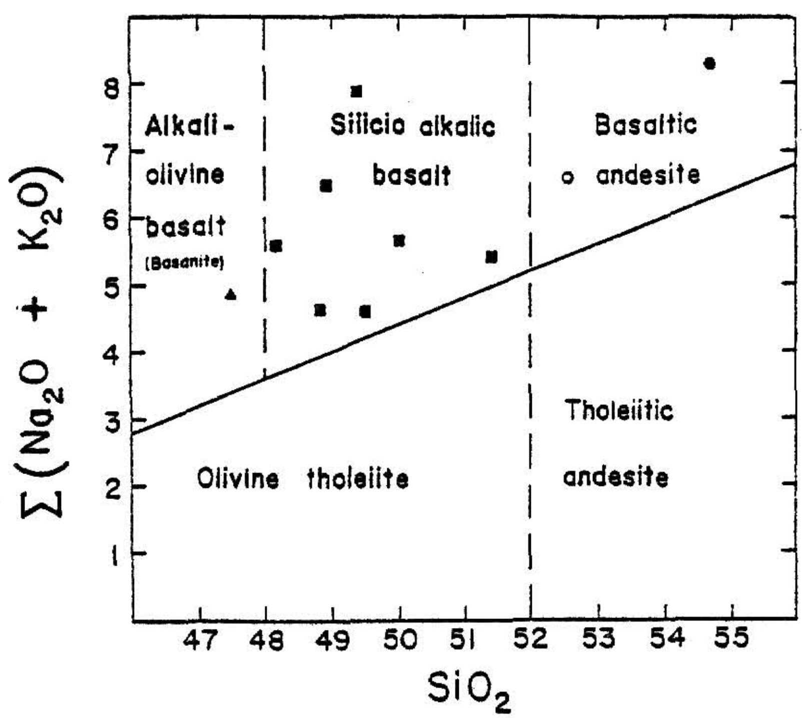

Figure 15. Chemical classification of Gravelly Range basalts based on alkali-silica variations and field boundaries between Hawaiian alkalic and tholeiitic basalts (MacDonald and Katsura, 1964). Alkali-olivine basalt (▲); Silicic-alkalic basalt (■); and basaltic andesite (●).

VARIATION DIAGRAMS

Normative nepheline is present in all mafic samples with the exception of two silicic-alkalic basalts (SR-24-79 and SR-14B-79). Crystal tuff and welded tuff samples (P-13F-77, SR-1C-79; and P-30B-77, SR-25A-79, and SR-25B-79) contain normative quartz and hypersthene. Differentiation indices increase in the order: alkali-olivine basalt < silicic-alkalic basalt, basaltic andesite, and andesitic-dacitic crystal tuff < rhyolitic ignimbrite

In terms of alumina saturation, the Gravelly Range volcanic rocks are peraluminous in the alkali-olivine basalt, basaltic andesite, and rhyolitic ignimbrite. Silicic-alkalic basalt ranges from metaluminous to peraluminous.

By plotting the weight percent oxides of ($\Sigma Na_2O + K_2O$) and CaO versus SiO_2 on the same graph and determining their intersection, the alkali-lime differentiation index is obtained. When basaltic through dacitic rocks are plotted on this type of diagram, the intersection falls in the alkali-calcic range (SiO_2 = 54.5).

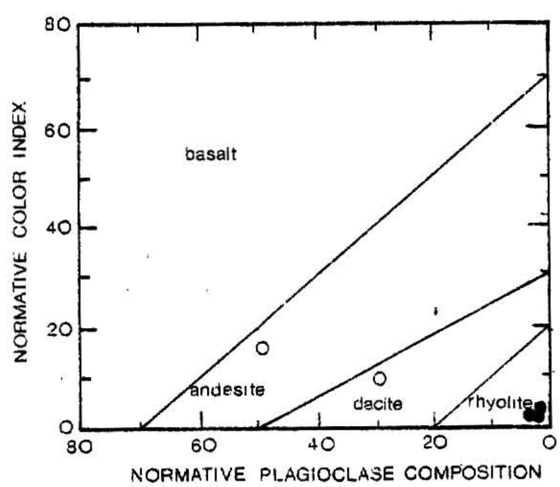

Figure 16. Chemical classification of Gravelly Range tuff based on the normative color index versus the normative plagioclase composition and field boundaries between basalt, andesite, dacite, and rhyolite (Irving and Barager, 1971). Crystal tuff (O) and ignimbrite (●).

The normative mineralogy and differentiation index (normative Q + Or + Ab + Ne + Le + Kl) of analyzed rocks were calculated (Table 4). Silicic sample FeO concentrations were calculated by using the equation suggested by Anderson (unpublished data, 1978):

$Fe_2O_3/(Fe_2O_3 + FeO) = 0.0281$ (weight percent $K_2O + Na_2O$) + 0.148.

Basaltic sample FeO concentrations were calculated using the equation suggested by Brooks (1976):

$$Fe_2O_3/(Fe_2O_3 + FeO) = 0.15.$$

Major-element variation diagrams for volcanic rocks from the Gravelly Range are obtained from the data of this study (Table 4; figs. 17 to 20). Plots of the weight percent of the major-element oxides versus the DI show a discontinuous trend from mafic to silicic rocks (fig. 17). SiO_2, Na_2O and K_2O increase with increasing DI whereas CaO, MgO and Fe_2O_3(T) (Fe_2O_3(T) denotes total Fe as Fe_2O_3) decrease with increasing DI. Al_2O_3 remains almost constant.

Plots of the ratios $CaO/(CaO + Na_2O)$ and Fe_2O_3 (T)/ Fe_2O_3 (T) + MgO versus Al_2O_3 (fig. 18) seperate Gravelly Range rocks into three groups: (1) the alkali basalt, (2) the crystal tuff, and (3) the rhyolitic ignimbrite. An increase in CaO with Al_2O_3 is suggested for the silicic samples whereas a slight decrease in CaO with Al_2O_3 is suggested for the mafic samples. Silicic samples decrease in Fe_2O_3 (T) as Al_2O_3 increases.

The alkali-basalt group and the crystal tuff group show a similar increase in alkali content (fig. 19). Rhyolitic tuffs show extremely high alkali content and low MgO concentrations. A gradual increase in K_2O relative to Na_2O within the mafic samples is observed with one exception, a silicic-alkalic basalt (SR-19-79) that is considerably higher in Na_2O content than expected for the trend (fig. 20). Seperate, though similar, trends are also displayed by the silicic rocks.

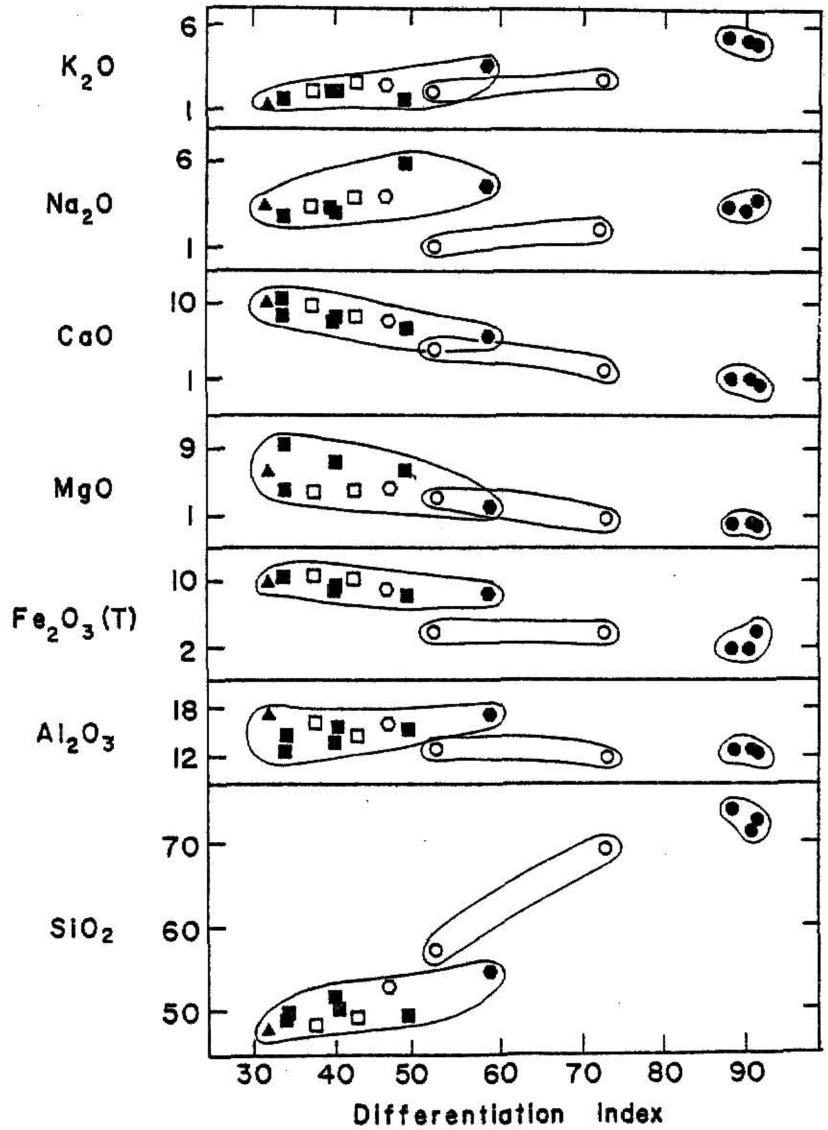

Figure 17. Major-element variation diagram for Gravelly Range volcanic rocks. Weight percent oxide versus differentiation index. Alkali-olivine basalt: aphanitic (▲); Silicic-alkalic basalt: aphanitic (■), phaneritic (□); Basaltic andesite: aphanitic (⬢), phaneritic (⬡); Crystal tuff: aphanitic (○); Rhyolitic ignimbrite: aphanitic (●).

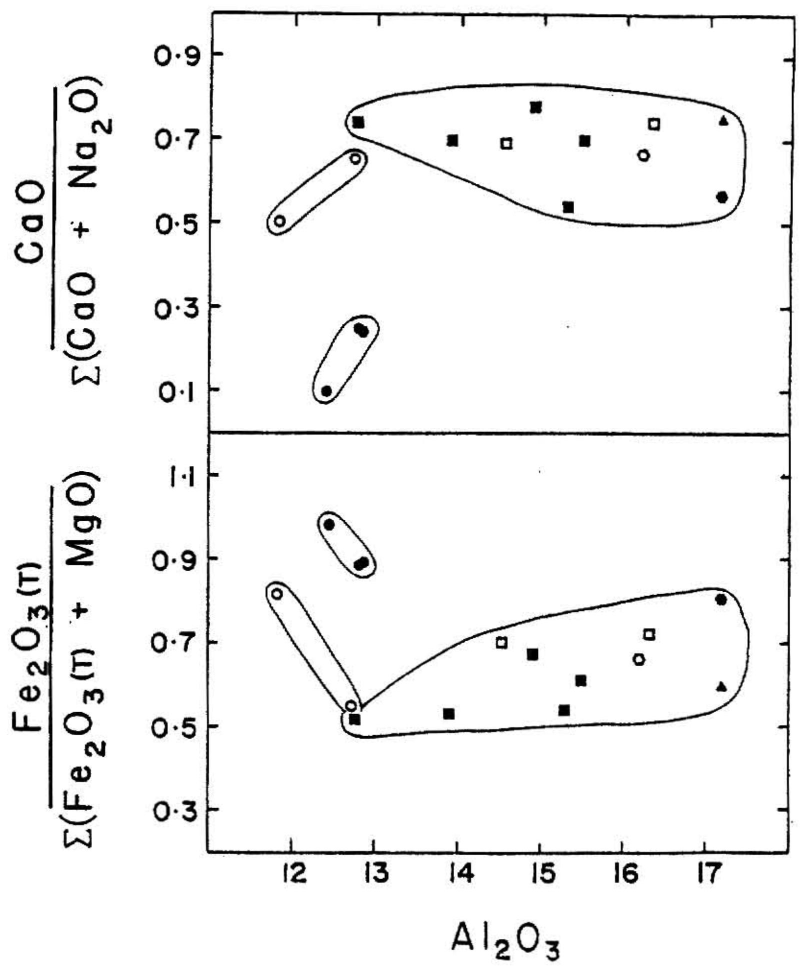

Figure 18. Major-element variation diagram for Gravelly Range volcanic rocks. $CaO/(CaO + Na_2O)$ ratio and $Fe_2O_3(T)/(Fe_2O_3(T) + MgO)$ ratio versus Al_2O_3 (weight percent). (See fig. 17 for explanation of symbols. '(T)' of the Fe_2O_3 denotes total iron as Fe_2O_3).

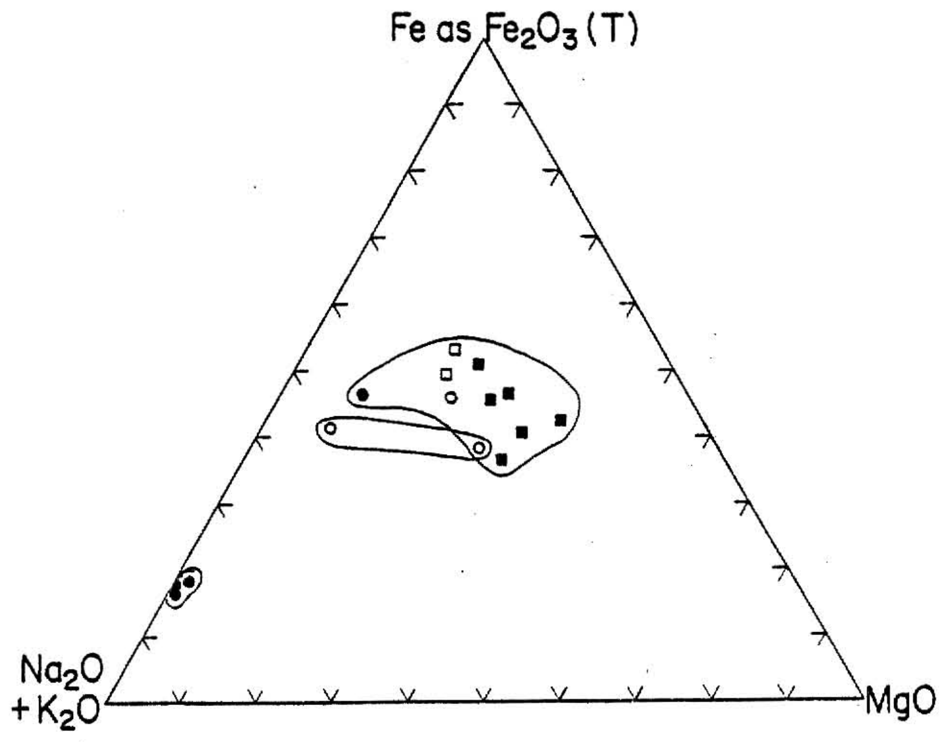

Figure 19. Major-element variation diagram for Gravelly Range volcanic rocks. AFM diagram (see fig. 17 for explanation of symbols).

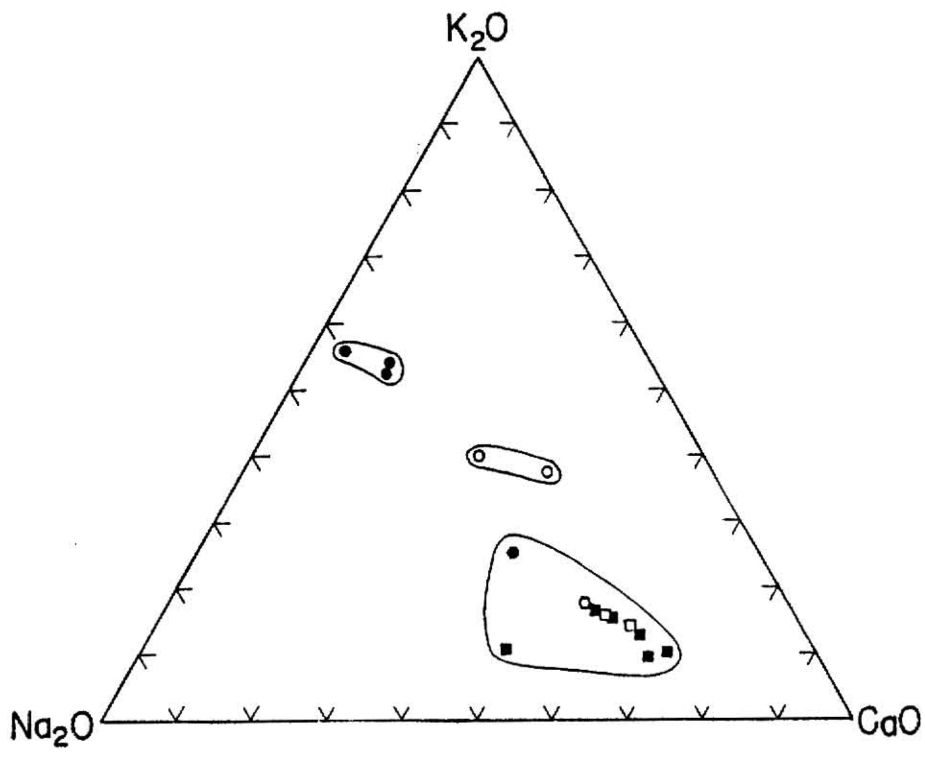

Figure 20. Major-element variation diagram for Gravelly Range volcanic rocks. CaO-K_2O-Na_2O diagram (see fig. 17 for explanation of symbols).

TRACE ELEMENTS

INTRODUCTION

Trace-element contents of representative samples of each of the volcanic rock units are reported in Table 5. REE (rare-earth element) contents not analyzed are estimated from chondrite-normalized curves (Haskin et al., 1968) to calculate ΣREE (total rare-earth element) contents. Ratios of La/Lu and Eu/Sm are calculated from their measured concentrations in each rock. The ratio Eu/Eu* is calculated from chondrite-normalized values where Eu is from the measured Eu content and Eu* is is extrapolated from Sm and Tb contents (assuming no fractionation of Eu). Both Eu/Sm and Eu/Eu* indicate depletion or enrichment of Eu relative to the other REE. Accounting for experimental error in this study, an Eu/Eu* value greater than 1.2 is considered a positive Eu anomaly, and an Eu/Eu* value less than 0.8 is considered a negative Eu anomaly. Analyzed rock types include alkali-olivine basalt (BB-9-77); silicic-alkalic basalt (P-5-77, BB-26B-77, SR-14B-79, SR-24-79, P-36A-77, SR-15B-79, and SR-19-79); basaltic andesite (SR-22B-79, and P-62B-78); andesitic-dacitic crystal tuff (P-13F-77 and SR-1C-79); and rhyolitic ignimbrite (SR-25A-79, SR-25B-79 and P-30B-79). Only the elemental contents of Ba, Rb, and Sr were determined for SR-24-79, P-36A-77, SR-15B-79, P-62B-78, and SR-1C-79.

TABLE 5. Trace-element contents (ppm) of Gravelly Range volcanic rocks.

Element(1)	Alkali-olivine Basalt	Silicic-alkalic Basalts						
	BB-9-77	P-5-77	SR-24-79	BB-26B-77	SR14B-79	P-36A-77	SR-15B-79	SR-19-79
Ba	788	862	---	1144	1019	---	---	1705
Co	41.6	46.7	---	23.6	36.6	---	---	27.8
Cr	118	377	---	14.2	262	---	---	201
Cs	0.297	0.835	---	0.316	0.450	---	---	0.932
Hf	3.75	4.45	---	5.49	4.35	---	---	4.40
Rb	42.7	44.4	49.0	58.7	62.3	66.0	69.0	51.9
Sb	---	---	---	---	---	---	---	---
Sc	28.6	19.9	---	27.1	17.0	---	---	15.7
Se	0.333	---	---	0.344	0.378	---	---	0.360
Sr	632	684	741	1090	564	125	771	1403
Ta	3.72	3.28	---	5.52	3.56	---	---	3.56
Th	5.06	4.87	---	7.53	6.38	---	---	9.34
U	0.496	0.834	---	1.56	1.30	---	---	1.69
Zn	35.2	163	---	54.9	98.2	---	---	1.19
La	30.8	33.8	---	45.3	36.6	---	---	88.1
Ce	58.6	67.8	---	85.5	65.2	---	---	154
Sm	5.29	6.61	---	7.72	5.88	---	---	8.58
Eu	1.73	1.75	---	2.19	1.78	---	---	2.28
Tb	0.58	0.82	---	0.90	1.29	---	---	0.670
Yb	1.76	1.57	---	3.56	1.44	---	---	1.57
Lu	0.38	0.23	---	0.53	0.237	---	---	0.268
ΣREE(2)	174	154.8	---	209	163.98	---	---	337.80
La/Lu	80.8	150	---	85.2	154	---	---	329
Eu/Sm	0.327	0.265	---	0.284	0.303	---	---	0.266
Eu/Eu*(2)	1.18	0.930	---	1.02	0.925	---	---	1.08

(1) Elemental contents determined by instrumental neutron activation except Rb and Sr which were determined by X-ray fluorescence.

(2) REE not analyzed were estimated from chondrite-normalized curves. Chondritic abundances taken from Haskin et al. (1968).

TABLE 5. (cont.) Trace-element contents (ppm) of Gravelly Range volcanic rocks.

	Basaltic Andesite		Andesitic-Dacitic Crystal Tuff				
	P-62B-78	SR-22B-79	Sr-1C-79	P-13F-77	SR-25A-79	SR-25B-79	P-30B-77
Ba	---	1675	---	625	550	676	748
Co	---	22.2	---	8.98	0.848	0.466	0.393
Cr	---	16.7	---	19.1	7.39	3.83	12.2
Cs	---	1.02	---	2.99	1.41	1.68	2.30
Hf	---	5.09	---	6.06	9.21	9.22	11.0
Rb	66.0	92.0	74	85.4	203	202	166
Sb	---	0.153	---	---	0.136	0.355	0.242
Sc	---	12.3	---	11.1	1.74	1.83	2.11
Se	---	0.417	---	0.836	1.12	0.880	1.47
Sr	710	936	314	212	16.0	11.6	10.8
Ta	---	3.91	---	1.08	4.45	4.53	4.63
Th	---	8.21	---	12.6	31.6	30.2	35.0
U	---	1.60	---	2.18	4.53	28.5	5.11
Zn	---	124	---	53.7	178	126	184
La	---	73.2	---	34.1	69.5	58.5	89.4
Ce	---	101	---	55.4	174	140	195
Sm	---	7.50	---	7.21	10.1	8.08	13.5
Eu	---	1.72	---	1.22	1.04	1.01	1.14
Tb	---	0.639	---	0.758	0.790	1.02	1.22
Yb	---	1.72	---	3.36	3.19	3.27	7.42
Lu	---	0.262	---	0.357	0.507	0.530	0.949
ΣREE*	---	247.90	---	150.45	346.89	290.81	423.20
La/Lu	---	279	---	95.5	137	110	94.2
Eu/Sm	---	0.229	---	0.169	0.103	0.125	0.084
Eu/Eu*	---	0.933	---	0.657	0.426	0.479	0.335

*REE not analyzed were estimated from chondritic-normalized curves. Chondritic abundances taken from Haskin et al. (1968).

RARE-EARTH ELEMENTS

Alkali-Basalt Suite

Chondrite-normalized plots of the REE contents of the mafic rocks from the alkali-basalt suite are illustrated in Figure 21. Similar moderate to highly fractionated REE patterns are displayed with La/Lu ratios from 81 to 329. Higher than average heavy rare-earth elements (HREE) are shown by one sample of silicic-alkalic basalt (BB-26B-77). Cross-over patterns are displayed by HREE, although these may be the result of experimental error for Tb. For mafic samples, the ΣREE ranges from 155 to 338.

Crystal Tuff

A chondrite-noramlized plot of the REE contents of the crystal tuff sample is shown in Figure 22. A moderately fractionated pattern, with a La/Lu ratio of 95.5, is accompanied by a negative Eu anomaly of Eu/Eu* = 0.657. For the crystal tuff, ΣREE is 150.

Rhyolitic Ignimbrite

Chondrite-normalized plots of the REE contents of the rhyolitic ignimbrite are indicated in Figure 22. Similar moderately fractionated REE patterns with La/Lu ratios from 94 to 137, and negative Eu anomalies with Eu/Eu* = 0.335 to 0.479 are the major characteristics of the REE For the rhyolitic ignimbrite, the ΣREE range from 291 to 423.

OTHER TRACE ELEMENTS

Alkali-Basalt Suite

Continuous, fairly colinear trends are observed in the relationship between trace-element contents and DI for the alkali basalt (fig. 23).

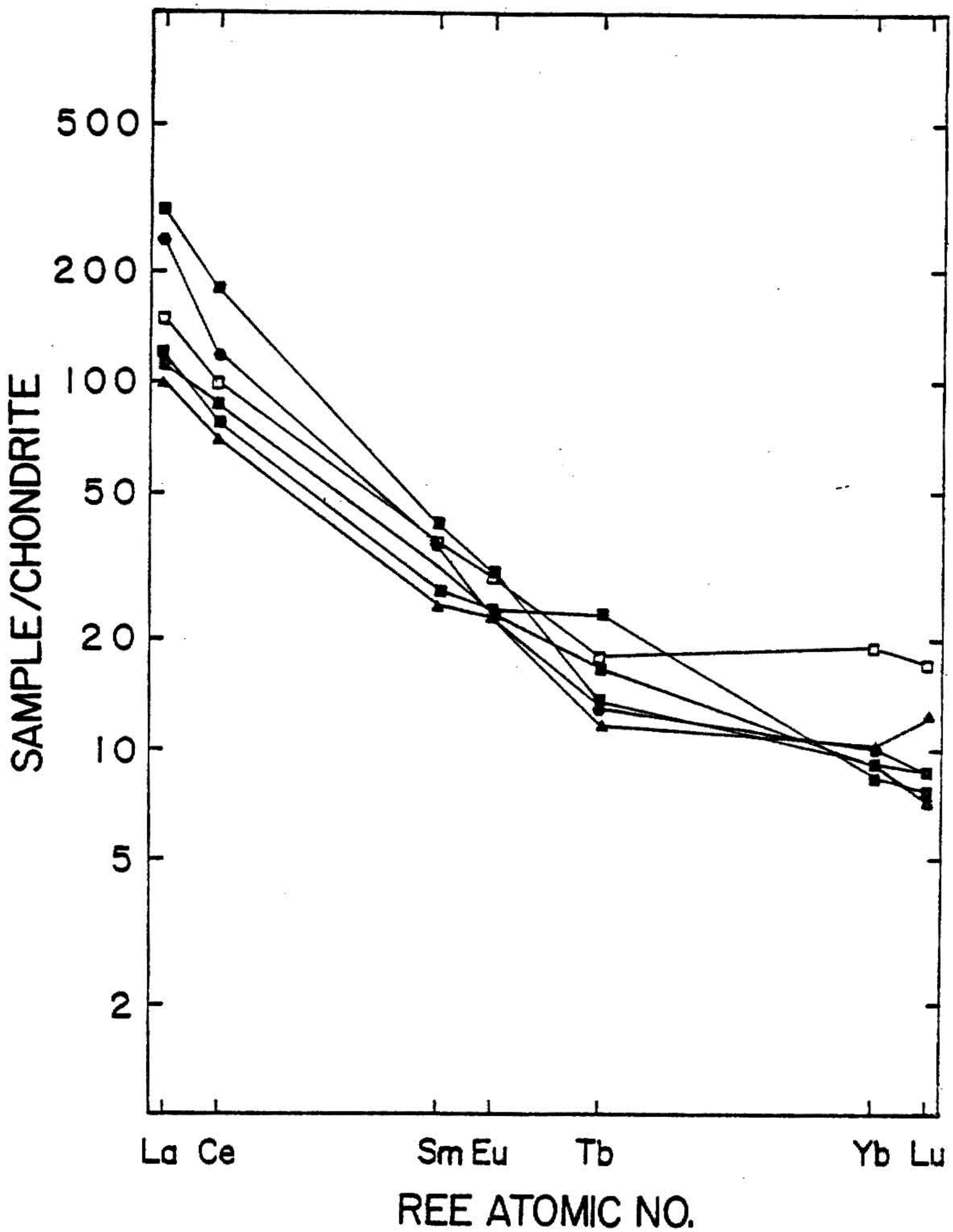

Figure 21. Chondrite-normalized REE plots for selected Gravelly Range basaltic rocks (see fig. 17 for explanation of symbols).

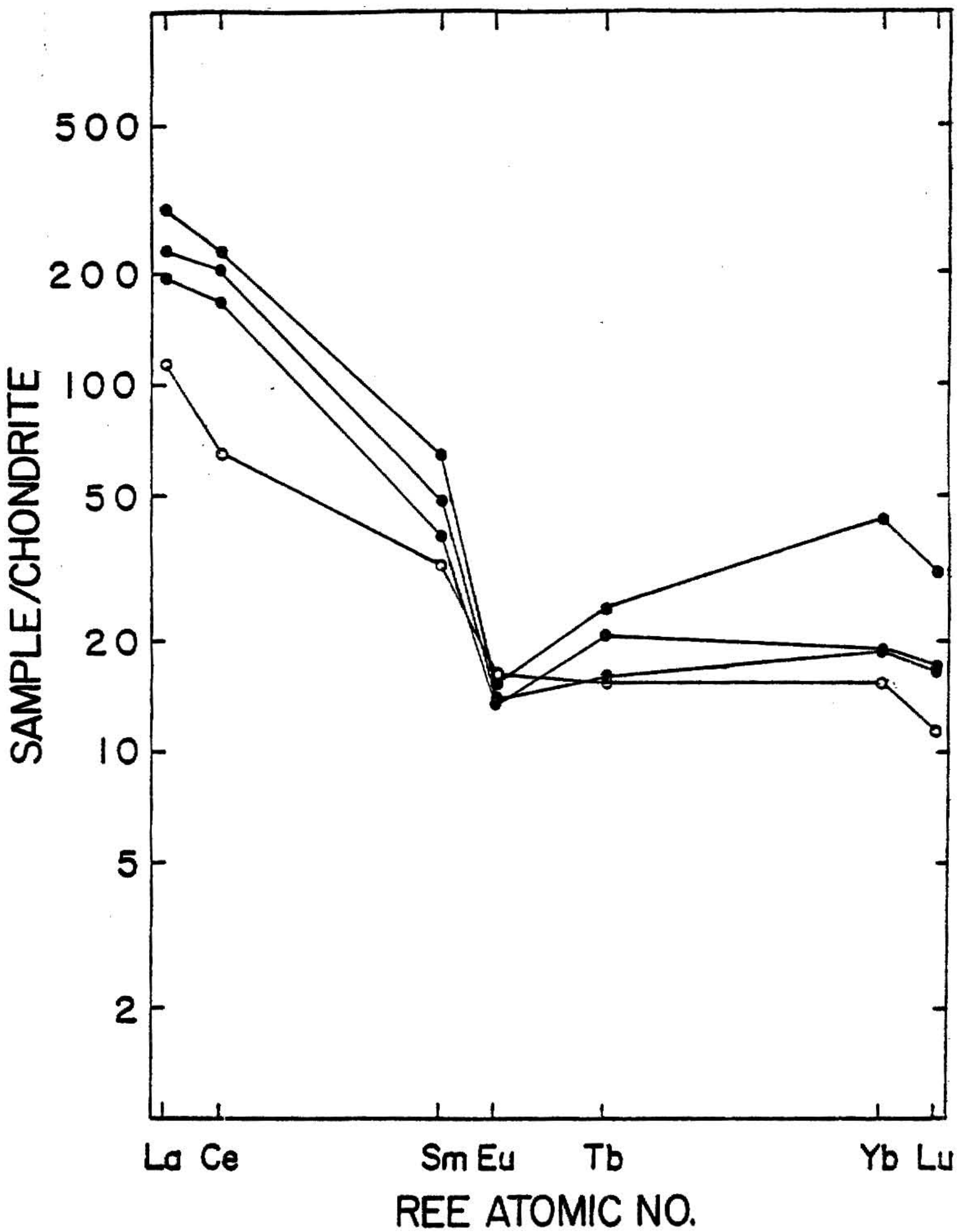

Figure 22. Chondrite-normalized REE plots for selected Gravelly Range andesitic-rhyolitic rocks (see fig. 17 for explanation of symbols).

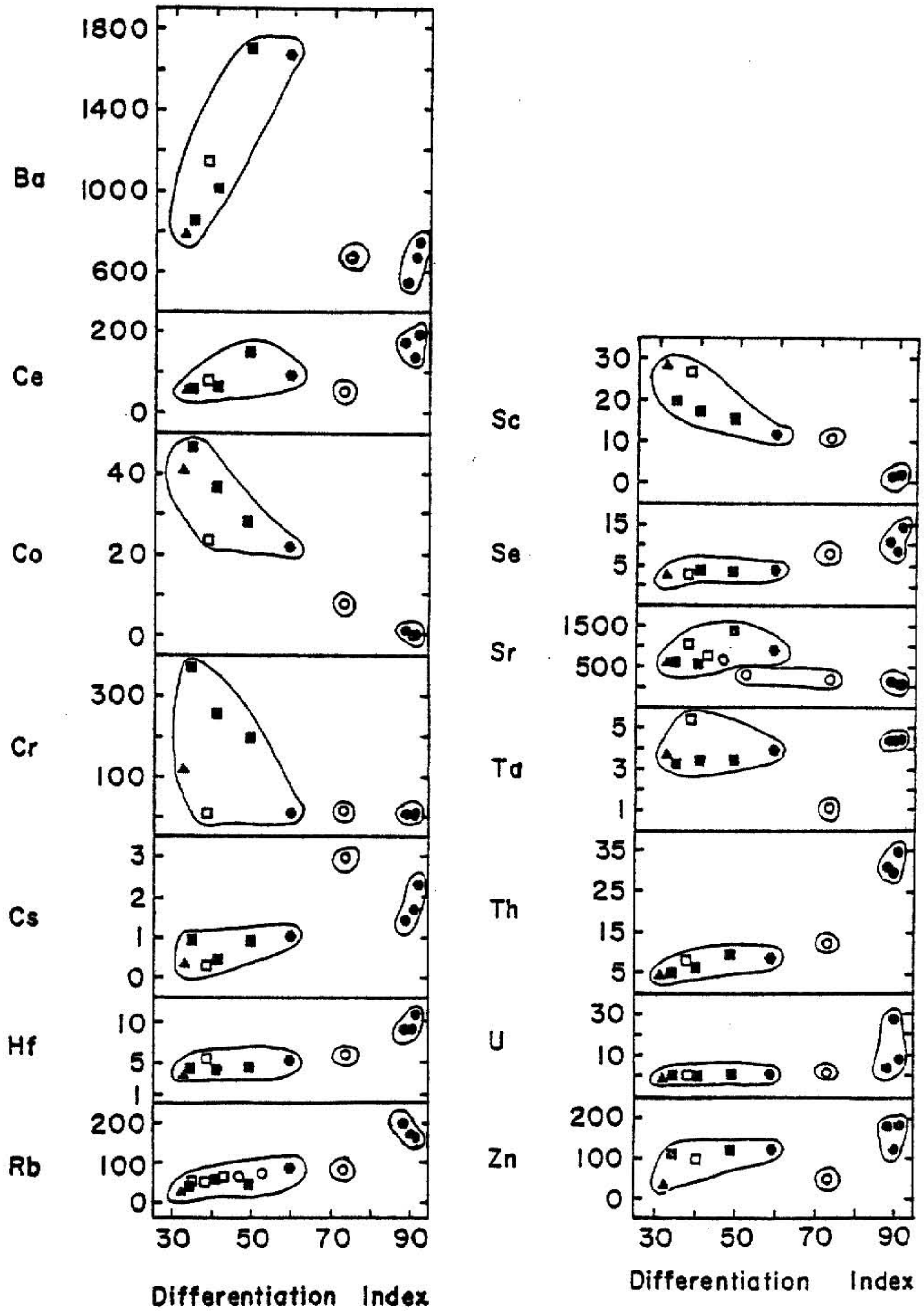

Figure 23. Trace-element variation diagrams for Gravelly Range volcanic rocks. Elemental content (ppm) versus differentiation index (see fig. 17 for explanation of symbols).

Incompatible trace elements (Ce, Ba, Cs, Hf, Rb, Se, Sr, Ta, Th, U, and Zn) increase as DI increases. Compatible trace elements (Co, Cr, and Sc) decrease as DI increases.

The alkali-basalt suite has smooth trends for trace elements in variation diagrams (figs. 24-26). Positive correlations are displayed by plots of Ba versus Sr (fig. 24), Rb versus K (fig. 25), and Ce versus K (fig. 26), whereas Rb versus Sr (fig. 24) shows a subhorizontal trend. however, one sample of silicic-alkalic basalt (SR-19-79) plots considerably off the trend on the Ce versus K plot (fig. 26).

Selected ratios of trace elements also indicate a relationship between the rocks of the alkali-basalt suite, although the trends are less linear (figs. 27 and 28). Poorly-defined negative correlations are displayed by plots of Sr/Ba versus K (fig. 27) and Sr/Ba versus Rb (fig. 28). A negative, near vertical correlation is displayed by a plot of K/Rb versus K (fig. 27).

Crystal Tuff

Trace-element contents versus the DI of the crystal tuff unit are plotted in Figure 23. For most compatible elements (Hf, Rb, Se, Th, and U), crystal tuff plots along the trend defined by the basaltic suite, and for some (Ba, Ce, Cs, Ta, and Zn) it plots off the trend. High mobility of the latter group of elements may account for the different trend in the crystal tuff. Ba shows much lower contents in the tuff than in the basaltic suite. Sr changes from an incompatible trend (basaltic suite) to a compatible trend for the crystal tuff. Other compatible-element trends for the basaltic rocks (Co, Cr, and Sc) remain compatible for the crystal tuff unit as salic mineral content increases.

Crystal tuff shows a continuation of the trends for most trace-element diagrams (figs. 25-26). Positive correlations are displayed by plots of Ba versus Sr (fig. 24) and Rb versus K (fig. 25) whereas a negative correlation is displayed by Rb versus Sr (fig. 24), and no correlation is displayed by K versus Ce(fig. 26).

A continuation of trends established by the basalt is shown by the

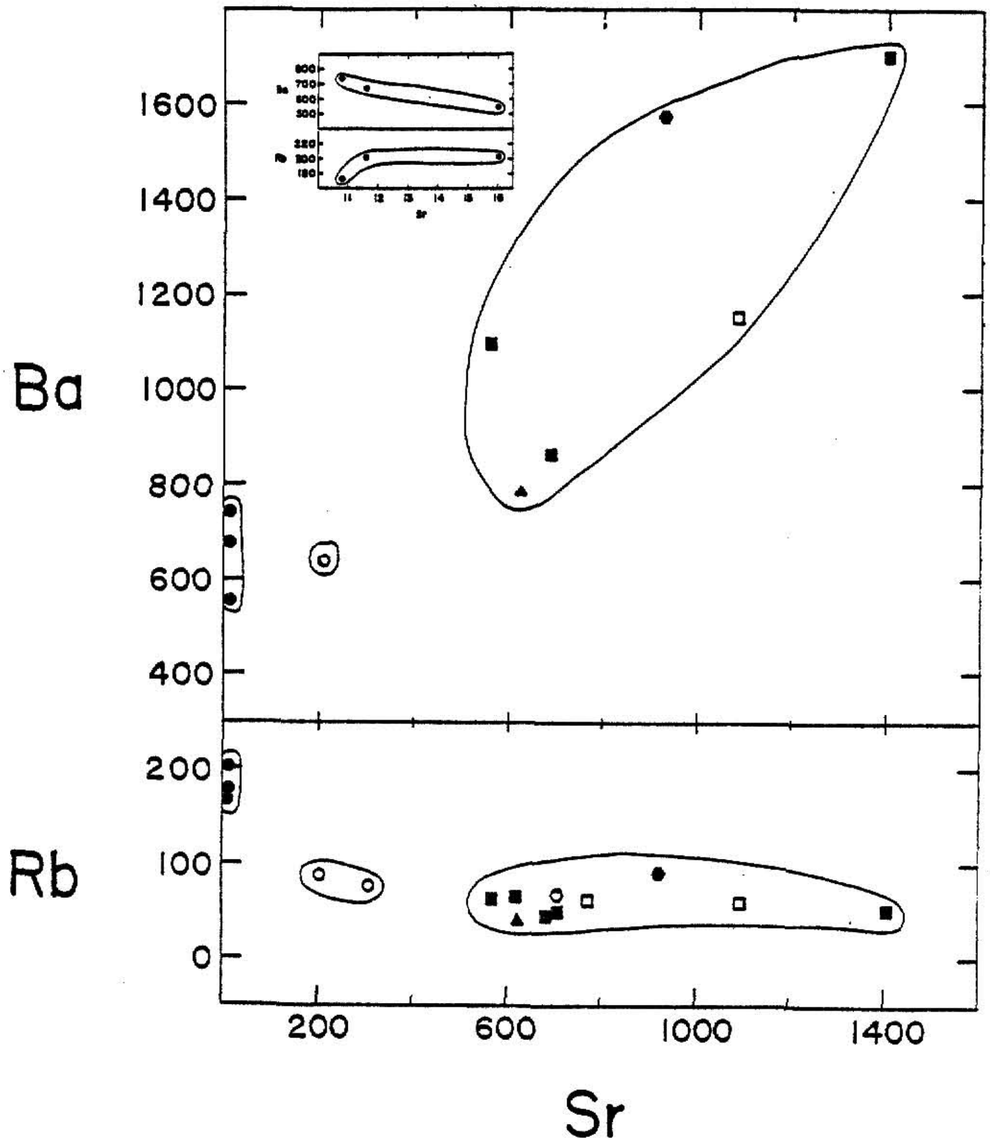

Figure 24. Trace-element variation diagram for Gravelly Range volcanic rocks with an expanded scale plot of rhyolitic ignimbrite samples. Elemental content (ppm) of Ba and Rb versus Sr(ppm) is plotted (see fig. 17 for explanation of symbols).

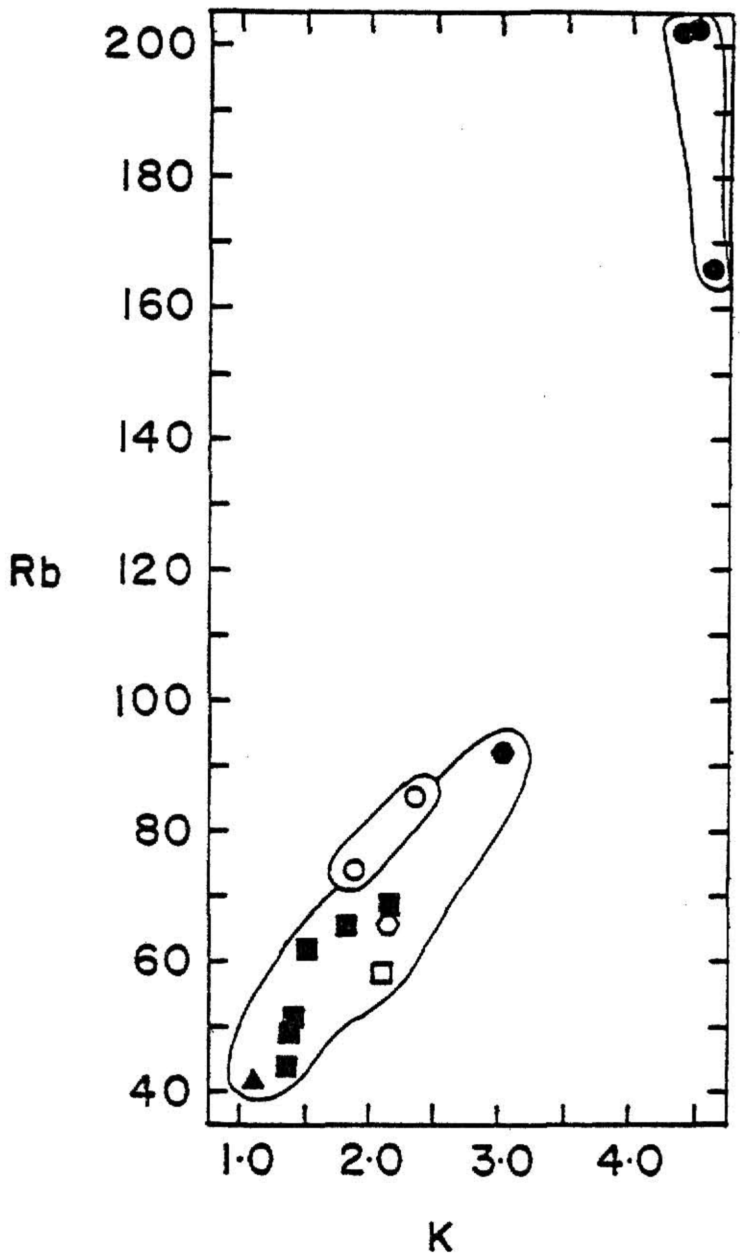

Figure 25. Trace-element variation diagram for Gravelly Range volcanic rocks. Elemental content (ppm) of Rb versus K (percent). (See fig. 17 for explanation of symbols).

crystal tuff for trace-element ratio diagrams (fig. 27 and 28). Negative correlations are displayed by plots of Sr/Ba versus K (fig. 27), and K/Rb versus K (fig. 27); a positive trend is displayed by Sr/Ba versus Rb (fig. 28).

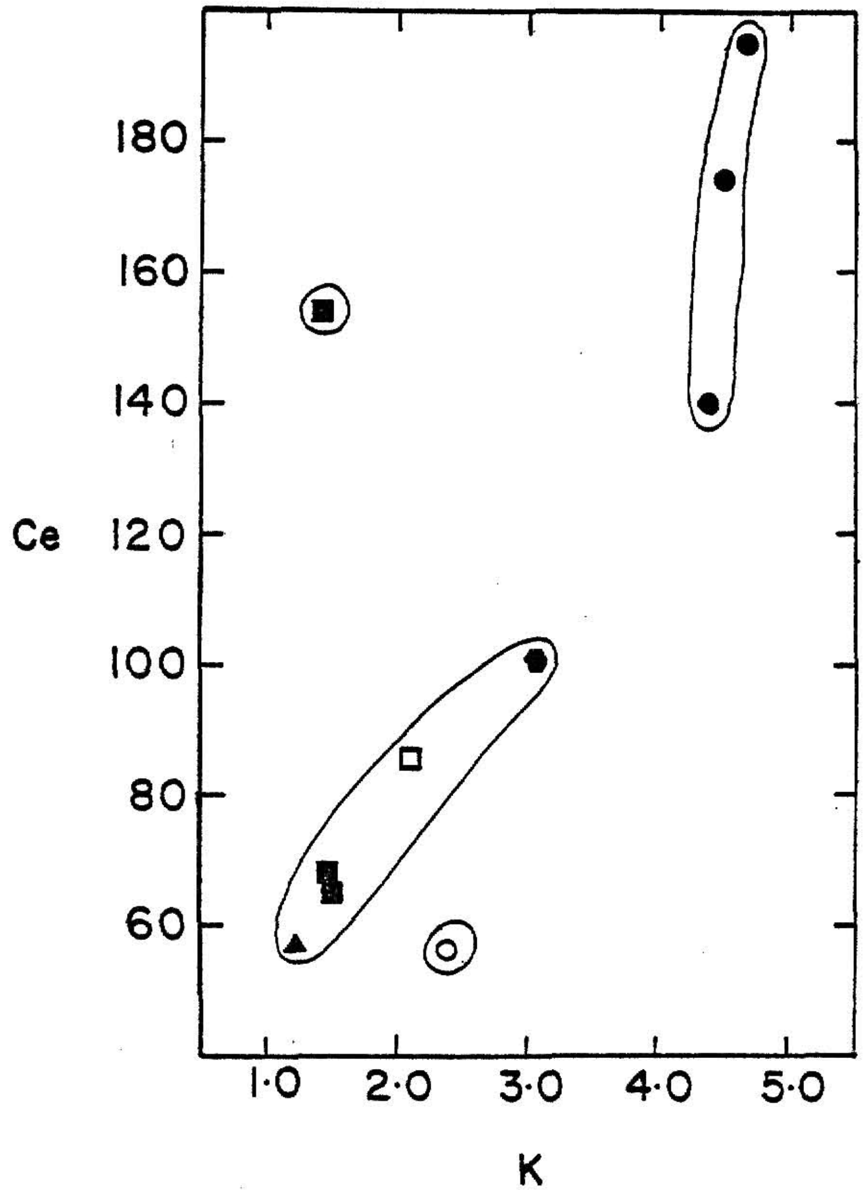

Figure 26. Trace-element variation diagram for Gravelly Range volcanic rocks. Elemental content of Ce (ppm) versus K (percent). (See fig. 17 for explanation of symbols).

Rhyolitic Ignimbrite

Trace-element contents versus DI are plotted for the rhyolitic ignimbrite (fig. 23). For most of the incompatible elements (Ce, Cs, Hf, Rb, Se, Ta, Th, U, and Zn), rhyolitic ignimbrite closely follows the trends defined by the basaltic rocks. Ba is much lower in the rhyolitic

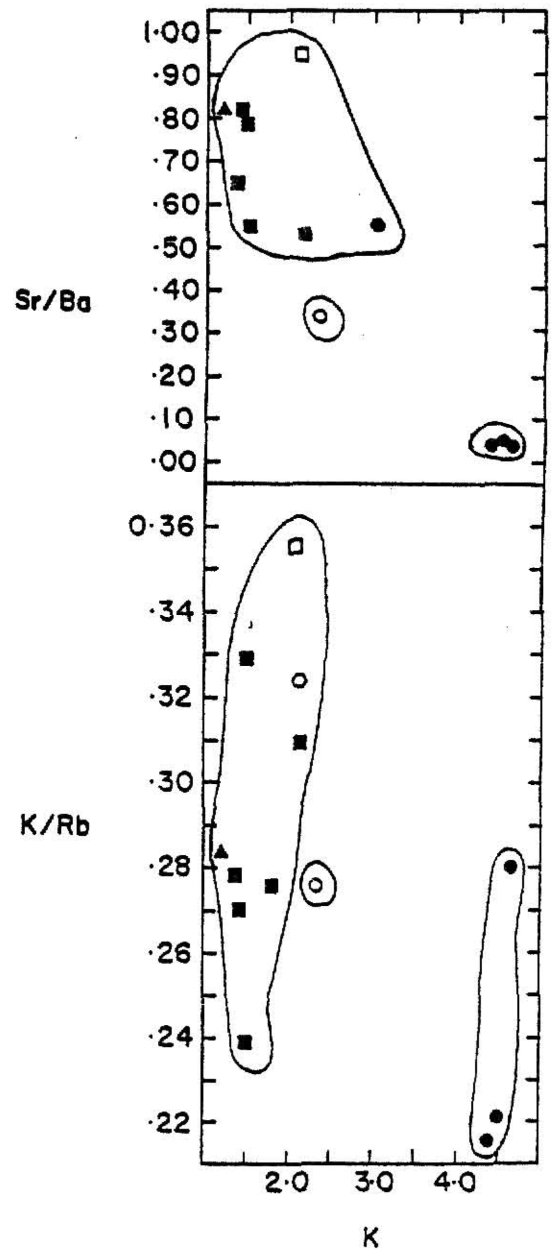

Figure 27. Trace-element variation variation diagram for Gravelly Range volcanic rocks. Elemental ratios of Sr/Ba and K/Rb versus K (percent). (See fig. 17 for explanation of symbols).

ignimbrite, and an incompatible trend is observed. Sr continues the compatible trend shown by the crystal tuff. Other compatible elements (Co, Cr, and Sc) continue trends defined by the basaltic rocks.

Rhyolitic ignimbrite follows most trends defined by basaltic rocks for other trace-element diagrams (fig. 24-26). On an expanded scale, a plot

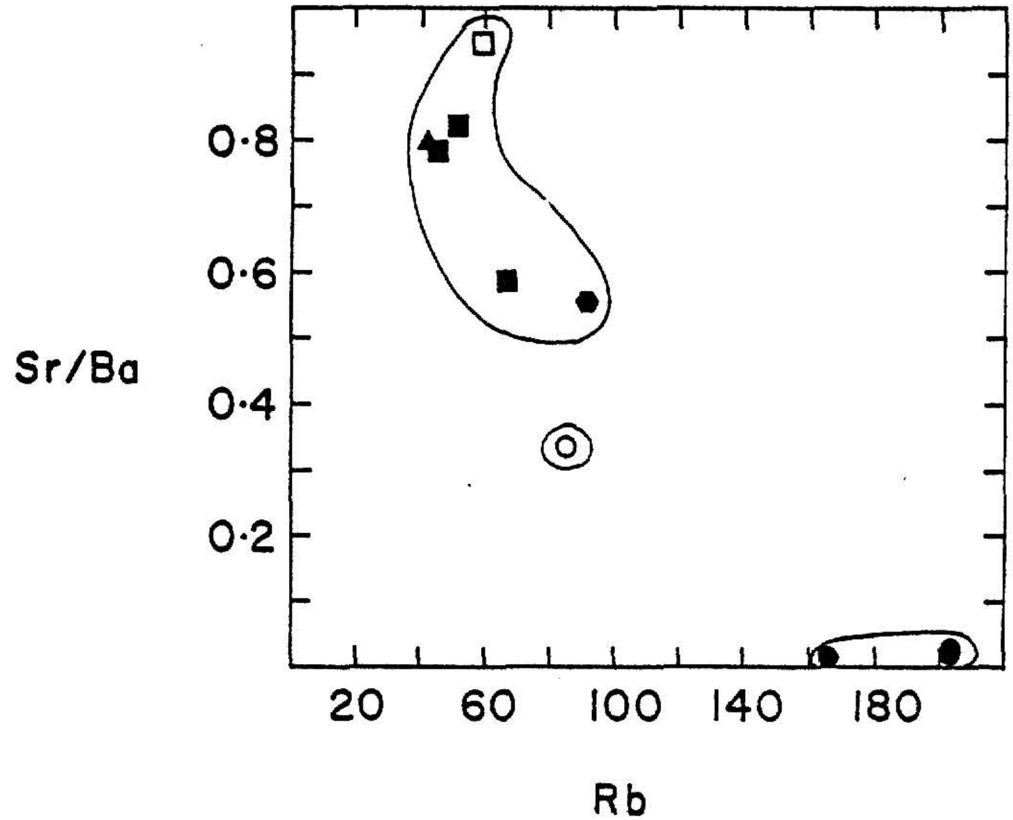

Figure 28. Trace-element variation diagram for Gravelly Range volcanic rocks. Elemental ratio of Sr/Ba versus Rb (ppm). (See fig. 17 for explanation of symbols).

of Ba versus Sr reveals a negative correlation; a plot of Rb versus Sr reveals a slight positive correlation (fig. 24). Total Rb contents are much greater in the rhyolitic rocks, and a plot of Rb versus K shows a negative trend (fig. 25). Total DI contents are also much greater in the rhyolitic rocks, and a positive, near vertical trend is observed on a plot of Ce versus K (fig. 26).

For trace-element ratio diagrams, rhyolitic ignimbrite follows the trends defined by the basaltic tocks for two of the plots (Sr/Ba versus K; fig. 27; and Sr/Ba versus Rb; fig. 28).

STRONTIUM ISOTOPES

INTRODUCTION

Elemental concentrations of Rb and Sr measured $^{87}Sr/^{86}Sr$, and calculated $^{87}Rb/^{86}Sr$ and $^{87}Sr/^{86}Sr_i$ ratios of Gravelly Range rocks are presented in Table 6. Analyzed samples include the following: alkali-olivine basalt (BB-9-77); silicic-alkalic basalt (P-5-77, BB-26B-77, and SR-19-79); basaltic andesite (SR-22B-79), and rhyolitic ignimbrite (SR-25B-79 and P-30B-77). The data are plotted on a Rb-Sr evolution diagram (fig. 29). No linearities are observed to permit the construction of an isochron. On an expanded scale, a negative correlation is observed within the basaltic suite (fig. 29).

INITIAL RATIOS

Alkali-Basalt Suite

Initial ratios of the basaltic suite are calculated with an assumed maximum age of mid-Oligocene (set at 35 m.y. B.P.). Considerable variability in the initial ratios is displayed with a range of values from 0.7044 (BB-9-77) to 0.7129 (SR-22B-79).

Additional variation diagrams of $^{87}Sr/^{86}Sr_i$ versus DI and versus 1/Sr content are plotted in Figures 30 and 31. There is positive correlation between the initial ratio and the DI (fig. 30) and a less negative correlation between the initial ratio and 1/Sr content (fig. 31).

Rhyolitic Ignimbrite

Initial $^{87}Sr/^{86}Sr$ ratios and ages of the rhyolitic ignimbrite samples (SR-25B-79 and P-30B-77) are unknown. Calculated initial ratios which

TABLE 6. Rubidium - strontium isotopic data of samples from Gravelly Range volcanic rocks.

SAMPLE	Rock Type	Rb(1) (ppm)	Sr(1) (ppm)	$^{87}Rb/^{86}Sr$	$(^{87}Sr/^{86}Sr)$ Corrected (2)	Age(3)	$(^{87}Sr/^{86}Sr)_i$ (4)
BB-9-77	Alkali-olivine basalt	42.7	632	0.195	0.7045 ± 0.0005	35 m.y.	0.7044
P-5-77	Silicic-alkalic basalt	44.4	684	0.187	0.7067 ± 0.0005	35 m.y.	0.7066
BB-26B-77	Silicic-alkalic basalt	58.7	1090	0.156	0.7084 ± 0.0005	35 m.y.	0.7083
SR-19-79	Silicic-alkalic basalt	51.9	1400	0.107	0.7088 ± 0.0005	35 m.y.	0.7087
SR-22B-79	Basaltic andesite	92.0	936	0.285	0.7130 ± 0.0005	35 m.y.	0.7129
SR-25B-79	Rhyolitic ignimbrite	176	11.6	43.97	0.7067 ± 0.0005	3.5 m.y.	0.7045
P-30B-77	Rhyolitic ignimbrite	166	10.8	44.58	0.7138 ± 0.0005	14.7 m.y.	0.7045

(1) Values obtained from X-ray fluorescence.
(2) Corrected for isotopic fractionation assuming $^{86}Sr/^{88}Sr = 0.1194$.
(3) Age of rhyolitic ignimbrite calculated for an initial ratio of 0.7045. For all other samples, the age represents a maximum value for initial ratio calculations.
(4) Initial ratios assumed for rhyolitic ignimbrite and calculated for all other samples.

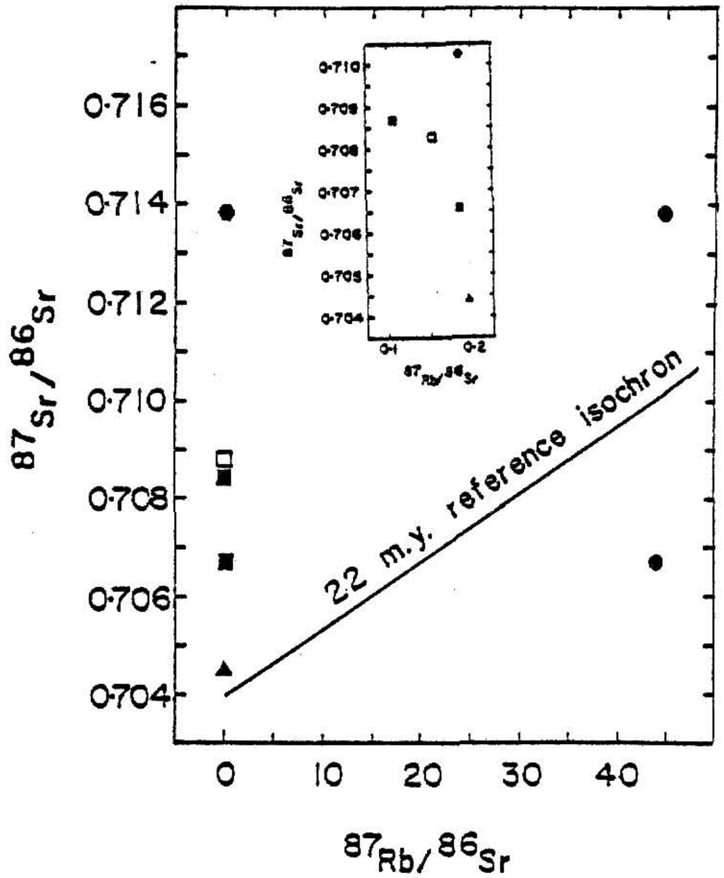

Figure 29. Rb-Sr evolution diagram for Gravelly Range volcanic rocks with basalt plotted on an expanded scale (see fig. 29).

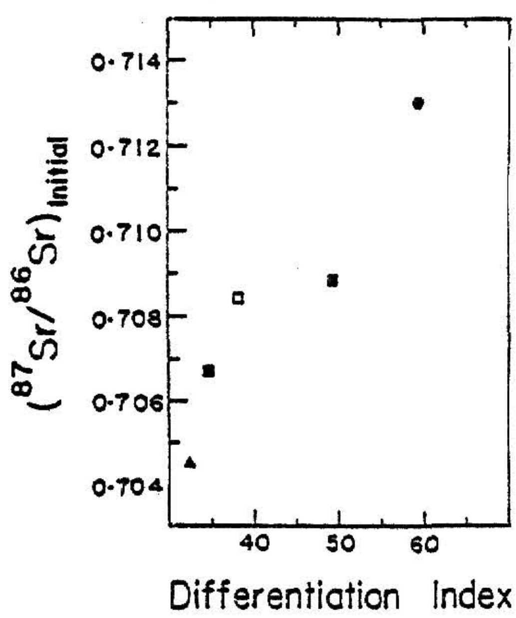

Figure 30. Isotopic variation diagram for Gravelly Range basaltic rocks. $^{87}Sr/^{86}Sr$ versus DI (see fig. for explanation of symbols).

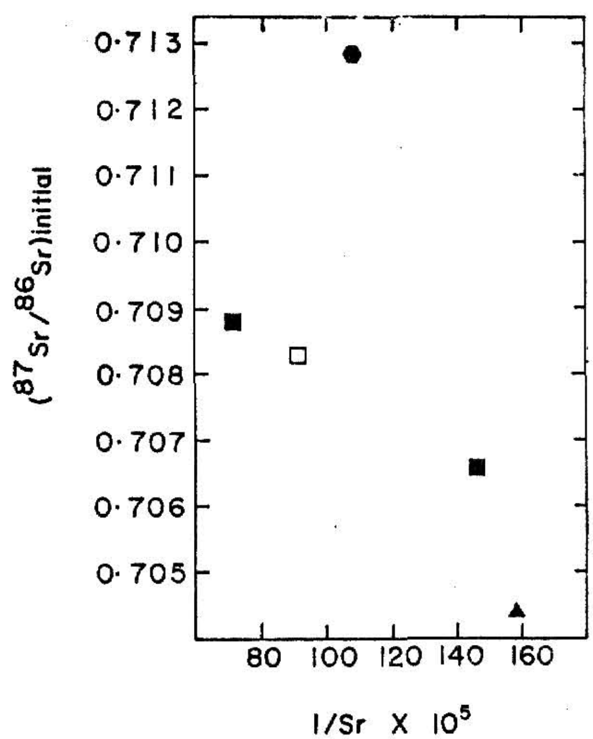

Figure 31. Isotopic variation diagram for Gravelly Range basaltic rocks. $^{87}Sr/^{86}Sr$ versus 1/Sr (ppm^{-1}). (See fig. 17 for explanation of symbols).

assumed an age as young as 20 m.y. B.P. resulted in unrealistic values (less than 0.7000). Assuming a closed system and a minimum ratio of 0.7045 for the initial ratio (lowest measured value in the area), maximum reasonable ages were calculated (Table 6). Ages of 14.7 m.y. B.P. for sample P-30B-77 and 3.5 m.y. B.P. for sample SR-25B-79 were obtained, in which case these rocks are younger than the mafic suite.

D I S C U S S I O N

INTRODUCTION

Field relations, petrographic, major-element, trace-element, and strontium isotope data restrict the possible sources and processes involved in the formation of Gravelly Range volcanic rocks. Analysis of these data yeilds a petrogenetic interpretation of these rocks and a possible, although not unique, model of the formation.

Quantative trace-element models are especially useful to limit models developed from other methods. A non-modal, aggregate-liquid model (Shaw, 1970) is used for calculations in this study, and it is expressed as:

$$Cl/Co = 1/F \left[1 - (1 - P^{F}/Do)\right]^{1/P}$$

where:

Cl = elemental concentration in liquid
Co = elemental concentration in source

F = fraction melted
P = proportionality coefficient
Do = overall distribution coefficient

with P and Do further defined as:

$P = P\alpha K\alpha + P\beta K\beta ...$

where:

$P\alpha,\beta$ = proportion of phase in the liquid

$K\alpha,\beta$ = distribution coeffieient of the element in the liquid

$Do = X\alpha D\alpha + X\beta D\beta ...$

where:

TABLE 7. Partition coefficients used in trace-element models.

	Orthopyroxene	Clinopyroxene	Plagioclase		Garnet
	B,I	B,I	B,I	S	B,I
La	0.020	0.10	0.14	0.30	0.027
Ce	0.024	0.15	0.12	0.27	0.028
Sm	0.054	0.50	0.067	0.13	0.29
Eu	0.054	0.51	0.34	2.2	0.49
Tb	0.12	0.53	0.067	0.13	1.0
Yb	0.34	0.62	0.067	0.049	11.5
Lu	0.42	0.56	0.060	0.046	11.9
Rb	0.001	0.001	0.01	0.041	0.001
Sr	0.017	0.12	2.2	4.4	0.012
Ba	0.001	0.001	0.023	0.31	0.002
Co	2	0.02	0.02	0.10	0.3
Cr	1.8	0.10	0.10	0.06	2
Sc	1.2	0.035	0.035	0.02	10

	Olivine	Biotite	Hornblende	Orthopyroxene	Quartz
	B,I	S	S	S	S
La	0.008	0.34	1.30	0.040	0.001
Ce	0.007	0.32	1.52	0.044	0.001
Sm	0.0066	0.26	7.77	0.18	0.001
Eu	0.0068	0.24	8.9	1.13	0.001
Tb	0.010	0.28	8.6	0.018	0,001
Tb	0.014	0.44	8,4	0,012	0.001
Lu	0.016	0.33	5.5	0.006	0.001
Rb	0.001	5.5	0.14	0.37	0.001
Sr	0.014	0.12	0.46	3.87	0.001
Ba	0.001	9.7	0.044	6.1	0.001
Co	3	20	10	0.01	0.001
Cr	2	12	2	0.01	0.001
Sc	0.03	11	15	0.06	0.001

B,I: Basaltic and Intermediate coefficients.
S : Silicic coefficients.
Compiled mainly from; Kilbane (1978), Philpotts and Schnetzler (1970a,b), and Cox, Bell and Pankhurst (1979).

$D\alpha, \beta$ = distribution coefficient of the element in the liquid

$X\alpha, \beta$ = fraction of the phase in the source

Haskin et al. (1970) present a mathematical equation which describes trace element behavior during fractional crystallization. Quantitative calculations from Gravelly Range rocks are based on this model, expressed as:

$$Cr/Ca = (1 - X)^{Do - 1}$$

where:

Cr = the average concentration of a particular element in the residual phase

Ca = the average concentration of a particular element in the system

X = the fraction of completion of the process

Do = overall distribution coefficient

with Do further defined as:

$$Do = X\alpha D\alpha + X\beta D\beta \ldots$$

where:

$D\alpha, \beta$ = distribution coefficient of the element in the phase

$X\alpha, \beta$ = fraction of the phase crystallizing

Distribution coefficient data have been compiled by numerous authors as summarized in Frey (1979). Data used in these calculations (Table 7) represent several sources (Kilbane, 1978; Philpotts and Schnetzler, 1970a; 1970b; and Cox et al., 1979).

RELATIONS BETWEEN VOLCANIC ROCKS

Major element and trace element data define two distinct, genetically unrelated groups of volcanic rocks in the Gravelly Range: (1) the basaltic suite and the andesitic-dacitic crystal tuff, and (2) the rhyolitic ignimbrite (figs. 14-28). Isotopic data support the distinction as the K-Ar age of a basalt from the Black Butte area (believed to be the youngest basaltic activity in the Gravelly Range) is 22.3 m.y. B.P. (Marvin and others, 1974), whereas $^{87}Sr/^{86}Sr$ ratios and their corresponding $^{87}Rb/^{86}Sr$ ratios limit the formation of the silicic ignimbrite to less than 14.7 m.y. B.P. Field studies also indicate that the basaltic suite is older than the rhyolitic ignimbrite. Crystal tuff may represent a third suite, although the majority of the data suggest that they are related to the alkali-basalt suite. Both major-element and trace-element data tend to show a contimuum in variation diagrams for the rocks of the basaltic suite (figs. 14-28).

Petrogenetic models (Holmes, 1931; Wager et al., 1965; Schmincke, 1969; Blake et al., 1965; Fenner, 1948) that could explain contemporaneous basaltic and rhyolitic compositions are summarized in Yoder (1973). Hypothesis include the following: (1) the magma was generated from separate magma chambers, or the sources for the magma were different, or both; (2) the silicic material was melted by the upwelling basaltic material; (3) there was one chamber which contained two immisicible liquids; (4) a common source was fractionally fused at different invariant points.

Major-element and trace-element data for Gravelly Range samples indicate that separate sources formed the mafic and silicic rocks. Major-element and trace-element variation diagrams show distinctly separate trends between the two rock types, and these criteria have been used to define the bimodal distribution of mafic and silicic suites in this area. Chondrite-normalized REE patterns reinforce the two-fold division by having no significant Eu anomaly for the mafic suite and a pronounced Eu anomaly for the silicic suite.

GENESIS OF THE ALKALI-BASALT SUITE

ISOTOPIC RELATIONS

The Rb-Sr isotopic data vary considerably among rocks of the Gravelly Range basaltic suite. The initial $^{87}Sr/^{86}Sr$ ratios range from 0.7044 (alkali-olivine basalt) to 0.7129 (basaltic andesite), and these ratios show a positive correlation with DI (fig. 30). The $^{87}Sr/^{86}Sr$ ratios have an apparent negative correlation with $^{87}Rb/^{86}Sr$ ratios (fig. 29), as do the initial $^{87}Sr/^{86}Sr$ ratios with 1/Sr values (fig. 31). The correlations among the rocks could be indicative of varied assimilation of crustal material by a parent magma; or of varied degrees of partial melting of a source region that was heterogeneous with respect to its Sr isotopic composition.

The lowest initial $^{87}Sr/^{86}Sr$ ratio of 0.7044 might be construed as the value of an uncontaminated mantle source region for the alkali-olivine basalt. A silicic-alkalic basalt from the same vent (BB-26B-77) has a higher initial ratio of 0.7083. If the parent magma of alkali-basalt composition were contaminated by a low Rb/Sr, high-radiogenic Sr material, such as a sedimentary carbonate rock, the increase in the initial $^{87}Sr/^{86}Sr$ ratio could be explained as well as the observed decrease in the $^{87}Rb/^{86}Sr$ ratio. The increase in overall Sr content (632 ppm in sample BB-9-77 to 1090 ppm in sample BB-26B-77) could be related to fractional crystallization of clinopyroxene from a parent magma.

The silicic-alkalic basalt, sample P-5-77, also has an initial ratio that is higher than that of the alkali-olivine basalt (0.7066 versus 0.7044), and a lower $^{87}Rb/^{86}Sr$ ratio (0.187 versus 0.195). Like in the silicic-alkalic basalt (BB-26B-77), an assimilation of crustal material from a low-Rb/Sr, high-radiogenic Sr source, such as a sedimentary carbonate rock, could explain the initial $^{87}Sr/^{86}Sr$ ratio of the basalt, P-5-77. Alternatively, a source that is heterogeneous with respect to $^{87}Sr/^{86}Sr$ and $^{87}Rb/^{86}Sr$ could also explain the variation in the initial ratio.

The silicic-alkalic basalt, sample SR-19-79, has an initial ratio of 0.7087 which is significantly higher than expected if it was derived from a mantle source similar to that of the alkali-olivine basalt (BB-9-77). A very high Sr content coupled with the high $^{87}Sr/^{86}Sr$ ratio of SR-19-79 will generally preclude consideration of an isotopically similar source for the two basalt units. The high $^{87}Sr/^{86}Sr$ ratio of the silicic-alkalic basalt, sample SR-19-79, is incompatible with its observed $^{87}Rb/^{86}Sr$ ratio of 0.107, as the calculated age is more than 6 b.y. B.P. From the isotopic consideration, the magma could not have been generated from a source having a single-stage model of isotopic evolution.

The basaltic andesite (SR-22B-79) which has the highest initial ratio (0.7129) is from the same vent area as the one of the silicic-alkalic basalt SR-19-79. The decrease in Sr content (from 1400 ppm in sample SR-19-79 to 936 ppm in SR-22-79) can be attributed to the higher degree of partial melting; however, the Rb/Sr would also be expected to decrease and not increase as has been observed for the andesite. The high $^{87}Sr/^{86}Sr$ ratio of the basaltic andesite could have resulted from incorporation of some crustal material having high $^{87}Sr/^{86}Sr$ and $^{87}Rb/^{86}Sr$ ratios, by magmas isotopically similar to that of the silicic-alkalic basalt (SR-19-79). A source that is heterogeneous with respect to $^{87}Sr/^{86}Sr$ and $^{87}Rb/^{86}Sr$ could also explain the variation in the initial ratios between the basaltic andesite and the silicic-alkalic basalt.

It has been shown in Figure 30 that the initial $^{87}Sr/^{86}Sr$ ratio increases with DI for the basaltic suite. Under constraints set by the isotopic data, the trend among the various rocks of the wuite cannot be explained as solely due to fractional crystallization from a parent magma. Nor could the relationship be produced if the rocks had originated as a result of varied degrees of partial fusion of a chemically and isotopically similar source. In both of these cases, the initial $^{87}Sr/^{86}Sr$ ratios for all the derivatives are expected to be similar. As an alternative to the above modes of evolution, a process of assimilation of crustal material by a magma typically derived from the mantle may be deduced to explain the observed relationship between the initial Sr isotopic composition and the DI. To be compatible with the model of assimilation of average crustal material, having Rb/Sr and $^{87}Sr/^{86}Sr$ ratios higher than those of a parent basaltic magma typified by the alkali-olivine basalt (BB-9-77), the $^{87}Sr/^{86}Sr$ ratios can be expected to increase with increasing $^{87}Rb/^{86}Sr$ ratios rather than decreasing which is true for these rocks. The negative trend between the $^{87}Sr/^{86}Sr$ and the $^{87}Rb/^{86}Sr$ ratios, illustrated in Figure 29, can be explained by considering assimilation of carbonate rocks having low Rb/Sr ratios. Because many Paleozoic carbonate rocks are known to occur in this region, these rocks can be potential contaminants in the assimilative process. Paleozoic carbonate rocks often contain less than 400 ppm of Sr and have $^{87}Sr/^{86}Sr$ ratios of 0.710 or less, and thus the hypothesis of assimilation of carbonate rocks is fraught with three major difficulties: (1) it would require incorporation of an unusually large amount (more than 75 percent) of carbonate rock to generate the observed $^{87}Sr/^{86}Sr$ ratios of some of the rocks, (2) it would not be possible to have a Sr content as high as 1000 ppm for some of the magmas unless they were accompanied by a large degree of pyroxene fractionation, and (3) the relationship between $^{87}Sr/^{86}Sr$ and 1/Sr whould be a positive one contrary to the negative one observed for these rocks.

From consideration of the Sr isotopic data, the choice of a chemically and isotopically uniform source for derivation of the magmas is prohibited. As an alternate to a homogeneous-source model, the isotopic data can be reconciled with evolution of these mafic rocks from isotopically and chemically varied sources.

VARIATION DIAGRAMS

Major-element and trace-element variation diagrams of the alkali-basalt suite display smooth linear trends. CaO and MgO show a definite compatible relationship with DI, whereas K_2O, Na_2O, and SiO_2 show a definite incompatible relationship with DI. In contrast, Al_2O_3 and Fe_2O_3(T) remain fairly constant with DI (fig. 17). Ce, Ba, Cs, Hf, Rb, Se, Sr, Ta, Th, U, and Zn also show an incompatible relationship with DI whereas Co, Cr, and Sc show a compatible relationship with DI (fig. 23).

These continuous major-element and trace-element variations for the suite may be explained by one or more of the following processes: (1) varied fusion of a source material; (2) fractional crystallization; (3) varied composition of the source region, and (4) crustal contamination; or (5) any combination of these processes (Cox et al., 1979).

Of the processes outlined above, only the varied composition of the source retion and the varied partial fusion processes are definitely supported by the variation of Ce with K (fig. 26). Sun and Hanson (1975) have shown that the presence or absence of a mineral in which K is an ESC (essential structural constituent) could affect the correlation of Ce with K during progressive partial fusion. Most Gravelly Range alkali basalt, with the exception of one (SR-19-79) show a positive correlation of Ce with K which would occur during progressive partial fusion of a source without a phase in which K is an ESC. The K content of sample SR-19-79 is much lower than expected and this may be the result of residual phlogopite or amphibole in which K is an ESC. Residual phlogopite is preferred because no anomalous behavior of K with Rb, as illustrated by Figure 25, is observed for this same sample.

REE data suggest that most rock types of the Gravelly Range basaltic suite have evolved from a source region that contains residual garnet as La/Lu ratios range from 81 to 329. Except for a negative Eu anomaly (Eu/Eu* = 0.657) for the dacitic tuff, the lack of any significant Eu anomaly is a common characteristic of the rocks of the basaltic suite. Low-pressure fractionation of plagioclase from a basaltic parent could account for the Eu anomaly observed for dacitic tuff. The lack of an Eu anomaly in the basaltic suite could be related to (1) absence of any significant plagioclase fractionation, (2) plagioclase fractionation accompanied by a much greater degree of clinopyroxene fractionation, or (3) plagioclase fractionation of a parent magma that had an inherently positive Eu anomaly.

Sample BB-26B-79 displays considerably higher HREE content than other rock samples. The source mineralogy that formed this rock may have been slightly different. The absence of residual garnet which retains HREE could explain the observed HREE content.

QUANTITATIVE PETROGENETIC MODEL

Experimental petrologists have shown that alkali basalt may originate by 2 to 15 percent partial melting of a mantle peridotite at pressures of 27 kb or greater (Kay and Gast, 1973; Ringwood, 1975). Alternatively, they could form by fractional crystallization of orthopyroxene from an olivine tholeiite parent magma at pressures between 13 and 18 kb pressure (Ringwood, 1975). Partial melting of mantle peridotite is the preferred principal formational process for Gravelly Range basaltic rocks because the presence of olivine tholeiite in the Gravelly Range has not been confirmed.

Kay and Gast (1973), based on REE patterns, suggested that alkali-olivine basalt forms by partial melting of mantle peridotite. Similarly, the preferred model presented here for Gravelly Range basalt (fig. 32) has a garnet lherzolite source (initial ratio of olivine/orthopyroxene/clinopyroxene/garnet = 40/30/28/02) which melts (in a ratio of orthopyroxene/clinopyroxene/garnet = 25/67/08) from 1 to 20 percent. REE contents of the source could vary, with increased enrichment of LREE/HREE resulting in greater fractionation for small degrees of fusion.

The sample of silicic-alkalic basalt (BB-26B-79), which has an olivine diabase texture, displays considerably less LREE/HREE fractionation than other rock types. Partial melting of a source that contains spinel instead of garnet could produce the observed REE pattern.

One sample of crystal tuff (P-13F-77) that appears to be related to the basaltic suite shows a considerable Eu anomaly and less LREE/HREE fractionation than most Gravelly Range basalt. Fractional crystallization (10-50 percent)

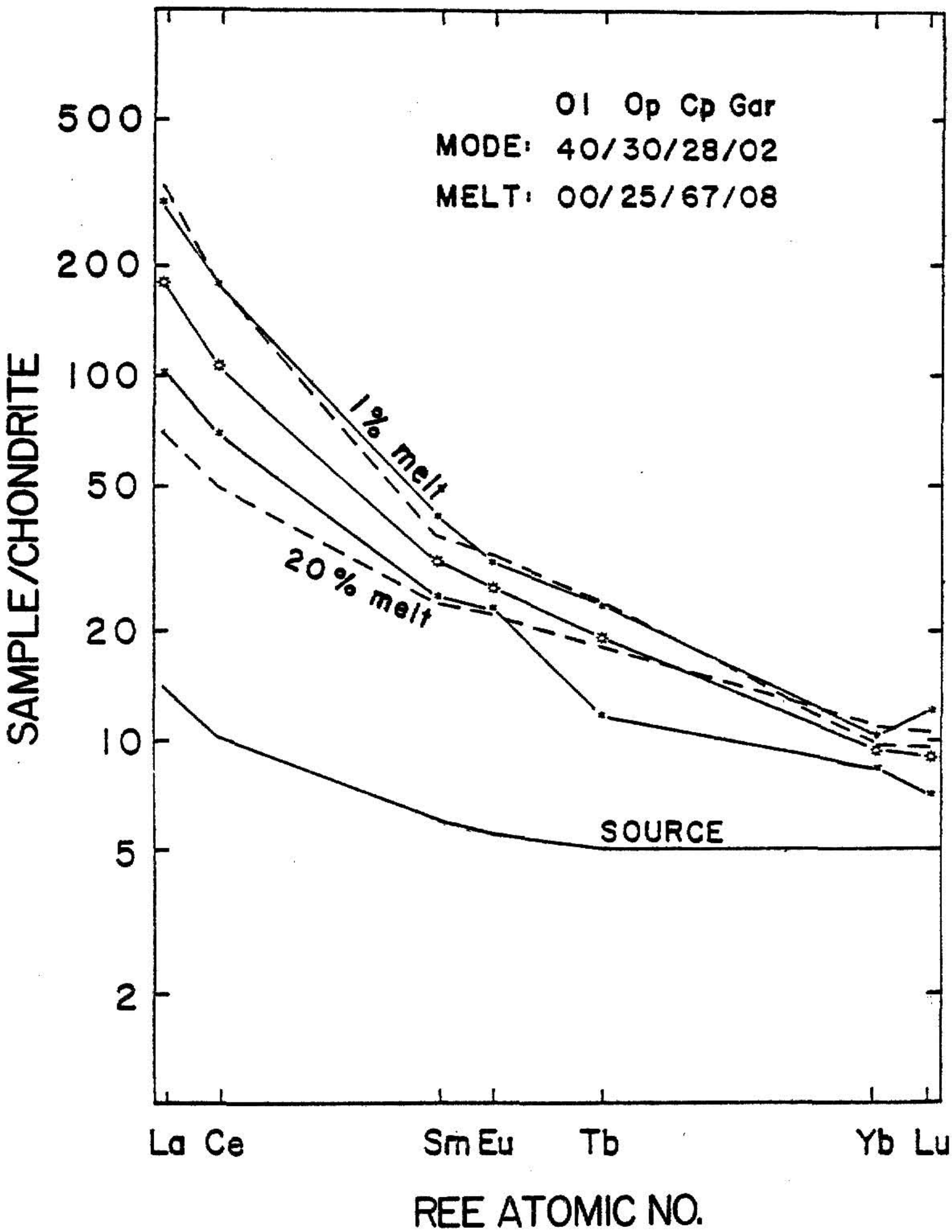

Figure 32. Chondrite-normalized REE plots of model melts for Gravelly Range alkali-basaltic magma. Solid lines (*) represent maximum and minimum values of Gravelly Range volcanic rocks. Solic line (✡) represents the average value for Gravelly Range basaltic rocks. Dashed lines represent model values with percent of fusion indicated. Garnet and clinopyroxene melt preferentially with an initial ratio of olivine/orhtopyroxene/clinopyroxene/garnet = 40/30/28/02 and a melt ratio of orhtopyroxene/clinopyroxene/garnet = 25/67/08.

of phenocryst minerals (in a ratio of clinopyroxene/plagioclase/orhtoclase = 30/35/35) from a silicic-alkalic basalt magma equivalent in composition to that of sample P-5-77 would produce a pattern similar to that observed for the crystal tuff (fig. 33). Although experimental petrologists have shown that a quartz normative liquid (such as sample P-13F-77) cannot be derived from a nepheline normative liquid (such as sample P-5-77) by low-pressure fractional crystallization of any phase, this liquid (P-5-77) may not be truly nepheline normative. Ratios of Fe_2O_3/FeO were estimated, and a slight adjustment of this ratio could result in a saturated or quartz-normative liquid.

Models developed from REE data are also supported by Co, and Sc data. Both Co and Sc model values bracket the values of Gravelly Range basalt (Table 8). Sr, Ba, and Rb values are slightly higher in the basalt than the model values.

GENESIS OF THE RHYOLITIC IGNIMBRITE

ISOTOPIC RELATIONS

Initial Sr isotopic compositions cannot be evaluated as the $^{87}Rb/^{86}Sr$ ratios of the rhyolitic ignimbrite samples are significantly high (43.97 to 44.58) and their ages are unknown. However, the Rb-Sr isotopic data do limit the maximum age of these rocks to less than 14.7 m.y. B.P. for sample P-30B-77, and less than 3.5 m.y. B.P. for sample SR-25B-79, if closed system behavior is assumed.

VARIATION DIAGRAMS

Rhyolitic ignimbrite forms a distinct suite when plotted on major-element and trace-element variation diagrams. The three samples analyzed are compositionally bery similar, which suggests that they may have evolved from similar sources.

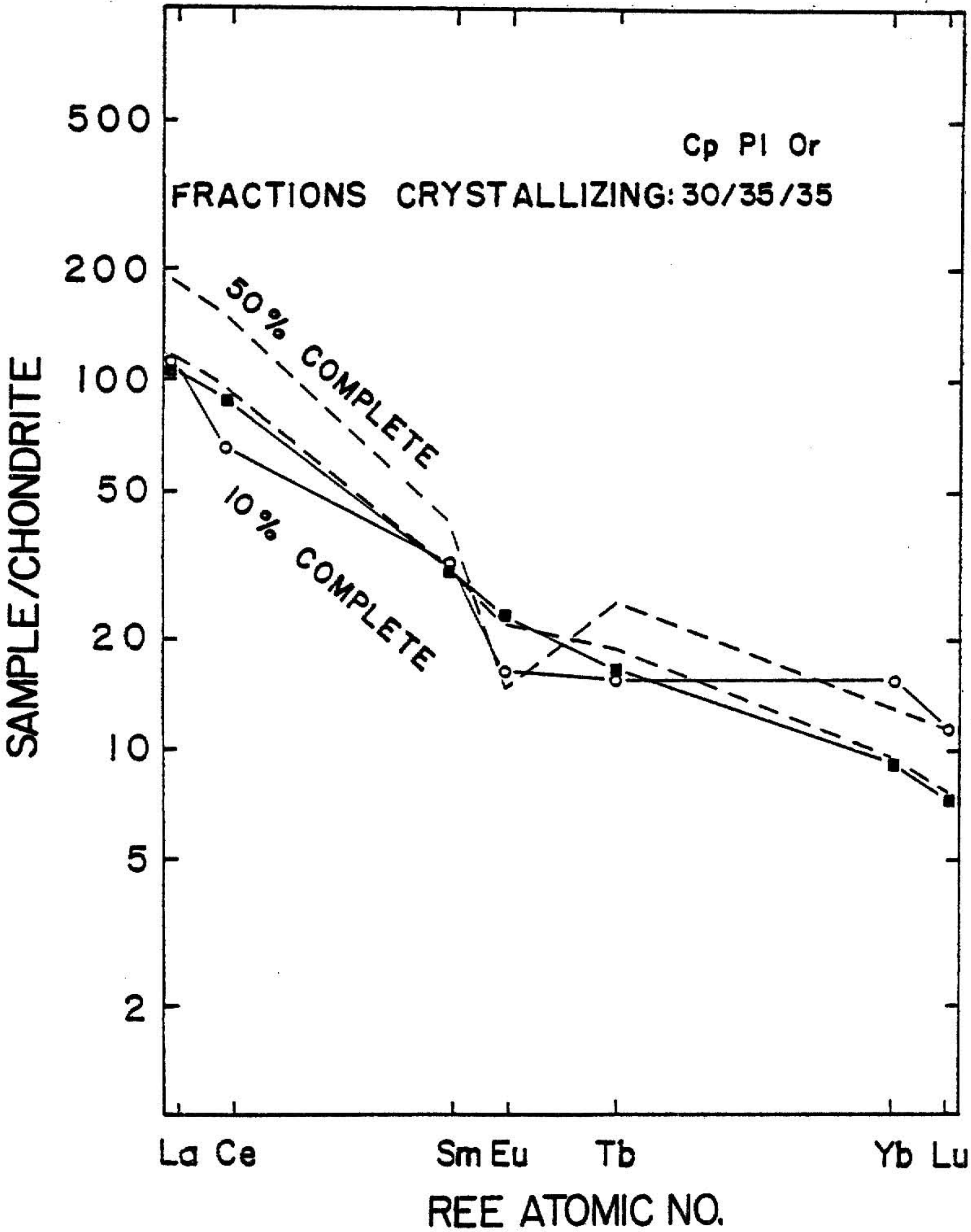

Figure 33. Chondrite-normalized REE plots of fractional crystallization models for a Gravelly Range crystal tuff. Solid line (■) represents a silicic-alkalic basalt source magma. Solid line (O) represents an observed crystal tuff. Dashed lines represent model values with percent of completion of the fractionation process indicated. Clinopyroxene preferentially crystallizes in a ratio of clinopyroxene/plagioclase/orthoclase = 30/35/35.

TABLE 8. Comparison of selected trace element contents in the hypothetical source with Gravelly Range basalts.

ELEMENT	Peridotite*	Gravelly Range Basalts	Predicted Content (1-20 pct. melt)
Co	35-120	22-47	19-66
Sc	5-15	12-29	9-26
Sr	10-40	560-1400	50-811
Ba	4-5	790-1700	20-500
Rb	2-8	43-92	10-800

*values compiled from Condie, 1967; and Condie et al., 1970.

Significant negative Eu anomalies (Eu/Eu* < 0.479) are displayed by the rhyolitic ignimbrite. Fractional crystallization of plagioclase could generate such an anomaly. Alternatively, the source could have had an inherent Eu anomaly. La/Lu ratios (94.2-137) reveal that significant fractionation has occurred; these ratios might be explained by the presence of residual hornblende in the source.

QUANTITATIVE PETROGENETIC MODEL

Winkler (1976) has shown partial fusion of a quartz, albite, anorthite, and orthoclase source will result in a melt which plots along a cotectic trace of the corresponding pressure on the Qz-Ab-An-Or tetrahedron. Gravelly Range rhyolitic samples plot between the 5 and 10 kb cotectic traces on a projection of the Qz-Ab-An-Or tetrahedron through the An apex (fig. 34).

An average Precambrian formation (Condie, 1970) that is enriched in LREE may represent a possible source for Gravelly Range rhyolitic rocks (initial ratio of quartz/plagioclase/orthoclase/biotite/hornblende = 20/34/20/25/01) that melt in a ratio of quartz/plagioclase/orthoclase/biotite = 30/35/30/05) from 1 to 30 percent (fig. 35) of this Precambrian source could generate the observed REE pattern. The same model can be used to explain the Ba, Rb, and Sr contents. The calculated model values and their observed values are in good agreement (Table 9).

REE data suggest that the rholitic ignimbrite could have formed by fractional crystallization of plagioclase from a mafic parent, however major-element and trace-element data reveal there are no intermediate compositions that would substantiate such a history. Alternatively, these rocks could have formed by varied partial fusion of a lower-crust assemblage such as an average Precambrian formation.

TABLE 9. Comparison of selected trace-element contents in the hypothetical source with Gravelly Range rhyolitic ignimbrite.

ELEMENT	Crustal Rocks*	Gravelly Range Silicic ignimbrites	Predicted Content (1-30 pct. melt)
Ba	900-2000	550-750	240-570
Rb	12-300	170-200	8-204
Sr	20-1100	11-16	9-540

*ranges compiled from Arth and Hanson (1975).

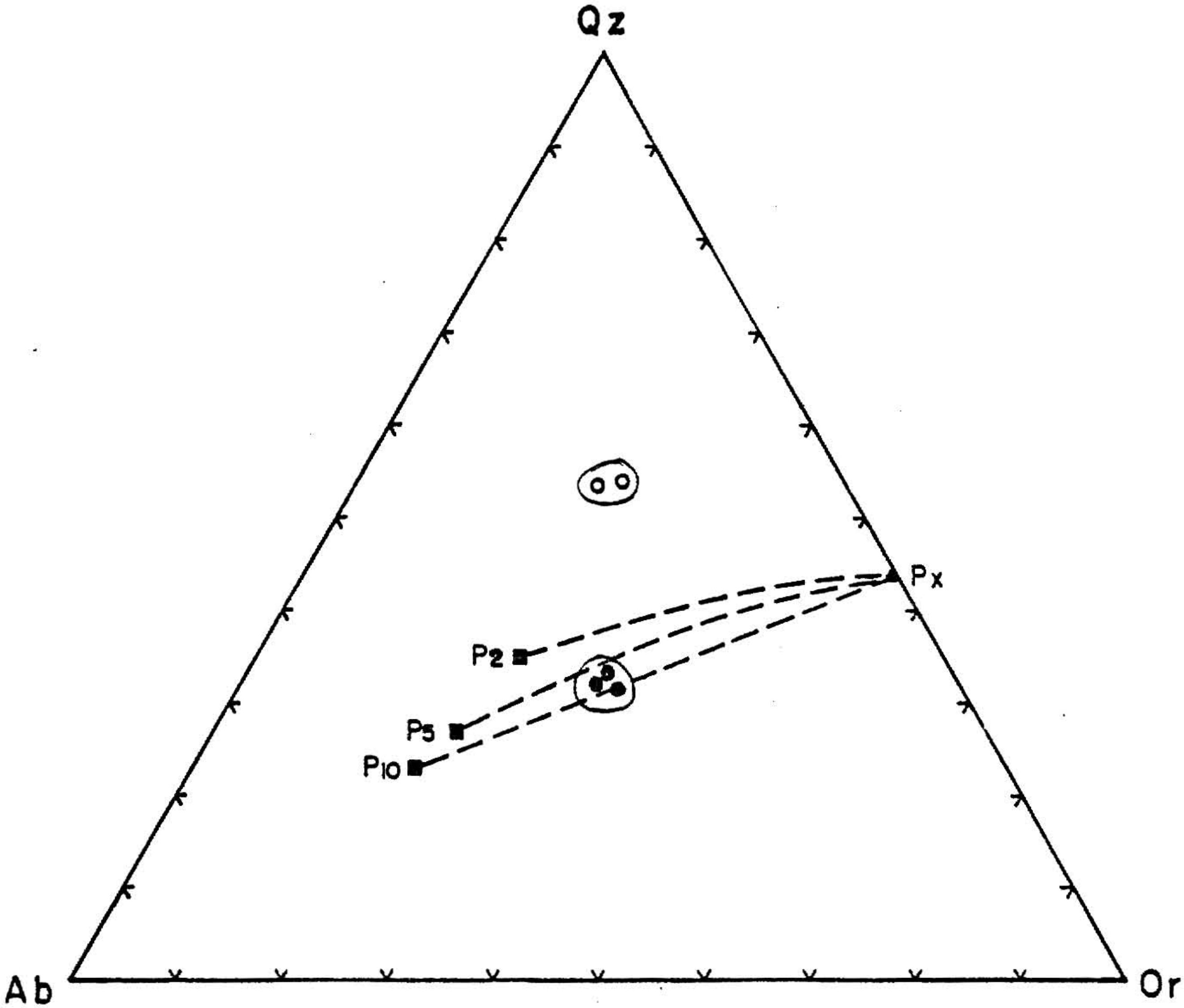

Figure 34. Projection of the Qz--Ab-An-Or tetrahedron through the An apex for Gravelly Range tuffs (Winkler, 1976). Minimum melt cotectic curves are shown at varied pressures. Point P (■) moves along these curves as anorthite content increases toward P(X). Rock types: rhyolitic ignimbrite (●); and crystal tuff (○).

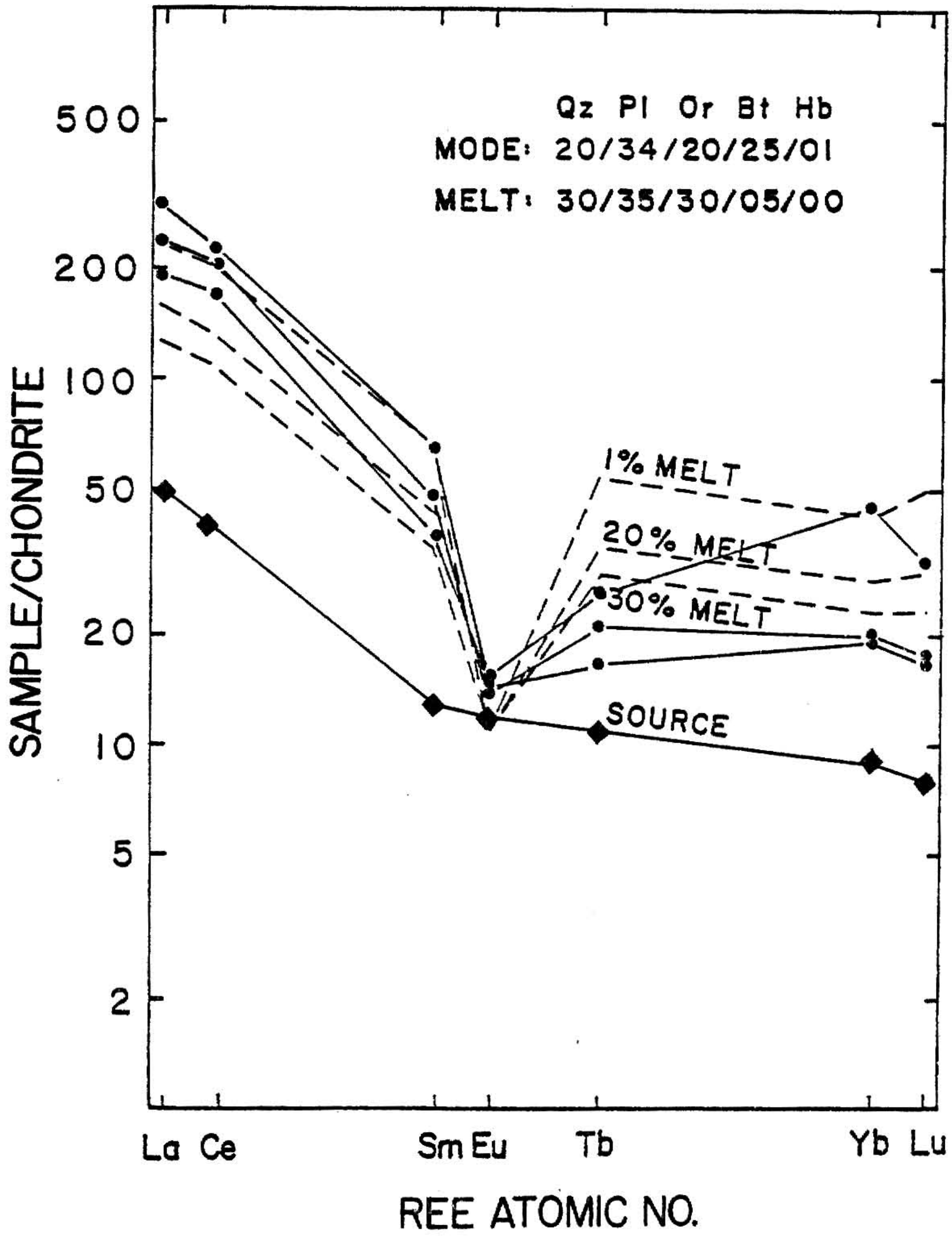

Figure 35. Chondrite-normalized REE plots of model melts for Gravelly Range rhyolitic magmas. Solid lines (●) represent rhyolitic ignimbrite. Solid line (◆) represents an average Precambrian formation (Condie, 1967; Condie et al., 1967; Condie et al., 1970). Dashed lines represent model values with percent of fusion indicated. Orthoclase and plagioclase preferentially melt with an initial ratio of quartz/plagioclase/orthoclase/biotite/hornblende = 20/34/20/25/01 and a melt ratio of quartz(plagioclase/orthoclase/biotite = 30/35/30/05.

RELATIONSHIP WITH THE SNAKE RIVER PLAIN-YELLOWSTONE REGION

Christiansen and Lipman (1972) and Lipman et al. (1972) have shown that post-orogenic volcanism in the western United States is fundamentally basaltic or bimodal and may be related to an extensional tectonic regime. Gravelly Range volcanic rocks represent a bimodal assemblage of alkali basalt and rhyolitic ignimbrite as do the volcanic rocks from the Snake River Plain-Yellowstone Region.

Field relations suggest the cycles of volcanism in the two areas are similar. Early activity in the Yellowstone Region involved the eruption of tholeiitic basalt followed by small rhyolitic flows and tuff (Eaton and others, 1975). Alkali basalt was first extruded from Gravelly Range centers. This was probably accompanied by zonation of a few magma chambers as suggested by the occurrence of a basal crystal tuff in some areas. Extrusion of small volumes of rhyolitic ignimbrite followed tha basaltic activity. Gravelly Range basaltic activity is much older (greater than 22 m.y. B.P.) whereas the activity in the Snake River - Yellowstone Region occurred much more recently (less than 15 m.y. B.P.).

Major-element contents of average Gravelly Range rock types are similar to those from the Snake River Plain - Yellowstone Region (Table 10), although the alkali contents ($Na_2O + K_2O$) are much greater in the Gravelly Range basalt, and SiO_2 is lower in the Gravelly Range rhyolitic ignimbrite. Because of the higher alkali contents, Gravelly Range rocks are classified as alkali basalt. Snake River Plain - Yellowstone basalt is classified as tholeiitic basalt. Thompson (1975) suggested, however, some Snake River basalt may not be tholeiitic (it may

TABLE 10. Comparison of major-element content (weight percent) of rock types from the Snake River Plain-Yellowstone Region with Gravelly Range rock types.

LOCALITY	Northwest Yellowstone Plateau			Snake River Plain		Gravelly Range		
ROCK TYPE	Basalt	Basaltic Andesite	Rhyolitic Ash-flow Tuff	Basalt	Silicic Rocks	Basalt	Basaltic Andesite	Rhyolitic Ignimbrite
REFERENCE	(1)	(1)	(1)	(2)	(2)	(3)	(3)	(3)
No. Analyses	1	2	4	9	?	8	2	3
SiO_2	46.7	49.8	76.6	47.2	74.6	49.2	53.6	72.5
Al_2O_3	15.7	15.6	12.4	15.8	12.4	15.1	16.7	12.7
Fe_2O_3	1.2	3.1	1.2	---	---	1.2	1.2	0.7
FeO	13.0	9.2	0.2	12.2*	2.3*	8.2	7.9	1.1
MgO	6.8	6.4	0.1	7.7	0.5	6.2	3.4	0.2
CaO	9.3	8.8	0.3	10.5	3.4	8.9	7.2	0.9
Na_2O	3.2	3.2	3.4	2.7	4.0	3.7	4.2	3.6
K_2O	0.5	0.8	4.9	0.7	4.4	2.0	3.1	5.4
TiO_2	2.4	2.0	0.1	2.5	0.4	1.9	1.5	0.1
P_2O_5	0.4	0.3	0.0	---	0.3	---	---	---
MnO	0.2	0.2	0.0	---	0.2	0.1	0.1	0.0

*Total iron as FeO.
(1) Leeman and Rogers (1970); (2) Hamilton (1963); (3) This study.

be nepheline normative) if measured Fe_2O_3 contents (Tilley and Thompson, 1970) are not representative of the original Fe_2O_3 contents.

Trace-element contents of average Gravelly Range rock types are quite different from average Snake River Plain rock types (Table 11). Ba, Rb, and Sr contents are much greater in Gravelly Range basalt and similar for Gravelly Range rhyolitic ignimbrite whereas Co, Cr, and Sc contents are lower in Gravelly Range basalt and similar for Gravelly Range ignimbrite. LREE contents are much greater in Gravelly Range rocks; HREE contents are lower.

Variations in initial $^{87}Sr/^{86}Sr$ ratios of Gravelly Range basalt (0.7044 to 0.7129) are similar to the variations of Snake River Plain basalt (0.7060 to 0.7180) determined by Leeman and Manton (1971). Higher values are associated with more evolved lavas in both areas. Leeman and Manton suggest that this is a source characteristic. Similar variation in source material is proposed in this study for the Gravelly Range basalt.

Trace-element data suggest Gravelly Range basalt could have formed by the partial melting of a garnet lherzolite or a spinel lherzolite (1-20 percent). Leeman and Vitaliano (1976) concluded that the Snake River basalt formed by partial melting of a spinel peridotite.

Although the basaltic activity in the Gravelly Range may have occurred earlier than in the Snake River Plain, the rhyolitic activity in the two areas may have been contemporaneous. Chemical data suggest that some source similarities as well as differences exist. REE data, however, indicate that the source area was much shallower for the Snake River basalt than for the majority of the Gravelly Range basaltic rocks. Rhyolitic volcanism could be from the same type of source region for both areas.

TABLE 11. Comparison of trace-element content of major rock types from the Snake River Plain-Yellowstone Region with Gravelly Range rock types.

LOCALITY	Snake River Plain		Gravelly Range		
ROCK TYPE	Olivine Tholeiite	Silicic Rocks	Basalt	Basaltic Andesite	Rhyolitic Ignimbrite
REFERENCE	(1)	(1)	(2)	(2)	(2)
No. Analyses	59	?	5	1	3
Ba	378	1100	1104	1675	658
Co	51	2.0	35.3	22.2	0.569
Cr	250	7.0	194	16.7	7.81
Rb	10	167.0	52.0	92.0	190
Sc	32	5.0	21.7	12.3	1.89
Sr	284	59.0	875	936	12.8
Rb/Sr	0.03	2.84	0.059	0.098	14.8
La	22	78.0	46.9	73.2	72.5
Ce	50	161.0	86.2	101	170
Sm	7.5	14.0	6.82	7.50	10.6
Eu	2.4	1.7	1.95	1.72	1.06
Tb	1.3	2.0	0.850	0.639	1.01
Yb	3.3	5.8	1.98	1.72	4.63
Lu	0.56	1.0	0.329	0.262	0.662
La/Lu	39.3	78.0	143	279	110

(1) Leeman (1976).
(2) Leeman et al. /1976).
(3) Average values from this study.

CONCLUSION

Tertiary igneous rocks of the Gravelly Range chemically, petrographically, and spatially , form two distinct suites: (1) the alkali-basalt suite and (2) the rhyolitic ignimbrite suite. Major-element and trace-element variation diagrams, despite being distinct between the two suites, form smooth trends for the rocks within an individual suite. These data suggest that they were not derived from similar sources. The basaltic suite is characterized by a high degree of fractionation of the REE and an apparent lack of Eu anomaly, whereas the ignimbrite suite has a low degree of fractionation of the REE and pronounced negative Eu anomalies.

The continuum of compositions for the rocks of the basaltic suite may be generated by: (1) fractional crystallization of a parent magma, (2) varied partial melting of a similar source, (3) varied amounts of crustal assimilation by a parent magma, (4) varied source composition, or (5) a combination of the above. Petrogenetic models based on the REE data can relate many of the rocks of the alkali-basalt suite to varied degrees of partial melting from a common peridotitic source in the mantle or to small degrees of fractional crystallization of olivine, pyroxene, and plagioclase from a parent magma. The Sr isotopic relationship among the rocks of the basaltic suite, however, serve to emphasize that they can neither be related by fractional crystallization from a common parent nor can they be related by varied degrees of partial fusion from n isotopically homogeneous source. The isotopic composition of these rocks requires that they be derived from partial melting of a varied source. The simplest explanation of the evolution of the rocks of the basaltic suite is that they were derived by partial melting of an upper-mantle source having a homogeneous REE pattern but a varied Rb/Sr ratio.

From the integrated study of chemical, isotopic and field relations of the basaltic igneous rocks of the Gravelly Range area, it is suggested that these rocks are the result of derivation from a varied mantle source material. The crystal tuff could have formed by fractional crystallization of plagioclase, clinopyroxene, and orthoclase from a basaltic parent. Rhyolitic ignimbrite could have formed by less than 30 percent fusion of an average Precambrian rock. The evolution of the Gravelly Range rocks is similar to that of the rocks of the Snake River Plain as suggested by Leeman and Manton (1971).

REFERENCES

Arth, J.G., Hanson, G.N., 1975, Geochemistry and origin of the early Precambrian crust of northeastern Minnesota. Geochim. Cosmochim. Acta 39, 325-362.

Atwood, W.W., Atwood, W.W., Jr., 1945, The physiographic history of an Eocene skyline moraine in western Montana. Jour. Geol. 53, 191-199.

Blake, D.H., Elwell, R.W.D., Gibson, I.L., Skelhorn, R.R., Walker, G.P.L., 1965, Some relationships resulting from the intimate association of acid and basic magmas. Quart. J. Geol. Soc. London 121, 31-50.

Brooks, C.K., 1976, The Fe_2O_3/FeO ratio of basalt analyses: an appeal for a standardized procedure. Bull. Geol. Soc. Denmark 25, 117-120.

Burke-Griffin, B.M., 1978, Geology, petrology, and geochemistry of Black Butte, volcanic, Gravelly Range, Montana. M.S. thesis, Wright State University, 102 p.

Burke-Griffin, B.M., Pushkar, P., 1979, Geology, petrology, and geochemistry of the Black Butte volcanic neck, Gravelly Range, Montana. (abstr.), Ohio Jour. Sci. 79, p. 25.

Chaudhuri, S., 1966, The geochronology of the Keeweenawan rocks of Michigan and the origin of the copper deposits. PhD. Thesis, Ohio State University, 200 p.

Chadwick, R.A., 1978, Geochronology of post-Eocene rhyolitic and basaltic volcanism in southwestern Montana. Isochron/West 22, 25-28.

Christiansen, R.L., Lipman, P.W., 1972, Cenozoic volcanism and plate-tectonic evolution of the western United States; II, Late Cenozoic. Phil. Trans. Royal Soc. London 271A, 249-284.

Condie, K.C., 1967, Geochemistry of early Precambrian graywackes from Wyoming. Geochim. Cosmochim. Acta 31, 2135-2149.

Condie, K.C., Macke, J.E., Reimer, T.O., 1970, Petrology and geochemistry of early Precambrian graywackes from the Fig Tree Group, South Africa. Geol. Soc. Am. Bull. 81, 2759-2776.

Condit, D.D., Finch, E.H., Pardee, T., Jr., 1927, Phosphate rock in the Three forks-Yellowstone Park region, Montana. U.S. Geol. Surv. Bull. 795,

Cox, K.G., Bell, J.D., Pankhurst, R.J., 1979, The Interpretation of Igneous Rocks. London, England: George Allen and Unwin Ltd., 450 p.

Dickinson, W.R., 1972, Evidence for plate-tectonic regimes in the rock record. Am. Jour. of Sci. 272, Summer, 551-556.

Douglas, E., 1909, A geological reconnaissance in South Dakota, Montana, and Idaho. Carnegie Museum, Pittsburgh, Annals 5, 201 p.

Eardley, A.J., 1960, Phases of Orogeny in the deformed belt of southwestern Montana and adjacent areas of Idaho and Wyoming. Billings Geol. Soc., 11th Annual Field Conference, 86-91.

Eaton, G.P., Christiansen, R.L., Iyer, H.M., Pitt, A.M., Mabey, D.R., Blank, H.R., Zietz, Jr., Gettings, M.E., 1975, Magma beneath Yellowstone National Park. Science 188, 787-796.

Eichen, D., 1979, The geology and petrology of the volcanic rocks in the southern Wolverine Basin, Gravelly Range, Montana. M.S. thesis, Wright State University, 60 p.

Eichen, D., Pushkar, P., 1979, Geology, petrology, and geochemistry of the basalts in Wolverine Basin, Gravelly Range, Montana. (abstr.), Ohio Jour. Sci. 79, p. 25.

Faure, Gunter, 1977, Principles of Isotope Geology. New York: John Wiley and Sons, 464 p.

Fenner, C.N., 1948, Immiscibility of igneous magmas. Amer. J. Sci. 246, 465-502.

Flanagan, F.J., 1973, 1972 values for international geochemical reference samples Geochim. Cosmochim. Acta 37, 1189-1200.

Flanagan, F.J., 1976, Descriptions and analyses of eight new U.S. Geological Survey rock standards. U.S. Geol. Surv. Prof. Paper 840, 131-184.

Frey, F.A., 1979, Trace element geochemistry: Application to the igneous petrogenesis of terrestial rocks. Reviews of Geophysics and Space Physics 17, no. 4, 803-823.

Gilluly, J., 1971, Plate tectonics and magmatic evolution. Geol. Soc. Am. Bull, 82, 2383-2396.

Gilluly, J., 1973, Steady Plate Motion and Episodic Orogeny and Magmatism. Geol. Soc. Am. Bull, 84, 499-514.

Gordon, G.E., Randle, K., Goles, G.G., Corliss, J.B., Beeson, M.H., Oxley, S.S., 1968, Instrumental Activation analysis of standard rocks with high-resolution X-ray detectors. Geochim. Cosmochim. Acta 32, 369-396.

Hamilton, W., 1960, Late Cenozoic tectonics and volcanism of the Yellowstone Region, Wyoming, Montana, and Idaho. Billings Geol. Soc., 11th Annual field Conference, 92-106.

Hamilton, W., 1963, Petrology of rhyolite and basalt, northwestern Yellowstone Plateau. U.S. Geol. Surv. Prof. Paper 475-C, C78-C81.

Haskin, L.A., Allen, R.O., Helmke, P.A., Paster, T.P., Anderson, M.R., Korotev, R.S., Zwiefel, K.A., 1970, Rare earths and other trace elements in Apollo 11 lunar samples. Proc. Apollo 11 Lunar Sci. Conf., Geochim. Cosmochim. Acta, Suppl. 1, 2, 1213-1231.

Haskin, L.A., Frey, F.A., Wildeman, T.R., 1968, Relative and terrestial abundances of the rare earths. In: Origin and Distribution of the Elements, Ahrens, L.H., Ed., Intern. Ser. Monography Earth Sci. 30, 889-912.

Holmes, A., 1931, The problem of the association of acid and basic magmas in central complexes. Geol. Mag. 68, 241-255.

Honkala, F.S., 1960, Structure of the Centennial Mountains and vicinity, Beaverhead County, Montana. Billings Geol. Soc., 11th Annual Field Conference, 197-113.

Hutchison, C.S., 1974, Laboratory Handbook of Petrographic Techniques. New York: Wiley, 500 p.

Irvine, T.N., Baragar, W.R.A., 1971, A guide to the chemical classification of the common volcanic rocks. Can. Jour. Earth Sci. 8, no. 5, 523-548.

Jacobs, J.W., Korstev, R.L., Blanchard, D.P., Haskin, L.A., 1977, A well-tested procedure for instrumental neutron activation analysis of silicate rocks and minerals. J. Radioanal. Chem. 40, 93-114.

James, H.L., Hedge, C.E., 1980, Age of the basement rocks of southwest Montana. Geol. Soc. Am. Bull. 91, Part I, 11-15.

Kay, R.W., Gast, P.W., 1973, The rare earth content and origin of alkali-rich basalts. Jour. Geol. 81, 653-682.

Kilbane, N.A., 1978, Petrogenesis of the McClure Mountain mafic-ultramafic and alkalic complex, Fremont County, Colorado. M.S. thesis, Kansas State University, 158 p.

Koch, R.J., 1978, Petrogenesis of the Precambrian Bevos and Musco Groups, St. Francois Mountains igneous complex, Missouri. M.S. thesis, Kansas State University, 105 p.

Kuenzi, W.D., Fields, R.W., 1971, Tertiary stratigraphy, structure, and geologic history, Jefferson Basin, Montana. Geol. Soc. Am. Bull, 82, 3373-3394.

Kuno, H., 1966, Lateral variation of basalt magma type across continental margins and island arcs. Bull. Volc. 29, 195-222.

Leeman, W.P., Manton, W.I., 1971, Strontium isotopic composition of basaltic lavas from the Snake River Plain, southern Idaho. Earth Planet. Sci. Lett. 11, 420-434.

Leeman, W.P., Rogers, J.J.W., 1970, Late Cenozoic alkali-olivine basalts of the Basin-Range province, U.S.A. Contrib. Mineral. Petrol. 25, 1-24.

Leeman, W.P., Vitaliano, C.J., 1976, Petrology and origin of McKinney basalt, Snake River Plain, Idaho. Geol. Soc. Am. Bull. 87, 1750-1771.

Lpman, P.W., Prostka, H.J., Christiansen, R.L., 1972, Cenozoic volcanism and plate tectonic evolution of the western United States. Phil. Trans. Royal Soc. London 271A, 217-284.

Lipman, P.W., Mehnert, H.H., 1975, Late Cenozoic basaltic volcanism and development of the Rio Grande Depression in the southern Rocky Mountains, Geol. Soc. Am. Mem. 144, 119-154.

MacDonald, G.A., Katsura, T., 1964, Chemical composition of Hawaiian lavas. Jour. Pet. 5, 82-133.

Mann, J.A., 1954, Geology of part of the Gravelly Range, Montana. Yellowstone Bighorn Research Project 190, Y.B.R.A., Inc.

Mann, J.A., 1960, Geology of the Gravelly Range area, Montana. Billings Geol. Soc., 11th Annual Field Conference, 114-127.

Marvin, R.F., Dobson, S.W., 1979, Radiometric ages: Compilation B, U.S. Geological Survey. Isochron/West, no. 6, 3-32.

Marvin, R.F., Wier, K.L., Mehnert, H.H., Merritt, V.M., 1974, K-Ar ages of selected Tertiary igneous rocks in southwestern Montana. Isochron/West, no. 10, 16-20.

Maxwell, J.A., 1968, Rock and mineral analysis. New York, Wiley, 584 p.

Medlin, J.H., Suhr, N.H., Bodkin, J.B., 1969, Atomic absorption analysis of silicates employing LiBO fusion. Atomic Absorption Newsletter 8, no. 2, March-April, 25-29.

Methot, R., 1973, Internal geochronologic study of two large pegmatites, Conneticut. Ph.D. thesis, Kansas State University, 123 p.

Peale, A.C., 1896, Three Forks, Montana, sheet. U.S. Geol. Surv. Geological Atlas, Folie 24, 5 p.

Philpotts, J.A., Schnetzler, C.C., 1970a, Phenocryst-matrix partition coefficients for K, Rb, Sr, and Ba with applications to anorthosite and basalt genesis. Geochim. Cosmochim. Acta 34, 307-322.

Philpotts, J.A., Schnetzler, C.C., 1970b, Speculations on the genesis of alkaline and sub-alkaline basalts following exodus of the continental crust. Can. Mineralogist 10, 374-379.

Ringwood, A.E., 1975, Composition and petrology of the earth's mantle. McGraw-Hill, Inc., 618 p.

Reitz, B.K., 1980, Evolution of Tertiary intrusive and volcanic rocks near Ravenna, Granite County, Montana. M.S. thesis, Kansas State University, 90 p.

Riley, J.P., 1958, Simultaneous determination of water and carbon dioxide in rocks and minerals. Analyst 83, 42-49.

Schmincke, H.V., 1967, Petrologie der phonolytischen bis rhyolitis-chen Vulkanite auf Gran Canaria, Kanarische Inseln. Habilitation Schrift, Ruprect Karl Universität zu Heidelberg, Heidelberg, Germany.

Scott, H.W., 1938, Eocene glaciation in southwestern Montana. Jour. Geol. 46, 628-636.

Shaw, D.M., 1970, Trace element fractionation during anatexis. Geochim. Cosmochim. Acta 34, 237-243.

Suhr, N.H., Ingamells, C.O., 1966, Solution Technique for analysis of silicates. Analytical Chemistry 38, 730-734.

Sun, S.S., Hanson, G.N., 1975, Evolution of the mantle: geochemical evidence from alkali basalts. Geology 3, 297-302.

Thompson, R.N., 1975, Primary basalts and magma genesis, II. Snake River Plain, Idaho, U.S.A. Contrib. Mineral. Petrol. 52, 213-232.

Tilley, C.E., Thompson, R.N., 1970, Melting and crystallization relations of the Snake River basalts of southern Idaho, U.S.A. Earth Planet. Sci. Lett. 8, 79-92.

Wager, L.R., Vincent, E.A., Brown, G.M., Bell, J.D., 1965, Marscoite and related rocks of the western Red Hill complex, Isle of Skye. Phil. Trans. Roy. Soc. London 257, 273-307.

Winkler, H.G., 1976, Petrogenesis of Metamorphic Rocks. 4th ed., Springer-Verlag New York, Inc., 334 p.

Yoder, H.S., Jr., 1973, Contemporaneous basaltic and rhyolitic magmas. Am. Mineral. 58, 153-171.

PETROGENESIS OF A BIMODAL ASSEMBLAGE OF ALKALI-BASALT AND RHYOLITIC IGNIMBRITE, GRAVELLY RANGE SOUTHWEST MONTANA

by

MALIA KAY SPAID-REITZ

B.A., Wright State University, 1978

AN ABSTRACT OF A MASTER'S THESIS

submitted in partial fulfillment of the

requirements of the degree

MASTER OF SCIENCE

Department of Geology

KANSAS STATE UNIVERSITY
Manhattan, Kansas
1980

ABSTRACT

The Tertiary volcanic rocks that occur along the crest of the Gravelly Range, Madison County, Montana, have been examined in this investigation. Major rock types that occur in the study area include, in ascending stratigraphic order, basal crystal tuff, alkali-basalt suite, olivine diabase, and rhyolitic ignimbrite. Field, petrographic, major-element, trace-element, and strontium isotopic data were studied from four of the major outcrop areas: Black Butte, Wolverine Basin, Lion Mountain-Windy Hill, and Divide Mountain.

Major-element contents of samples of the major rock types that occurred in each area were determined. Representative samples were then analyzed for Ba, Ce, Cr, Co, Cs, Hf, Rb, Sc, Se, Sr, Ta, Th, U, Zn, for REE (rare-earth elements) contents, and for Rb-Sr isotopic compositions. Two distinct suites are suggested by these data: (1) an alkali-basalt suite that includes alkali-olivine basalt, silicic-alkalic basalt, basaltic andesite, and crystal tuff, and (2) a rhyolitic ignimbrite. Variation diagrams reveal significant discontinuities between the basaltic suite {DI (differentiation index) ≤ 73.10, Eu/Eu* ≥ 0.657, and $^{87}Rb/^{86}Sr \leq 0.285$} and the rhyolitic ignimbrite (DI ≥ 88.35, Eu/Eu* ≤ 0.479, and $^{87}Rb/^{86}Sr \geq 44.58$).

Major-element and trace-element variation diagrams display continuous colinear trends for rock types within the basaltic suite. Processes that could explain these trends include the following: (1) varied partial fusion of source material, (2) fractional crystallization of a parent magma, (3) varied omposition of the source region, (4) assimilation of crustal material, or (5) any combination of the above processes. Rb-Sr isotopic data indicate that a

chemically and isotopically varied source region formed the basaltic suite. The REE data tend to suggest that the Gravelly Range basaltic rocks could have formed by less than 20 percent fusion of a mantle assemblage such as a garnet or spinel lherzolite, whereas the crystal tuffs could have formed by fractional crystallization of plagioclase and clinopyroxene from a basaltic magma.

Major-element and trace-element data are similar for analyzed samples of rhyolitic ignimbrite, and a genetic relationship is suggested by their normative quartz, albite, anorthite, and orthoclase contents. Partial fusion of an average Precambrian formation from 5 to 10 kb pressure could produce a melt with the observed composition of the rhyolitic ignimbrite. Sr isotopic data suggest that these rocks may be 8 to 20 m.y. younger than the most recent known basaltic activity (23 m.y. B.P.) of the area.